Order Number 9424201

A boundary integral equation approach to three dimensional electromagnetic wave scattering problems

Chao, Joseph Chiu, Ph.D.

Iowa State University, 1994

U·M·I
300 N. Zeeb Rd.
Ann Arbor, MI 48106

A boundary integral equation approach to three dimensional electromagnetic wave scattering problems

by

Joseph Chiu Chao

A Dissertation Submitted to the

Graduate Faculty in Partial Fulfillment of the

Requirements for the Degree of

DOCTOR OF PHILOSOPHY

Department: Electrical Engineering and Computer Engineering
Major: Electrical Engineering (Electromagnetics)

Approved: Members of the Committee:

Signature was redacted for privacy.

Signature was redacted for privacy.

In Charge of Major Work

Signature was redacted for privacy.

For the Major Department

Signature was redacted for privacy.

For the Graduate College

Iowa State University
Ames, Iowa

1994

To My Parents, Chun-Yun and Pi-Lien,
without their encouragement,
this would only be a dream that would never come true.

TABLE OF CONTENTS

LIST OF TABLES

LIST OF FIGURES

ACKNOWLEDGMENTS

It has been a great honor and pleasure to have the guidance and support from Professor Lalita Udpa and Professor Frank Rizzo throughout my doctoral work. I would like to express my sincere gratitude to Professor Udpa for her invaluable suggestions and encouragement, and to Professor Rizzo, who, in spite of his busy schedule, has always taken the time and patience to guide me through the many obstacles encountered in this research. Both Professor Udpa and Professor Rizzo have shown me, through example, what a true scholar should be.

Special thanks are due Dr. Yijun Liu for generously sharing his wisdom in the area of boundary element method. The help he provided me through the course of completing the computer programs for this research is much appreciated.

I would like to thank Professor Satish Udpa, Professor William Lord, and Professor Thomas Rudolphi for taking the time to serve on my committee and for kindly reviewing my dissertation. I am grateful to Dr. Mani Mina and the soon-to-be Dr. Ibrahim El-Shafiey for providing me with valuable insight into the subject of electromagnetism. Also, I would like to acknowledge the financial support provided by the Electrical Power Research Institute during my graduate study.

Finally, I am forever indebted to my loving family: My parents, Chun-Yun and Pi-Lien, and my sisters, Marian and Mei-Ling for their constant encouragement and support. Special thanks are due my father for taking the initiative to change my life for the better. Most of all, I would like to thank my dear wife, Anastasia, for providing me the inspiration and friendship I needed during the difficult times. All of them have sacrificed so much to make all this possible.

ABSTRACT

Electromagnetic scattering models are finding increasing interest in many applications ranging from nondestructive evaluation (NDE) to design of optical systems. The availability of a computational scattering model characterizing the underlying system serves several purposes. First, it serves as an inexpensive test bed to simulate a variety of test situations. For instance, the forward model can be used to evaluate various polarizations and incidence angles of the incident source fields and the corresponding spatial distribution of the scattered fields which in turn provides information useful for optimizing the measurement of scattered fields. By preserving some of the realism that is usually possible in purely analytical methods, it provides valuable insight into the physics of actual problems. Second, forward scattering models are important in solving the inverse problem where the scattered fields are used for characterizing the size, the shape and the constitution of the scatterer.

The development of theoretical models largely relies on the use of numerical techniques such as boundary element method (BEM), finite element method (FEM), or finite difference method (FDM). However, no single numerical method has emerged as the optimal method for solving all electromagnetic scattering problems. One numerical method might be preferred over others, depending on the nature of the problem. For instance, problems which involve homogeneous scatterers and propagation of waves in an infinite medium are typically solved using the BEM whereas problems which involve a naturally truncated region are modeled using FEM and FDM.

This dissertation presents a boundary integral equation (BIE) formulation for the problem of electromagnetic scattering due to homogeneous dielectric scatterers. The governing BIEs are then evaluated numerically using the BEM. Several fundamental electromagnetic scattering geometries are considered. The first problem involves solving for

the scattered fields in the presence of a single, three dimensional, arbitrarily shaped, dielectric scatterer suspended in an infinite medium. The formulation is then extended to modeling the scattered fields in the presence of multiple dielectric scatterers as well as a dielectric scatterer in the proximity of an infinite perfect conducting plane. Lastly, the problem of a dielectric scatterer situated close to a dielectric half-space is discussed. The geometries are chosen so that the work presented in this dissertation will serve as a basic model and solutions to a large range of problems can be obtained by modifying one or more of the configurations presented.

CHAPTER 1. INTRODUCTION

Background

The problem of electromagnetic scattering by homogeneous dielectric scatterers is of interest in many applications ranging from remote sensing to nondestructive evaluation. One such application is the detection of contaminants such as dust particles on semiconductor devices and optical surfaces during manufacture. The presence of such contaminants can affect yield as well as cause reliability problems. In the integrated and digital storage media industries, optical techniques are beginning to find widespread application as a powerful tool for surface inspection and contaminant detection. Commercial detection instruments are currently available for scanning a smooth surface with a laser and using the scattered light to count individual contaminant scatterers, with dimension comparable to the laser wavelength. Although these instruments display high sensitivity to the presence of scatterers, the calibration process (i.e. the size vs. scatterer relationship) must be experimentally determined for each substrate/contaminant combination. An accurate forward model can not only predict the appropriate orientation of the incident fields, but also determine the best possible locations where the scattered fields should be measured in order to reliably detect the presence of the contaminants every time. Consequently, an accurate forward model predicting the calibrating process is of significant interest to the industry.

Prior to the advent of large scale computers, solutions obtained for electromagnetic scattering problems had been largely limited to canonical geometries with boundaries of the scatterer parallel to the axes of an orthogonal coordinate system. An example of such a problem is the Mie theory where solutions to scattering problems in the presence of a sphere or a cylinder can be calculated exactly. However, in the last two decades, with the availability of large scale computers, numerical methods have emerged as the main vehicle for solving electromagnetic scattering problems. A variety of numerical methods have been proposed for solving electromagnetic field problems. These methods can be categorized into one of three

classes: 1. Field approximation method where the problem is solved in terms of the governing differential equations. 2. Source approximation method where the governing differential equations are recast into a set of integral equations which involve equivalent sources on the domain surface. 3. Hybrid method which is a combination of 1 and 2. The finite element method (FEM) and the finite difference method (FDM) are among the more commonly used numerical methods for solving complicated problems. Areas of application include fluid and solid mechanics, heat transfer, and electromagnetic field problems. The FEM, together with the FDM, can be categorized as "field approximation methods". Typically, the FEM involves approximating the problem domain by elements and the FDM involves approximating the governing differential equation by difference equations through a set of discretizing nodes. Both methods require the discretization process to take place throughout the region of interest and are therefore, generally computationally intensive. Both methods have been used successfully in the solution of interior problems where the Dirichlet and/or Neumann boundary conditions apply at the boundary surface. An example is the calculation of electromagnetic fields inside wave guides and cavities where a bounding surface, such as the wave guide walls, exactly terminates the problem domain.

In contrast, exterior problems, such as the calculation of scattered fields are characterized by the lack of a finite boundary surface on which the boundary conditions are exactly specified. The problem domain in the exterior problem is unbounded and extends to infinity where the Sommerfeld radiation condition is enforced, either exactly or approximately. Approximate methods usually truncate at a region where only local field information is used at each node. Exact methods, on the other hand, use information from the entire mesh boundary. These methods are generally more computationally intensive. Approximate absorbing boundary conditions (ABC) provide a computationally efficient enforcement of the radiation condition because they are implemented locally at each boundary node and do not disturb the desired sparsity characteristics of the resulting finite element matrix [1] [2]. However, these approximate methods become more accurate when they are far from the scatterer, thus, expanding the domain of discretization outside the scatterer body. An alternate way of solving this problem is through the use of a unimoment method [3]. In this approach, an imaginary surface enclosing the scatterer is used as the truncated boundary. In general, the geometry of the imaginary surface is of a canonical form with the boundary surface parallel to the orthogonal coordinate system. The fields in the

exterior region are then expanded using an eigenfunction expansion and coupled with the fields inside, solved using the FEM. A set of unknown coefficients expanding the fields can then be solved and subsequently used for calculating the external scattered fields. This method, however, is fundamentally limited to scatterers which conform to the bounding surface, and becomes inefficient for elongated scatterers.

Hybrid methods are another way of solving unbounded scattering problems where the interior region is solved using the FEM and the exterior region is solved using integral equation methods. An example of a hybrid method is the bymoment method. This method decouples the exterior and the interior regions by using a surface that conforms to the scatterer. On the surface, the tangential fields are expressed in terms of a set of basis functions whose coefficients are to be determined. The interior solution is solved using a method similar to the unimoment method and is expressed in terms of the unknown coefficients used in the expansion of the tangential fields on the surface. Next, an application of Green's theorem over the enclosed surface on the inside of the finite element mesh and the surface at infinity allows the coupling of the interior solution to the exterior solution which leads to the determination of coefficients [4]. Other hybrid methods have also been developed [5] [6] [7] [8] [9] [10] [11]. These models differ from one another in the way the interior region is coupled to the exterior solution. For inhomogeneous scatterers, the hybrid method is well suited for solving the scattered fields since the interior region of the scatterer requires volume discretization. However, for homogeneous scatterers, the hybrid method tends to be computationally intensive. In such problems, a boundary integral equation (BIE) method is a more economical candidate.

The BIE methods are well suited for homogeneous body scattering problems for two primary reasons. First, the discretization needs to be performed only on the bounding surface of the scatterer in contrast to volume discretization. Second, because of the nature of the kernel function used in the integral equations, the calculated scattered waves automatically satisfy the Sommerfeld radiation condition without the need for further constraints. Over the years, a considerable amount of work has been done in solving scattering problems using the BIE approach. For instance, the scattering problem of two dimensional scatterers has been successfully solved using BIE based methods [12] [13] [14]. The effectiveness of the BIE

methods has also been shown for a more complicated three dimensional scattering problem [15] [16] [17] [18]. Several different formulations of BIEs can be used. For example, the magnetic field integral equation (MFIE) formulation was used to solve a three dimensional scattering problem [19]. The drawback of using this formulation is that the solution becomes degenerate at certain fictitious resonant frequencies. To overcome this problem, a linear combination of the governing BIEs was taken to circumvent the resonance problem at all frequencies [20]. A number of tutorials are available for a more in-depth discussion on the resonance problem associated with the integral equation approach [21][22].

Scope of the dissertation

The major objective of this dissertation is to develop a boundary integral equation (BIE) approach for solving three dimensional electromagnetic scattering problems. The BIE approach has been shown to be an efficient method for solving complex problems governed by differential equations. By recasting the differential equations into a set of integral equations, the dimensionality of the problem is automatically reduced by one. This is a highly desirable feature in terms of numerical computation.

The dissertation is organized as follows. Chapter 2 is devoted to the discussion on various techniques used for solving electromagnetic scattering problems. These include both the analytical approaches as well as numerical approaches. A comparison is made between several numerical methods for solving scattering problems outlining their advantages and disadvantages. In Chapter 3, the development of governing BIEs for scattering problems is presented. The integral equations obtained are for the single body scattering case but can be easily modified to solve for multiple-body scattering problems. In addition, the problem of spurious resonance is discussed and methods for circumventing this problem are presented. The scattering problem due to multiple scatterers is presented in Chapter 4. It is shown that the governing BIEs for this problem can be obtained by modifying the BIEs derived in Chapter 3. Chapter 5 considers the problem where a dielectric scatterer is situated next to a perfect conducting half-space. It is demonstrated that by the use of image theory, this problem can be transformed into a multiple scatterer problem. Chapter 6 discusses aspects pertaining to the numerical implementation of BIEs. In particular, by discretizing the problem surface domain into a set of discrete nodal points, the BIEs are transformed into a set of linear

algebraic equations. In addition, a process called regularization is introduced to handle the high order singular kernel functions inherent in BIEs. Numerical results obtained by using the BIE approach are presented in Chapter 7. These results are validated by comparing them with other published results. Finally, Chapter 8 presents some conclusions and an outline of the future topics to be pursued.

CHAPTER 2. ELECTROMAGNETIC SCATTERING PHENOMENA

Introduction

The scattering of electromagnetic waves by any system is related to the heterogeneity, at a molecular level, of that system. All matter is comprised of discrete electric charges such as electrons and protons. If an obstacle, whether it be a charged particle or a collection of molecules, is illuminated by an incident electromagnetic wave, electric charges in the obstacle are set into vibratory motion by the electric field of the incident wave. Accelerated electric charges radiate electromagnetic energy in all directions and it is this second radiation that is called the "radiation" scattered by the obstacle. The magnetic counterpart is also present. In addition, the excited charges may convert part of the incident electromagnetic energy into other forms of energy such as heat. This conversion process is called "absorption." It is these two phenomena that are generally associated with "scattering" [23].

The scattering phenomenon due to a single scatterer can be explained qualitatively without any computation. Consider an arbitrary scatterer which is conceptually subdivided into small regions as shown in Figure 2.1. An applied oscillating incident field induces a dipole moment in each region where the dipoles oscillate at the frequency of the incident field and scatter radiation in all directions. The total scattered fields at a location P can be calculated by the superposition of individual scattered wavelets induced by each of the dipole regions, where the individual phase differences are taken into consideration. In general, phase relations change as a function of direction and the scattered field is therefore, expected to change as a function of direction. Typically, if the scatterer is much smaller than the incident wavelength, the scattered wavelets can be considered to be in phase, and there will be no significant variation in scattered fields as a function of direction. On the other hand, as the dimension of the scatterer increases, the scattered fields exhibit phenomena of mutual construction and cancellation, resulting in peaks and valleys in the scattering diagram. Other

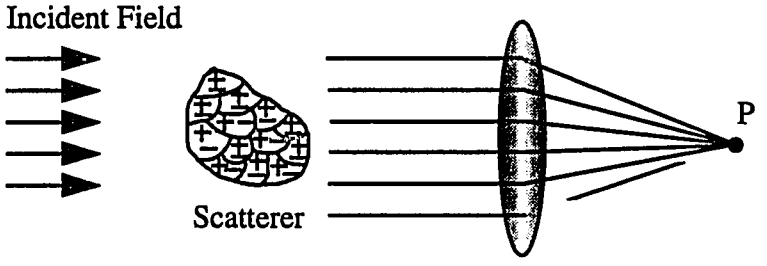

Figure 2.1 A scatterer divided into small dipole regions

factors which all affect the scattering patterns include the shape and the material composition of the scatterer.

In real world applications, multiple scatterer problems (scattering due to multiple scatterers) are encountered more often than single scatterer problems. The multiple scattering phenomenon is considerably more complex since the particles are electromagnetically coupled. Each particle is excited by the external incident field and the resultant field scattered by all the other particles, and the field scattered by a particle also depends on the total field incident on it. Simplification techniques exist for this problem. A commonly used simplification is to assume that each particle is sufficiently small and is separated sufficiently far away from other particles. Consequently, the total scattered field can be approximated by the superposition of the single scattered fields due to each particle. This approach completely neglects the coupling effect and often oversimplifies the original problem.

Maxwell's equations

In a source-free region, all time harmonic electromagnetic waves are governed by the set of frequency domain Maxwell's equations

$$\nabla \times \varepsilon \vec{E} = 0 \tag{2.1}$$

$$\nabla \cdot \mu \vec{H} = 0 \tag{2.2}$$

$$\nabla \times \vec{E} = j\omega\mu \vec{H} \tag{2.3}$$

$$\nabla \times \vec{H} = -j\omega\varepsilon \vec{E} \tag{2.4}$$

where
$\vec{E}$ is the electric field intensity,
$\vec{H}$ is the magnetic field intensity,
μ is the permeability of the medium,
ε is the permittivity of the medium, and
ω is the time-harmonic radial frequency of the fields.

The constitutive parameters ε and μ are constants in a linear, isotropic, homogeneous medium. From equations (2.1) through (2.4), the vector Helmholtz (wave) equations can be obtained by using the vector identity

$$\nabla \times \left(\nabla \times \vec{A}\right) = \nabla\left(\nabla \cdot \vec{A}\right) - \nabla \cdot \left(\nabla \vec{A}\right) \tag{2.5}$$

which yields

$$\nabla^2 \vec{E} + k^2 \vec{E} = 0 \tag{2.6}$$

$$\nabla^2 \vec{H} + k^2 \vec{H} = 0 \tag{2.7}$$

where

$$k^2 = \omega^2 \mu\varepsilon \tag{2.8}$$

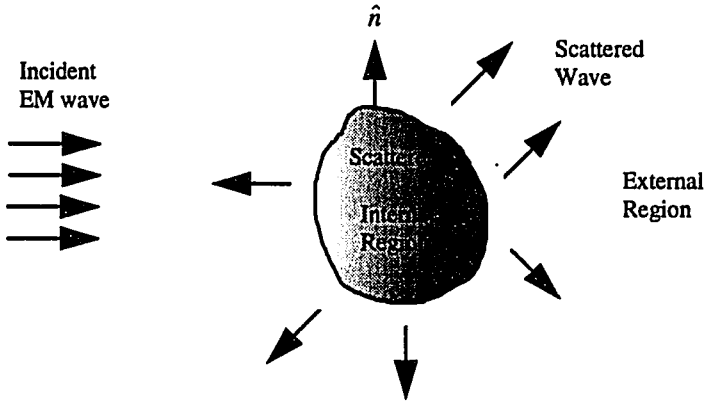

Figure 2.2 A typical scattering configuration

A typical electromagnetic scattering problem is shown in Figure 2.2 where a plane electromagnetic wave is incident upon an arbitrarily shaped particle. The fields are defined using the following notation

$\vec{E}_{inc}$, $\vec{H}_{inc}$ are the incident electromagnetic fields,
$\vec{E}_s$, $\vec{H}_s$ are the scattered fields in the external region, and
$\vec{E}_i$, $\vec{H}_i$ are the fields internal to the scatterer.

The total fields in the external region are

$$\vec{E} = \vec{E}_{inc} + \vec{E}_s \tag{2.9}$$

$$\vec{H} = \vec{H}_{inc} + \vec{H}_s \tag{2.10}$$

All electromagnetic fields are required to satisfy the Maxwell's equations at all points in space. However, as the fields cross the boundary between the scatterer and the medium, there is an abrupt change in these material properties. This change occurs over a transition

region with thickness of the order of atomic dimensions. This transition, macroscopically, is viewed as a discontinuity at the boundary. The boundary conditions at the interface between the scatterer and the medium can be derived using the integral form of Maxwell's equations.

$$\hat{n} \times \bar{E}(p) = \hat{n} \times \bar{E}_i(p) \tag{2.11}$$

$$\hat{n} \times \bar{H}(p) = \hat{n} \times \bar{H}_i(p) \tag{2.12}$$

where p is a point on the boundary and $\hat{n}$ is an unit normal directed outward away from the surface S of the scatterer.

Analytical methods

As mentioned in the previous chapter, many factors influence the electromagnetic scattering phenomenon of an object. The first factor of importance is the shape of the scatterer, since the scatterer shape helps to choose a particular coordinate system which enables the boundary conditions to be expressed in a tractable form. The wave equation is then formulated using these coordinates. For a spherical scatterer, a spherical coordinate system is used to express the necessary boundary conditions. The second major factor affecting the scattering pattern is the size of the scatterer relative to the wavelength of the incident field. Based on the scatterer size, approximate methods such as Rayleigh scattering or geometrical optics techniques may be used to obtain a closed form solution.

Exact methods

Mie theory solutions to electromagnetic scattering phenomena due to a dielectric sphere were first developed in 1908 by Gustav Mie in an effort to understand the varied colors in absorption and scattering exhibited by small colloidal particles of gold suspended in water [24]. The same scattering problem was also considered by Debye at approximately the same time. Whereas Mie used a series expansion of the field vectors using vector harmonics, Debye introduced a set of auxiliary potential functions and expanded these potential functions using similar vector harmonics. The Mie solution for spherical scatterers is described below.

In a source-free, linear, isotropic, homogeneous medium, the time-harmonic electromagnetic fields must satisfy the wave equations

$$\nabla^2\vec{E}+k^2\vec{E}=0 \tag{2.6}$$

$$\nabla^2\vec{H}+k^2\vec{H}=0 \tag{2.7}$$

Consider a scalar function ψ and arbitrary constant vector $\vec{c}$, so that a vector function $\vec{M}$ is constructed as

$$\vec{M}=\nabla\times(\vec{c}\psi) \tag{2.13}$$

Since the divergence of the curl of any vector function vanishes

$$\nabla\cdot\vec{M}=0 \tag{2.14}$$

The vector $\vec{M}$ can be shown to satisfy the equation

$$\nabla^2\vec{M}+k^2\vec{M}=\nabla\times\left[\vec{c}\left(\nabla^2\psi+k^2\psi\right)\right] \tag{2.15}$$

Therefore, $\vec{M}$ satisfies the vector wave equation if ψ is a solution to the scalar wave equation

$$\nabla^2\psi+k^2\psi=0 \tag{2.16}$$

A similar vector function $\vec{N}$ can be constructed from $\vec{M}$

$$\vec{N}=\frac{\nabla\times\vec{M}}{k} \tag{2.17}$$

with zero divergence. $\vec{N}$ satisfies the vector wave equation

$$\nabla^2\vec{N}+k^2\vec{N}=0 \tag{2.18}$$

and

$$\nabla \times \vec{N} = k\vec{M} \tag{2.19}$$

$\vec{M}$ and $\vec{N}$ have all the required properties of an electromagnetic field: they satisfy the vector wave equation, they are divergence free, the curl of $\vec{M}$ is proportional to $\vec{N}$, and the curl of $\vec{N}$ is proportional to $\vec{M}$. Thus, the problem of finding solutions to the propagation equations is reduced to a relatively simpler one of finding solutions to a scalar wave equation given in equation (2.16). ψ is often called the generating function; $\vec{M}$ and $\vec{N}$ are the vector harmonics; $\vec{c}$ is referred to as the guiding vector. The choice of ψ to be used is primarily dictated by the symmetry of the problem. For a spherical scatterer, the function ψ is chosen such that it satisfies the wave equation in spherical coordinate system. In this case, $\vec{M}$ and $\vec{N}$ are called the spherical vector harmonics and $\vec{c}$ is chosen to be $\vec{r}$, a radius vector. Consequently,

$$\vec{M} = \nabla \times (\vec{r}\psi) \tag{2.20}$$

is a solution to the vector wave equation in spherical coordinate system. For problems involving spherical symmetry, the $\vec{M}$ defined in equation (2.20) and the associated $\vec{N}$ are taken as the fundamental solution to the wave equation. Note that $\vec{M}$ is tangential everywhere to any sphere $|\vec{r}|$ = constant (i.e. $\vec{r} \cdot \vec{M} = 0$). Solving the scalar wave equation (2.16) in spherical coordinates and performing a separation of variables, it can be shown that

$$\psi_{emn} = \cos m\phi \, P_n^m(\cos\theta) \, z_n(kr) \tag{2.21}$$

$$\psi_{omn} = \sin m\phi \, P_n^m(\cos\theta) \, z_n(kr) \tag{2.22}$$

and

$$\vec{M}_{emn} = \nabla \times (\vec{r}\psi_{emn}) \tag{2.23}$$

$$\vec{M}_{omn} = \nabla \times (\vec{r}\psi_{omn}) \tag{2.24}$$

$$\vec{N}_{emn} = \frac{\nabla \times \vec{M}_{emn}}{k} \tag{2.25}$$

$$\vec{N}_{omn} = \frac{\nabla \times \vec{M}_{omn}}{k} \tag{2.26}$$

where P_n^m is the associated Legendre function of the first kind of degree n and order m, and z_n is a spherical Bessel function of either the first or second kind.

Given an arbitrary incident plane wave

$$\vec{E}_{inc} = E_0 e^{jkr\cos\theta}\hat{y} \tag{2.27}$$

it can be shown that $\vec{E}_{inc}$ can be expanded using the spherical harmonics as

$$\vec{E}_{inc} = E_0 \sum_{n=1}^{\infty} j^n \frac{2n+1}{n(n+1)}\left(M_{o1n}^B - j N_{e1n}^B\right) \tag{2.28}$$

and the scattered field can be expanded as

$$\vec{E}_s = E_0 \sum_{n=1}^{\infty} j^n \frac{2n+1}{n(n+1)}\left(j a_n N_{e1n}^H - b_n M_{o1n}^H\right) \tag{2.29}$$

where the superscripts B and H represent spherical harmonics that are generated by the spherical Bessel functions and the spherical Hankel functions, respectively; a_n and b_n are scattering coefficients which can be determined from the boundary conditions. Consequently, the relation between the incident wave and the scattered wave amplitude is written in matrix form as

$$\begin{pmatrix} E_{\parallel s} \\ E_{\perp s} \end{pmatrix} = \frac{e^{jk(r-z)}}{-jkr}\begin{pmatrix} s_2 & 0 \\ 0 & s_1 \end{pmatrix}\begin{pmatrix} E_{\parallel inc} \\ E_{\perp inc} \end{pmatrix} \tag{2.30}$$

where $\parallel$ and $\perp$ indicate the parallel and the perpendicular components of the fields with respect to the scattering plane, respectively [23]. The scattering coefficients s_2 and s_1 are obtained from

$$s_1 = \sum_n \frac{2n+1}{n(n+1)}(a_n \pi_n + b_n \tau_n) \tag{2.31}$$

$$s_2 = \sum_n \frac{2n+1}{n(n+1)}(a_n \tau_n + b_n \pi_n) \tag{2.32}$$

and

$$\tau_n = \frac{dP_n^1}{d\theta} \tag{2.33}$$

$$\pi_n = \frac{P_n^1}{\sin\theta} \tag{2.34}$$

The series described in equations (2.31) and (2.32) is usually terminated after a finite number of terms using an appropriate criterion [23]. As can be seen from equation (2.30), the electromagnetic scattering phenomenon due to the presence of a sphere is expressed in a closed analytical form. Similar steps are also applied to scatterers with other canonical geometry. For instance, in the case of a cylindrical scatterer, the cylindrical vector harmonics are used instead of the spherical vector harmonics.

Approximate methods

In the analyses of electromagnetic scattering, exact analytical solutions such as Mie theory (eigenfunction series expansion) are limited to a small class of problems involving simple scatterer shapes. Various approximate techniques have been proposed to cover a wider class of problems depending on the dimensions of the scatterer relative to the wavelength of incident wave, and the material composition of the scatterer. For dielectric scatterers whose dimensions are much smaller than the incident wavelength, the Rayleigh approximation method provides a simple tool for calculating the scattered fields. On the other hand, for scatterers whose dimensions are much larger than the wavelength, optical methods such as geometrical optics and geometrical theory of diffraction (GTD) constitute easy, yet elegant approaches [25]. For scatterers whose relative dielectric constant ε_r is close to unity, the

Rayleigh-Debye method (Born approximation) is typically used to solve for the scattered fields.

Rayleigh scattering The Rayleigh method is generally used when the dimensions of the scatterer are significantly smaller than the incident wavelength. Consider the case of a dielectric sphere whose radius, a, is much smaller than the wavelength, λ. In such cases, the impinging electric field within and near the sphere must behave as an electrostatic field [26]. It is known in electrostatics that when a constant field $\vec{E}_{inc}$ is applied to a dielectric sphere, the electric field $\vec{E}$ inside the sphere is uniform and given by [27]

$$\vec{E} = \frac{3}{\varepsilon_r + 2} \vec{E}_{inc} \tag{2.35}$$

and the scattering cross section σ_s can be shown to be [26]

$$\sigma_s = \frac{128\pi^5 a^6}{3\lambda^4} \left| \frac{\varepsilon_r - 1}{\varepsilon_r + 2} \right|^2 \tag{2.36}$$

This Rayleigh equation is valid only for small ka problems. The approximate upper limit of the radius of the scatterer is generally taken to be $a = 0.05\lambda$. At this radius, the error of the Rayleigh equation is less than 4%.

High frequency approximation method Geometrical optics is a popular, high frequency approximation method primarily because of its applicability to a wide class of scatterers of arbitrary shapes. Based on Fermat's principle, it represents an easy and intuitive understanding of the phenomena. However, the shortcoming of geometrical optics is that it treats only a principal contribution in high frequency asymptotic without expressing the diffraction effects in higher order terms. To include the diffraction effects, [28] introduced the geometrical theory of diffraction (GTD) with the following assumptions:

1) Diffraction is a phenomenon that depends only on the local environment which includes the scatterer shapes and the characteristics of the incident waves in the vicinity of the ray path.

2) Diffracted ray paths must satisfy the extended Fermat's principle where the amplitude and the phase of the field in diffracted rays vary in a manner similar to the geometrical optics field.

GTD is a high frequency technique based on ray theory solution for diffraction by scatterers. As a result, GTD becomes more accurate as the size of the scatterer becomes larger relative to the wavelength of the incident wave. However, the local property of the phenomenon assures GTD to be more widely applicable for scatterers with arbitrary macroscopic shapes, provided the local shape can be regarded as part of a canonical shape. Nonetheless, as in the case of geometrical optics, GTD often encounters problems such as singularities of fields at shadow and reflection boundaries. The mathematical backgrounds of geometrical optics and GTD is beyond the scope of this dissertation but can be found in [29] [30].

Rayleigh-Debye method (Born approximation) Consider the scattering characteristics of a scatterer whose dielectric constant ε_r is close to unity. In this case, the field inside the scatterer may be approximated by the incident field

$$\bar{E} \approx \bar{E}_{inc} \tag{2.37}$$

The resulting scattering amplitude function F in the case of a homogeneous sphere of radius a can be shown to be

$$F(\theta) = \frac{3}{k_s^3 a^3}(\sin k_s a - k_s a \cos k_s a) \tag{2.38}$$

where $k_s = 2k\sin\left(\frac{\theta}{2}\right)$.

This approximation is valid when $2(\varepsilon_r - 1)ka << 1$ [26].

Numerical methods

The non-canonical shapes or geometry of scatterers involved in the majority of practical electromagnetic scattering problems have long been an obstacle to obtain a complete, closed form analytical solution. Prior to the advent of large scale computers, researchers had to either perturb or extrapolate results obtained from canonical scattering problems. To a limited extent, these methods provide a good qualitative analyses of the scattering phenomena. Quantitatively speaking, the results obtained from using these methods tend to deviate from the solutions as the scatterer becomes more and more irregularly shaped. However, within the last two decades, digital computers have quickly emerged as an invaluable tool for solving complex scattering problems. Consequently, many numerical techniques have been developed which allow dependable and accurate approximate solutions to a wide class of problems with irregularly shaped geometry. Two of the more commonly used methods are the finite element method and the boundary element method.

Finite element method

The finite element method (FEM) is among the more commonly used numerical methods for solving complex, real world problems. Areas of applications include fluid and solid mechanics, heat transfer, and electromagnetic field problems. The FEM has its origins in the field of structural engineering where it is used to calculate stresses and deformations in beams with various constraints [31]. The key steps involved in the FEM are as follows:

1) Domain discretization into a set of volume elements
2) Minimization of the energy function, obtained from using variational methods, whose solution also satisfies the original governing differential equations, or a weighted residual approach on the governing differential equations can be taken.
3) Interpolation of the unknown parameters using a set of basis functions within an element.
4) Solving a set of linear equations obtained from substituting 3) into 2).

The volumetric discretization of the problem domain, inherent in FE modeling, gives the capability to handle problems dealing with anisotropy and nonlinearity in the medium or the scatterer. However, since FEM is a "field approximate method", the memory requirement for implementing the volume discretization is generally large. This problem becomes even more severe for unbounded problems, such as electromagnetic scattering problems. As a solution, researchers over the years have proposed numerous alternatives to circumvent this problem. One alternative is to truncate the discretization region at a finite imaginary boundary outside the scatterer and impose an absorbing boundary condition at the imaginary boundary. This imposition assures that the calculated scattered wave propagates in an outward going direction, so as to satisfy the Sommerfeld radiation condition. Another alternative adopted by many engineers is a hybrid approach where both the FEM as well as boundary integral equations (BIE) method are integrated. In this approach, both the FEM and the BIE methods are coupled at the scatterer boundary and the unknowns to be solved are values at the scatterer boundary. After the boundary values have been calculated, the boundary integrals are used to calculate the scattered fields in the exterior region. This method is appropriate for unbounded problems since the BIE approach inherently satisfies the Sommerfeld radiation condition. Nonetheless, for scattering problems involving isotropic, homogeneous scatterers, boundary element method, to be described next, is a more efficient technique since the discretization only takes place at the scatterer's bounding surface.

Boundary element method

The boundary element method (BEM) represents yet another powerful numerical method for solving electromagnetic scattering problems. There are, however, distinct fundamental differences between BEM and FEM that must be emphasized. In the BEM, the original problem expressed in differential equations form is recast analytically into integral equations form using the prescribed boundary conditions [32]. The equation reformulation process uses the fundamental singular solution to the original governing differential equations. Next, using Green's theorem, the integral equation is defined on the domain boundary rather than the 'field region', which results in a reduction in dimension of the problem by one. For instance, a three dimensional integration problem can be reduced to a two dimensional problem of integration over only the domain surface boundary. The reduced dimension problem generally results in smaller but fully populated matrix system of equations which approximate the integral equations. These matrices are generally well

conditioned due to the singular characteristics of the fundamental solution used during the reformulation process. Furthermore, the boundary at infinity is incorporated analytically where the Sommerfeld radiation condition can be directly applied. Thus the problem of truncating the elements at an imaginary boundary never occurs as in the FEM. The only disadvantage associated with the BEM is the difficulty involved in solving problems where the medium is characterized by anisotropy and nonlinearity, although a number of researchers have reported success with these types of problems. A typical procedure for applying the BEM is as follows:

1) Recast the governing differential equations into a set of boundary integral equations using the prescribed boundary conditions and the Green's theorem.
2) Discretize only the bounding surface of the object of interest.
3) Interpolate the unknown quantities on the surface of the object using a set of basis expansion functions.
4) Solve the set of linear algebraic equations for the expansion coefficients.
5) Calculate the scattered fields, either internal or external to the scatterer, using the governing integrals.

The specific detail of employing the BEM approach for solving scattering problems due to both single scatterer and multiple scatterers is discussed in the next two chapters.

CHAPTER 3. SINGLE BODY SCATTERING

Scattering integral equations

The problem of single homogeneous body scattering is probably the least difficult one among all the possible scenarios in electromagnetic scattering problems. The scattering problem to be considered is shown in Figure 3.1 where the scatterer is characterized by the constitutive parameters μ_i and ε_i, and the external medium is characterized by μ_e and ε_e. The incident wave impinging on the scatterer is assumed to be an unit-amplitude, time-harmonic plane wave. To utilize the BIE method, the

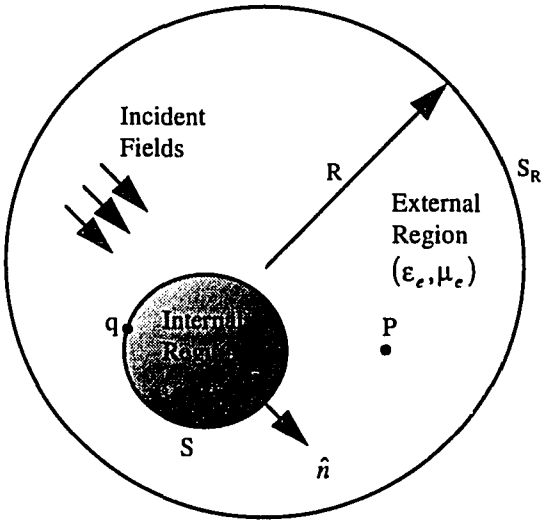

Figure 3.1 Single body scattering problem

governing differential equation is first recast into an integral equation by using the fundamental singular solution and applying the Green's theorem. The governing differential equation for this problem is the vector Helmholtz wave equation,

$$\nabla^2 \vec{E}_i(q) + k_i^2 \vec{E}_i(q) = -\vec{f}(q) \tag{3.1}$$

and the Green's function satisfying the equation

$$\nabla^2 G_i(P,q) + k_i^2 G_i(P,q) = -\delta(P-q) \tag{3.2}$$

where

- $\vec{E}_i$ is the internal electric field,
- $\vec{f}$ is the source or the forcing function,
- G_i is the Green's function characterized by the internal material properties,
- k_i is the wave number associated with the internal region, and
- δ is the dirac delta function.

Applying the Green's theorem for a vector field [32]

$$\int_v \left[G_i \nabla^2 \vec{E}_i - \vec{E}_i \nabla^2 G_i \right] dv = \int_S \left[(\nabla \cdot \vec{E}_i) G_i \hat{n} - (\hat{n} \cdot \vec{E}_i) \nabla G_i - \hat{n} \times (\nabla \times \vec{E}_i) G_i \right.$$
$$\left. - (\hat{n} \times \vec{E}_i) \times \nabla G_i \right] dS \tag{3.3}$$

Multiplying equation (3.1) by G_i and equation (3.2) by $\vec{E}_i$ and subtracting equation (3.2) from (3.1) and integrating over the entire scatterer volume to get

$$\int_v \vec{f}(q) G_i(P,q)\, dv + \int_S \left\{ \left[(\nabla \cdot \vec{E}_i(q)) \hat{n} - \hat{n} \times (\nabla \times \vec{E}_i(q)) \right] G_i(P,q) \right.$$
$$\left. - (\hat{n} \cdot \vec{E}_i(q)) \nabla G_i(P,q) - (\hat{n} \times \vec{E}_i(q)) \times \nabla G_i(P,q) \right\} dS_q = \begin{cases} 2\vec{E}_i(P) & \text{P inside S} \\ 0 & \text{P outside S} \end{cases} \tag{3.4}$$

which is one of the governing integrals for the internal equivalence representation discussed in Appendix A. In the case of a homogeneous, isotropic, dielectric scatterer, equation (3.4) reduces to

$$\int_S \left\{ \left[\hat{n} \times \left(\nabla \times \vec{E}_i(q) \right) \right] G_i(P,q) + \left(\hat{n} \cdot \vec{E}_i(q) \right) \nabla G_i(P,q) + \left(\hat{n} \times \vec{E}_i(q) \right) \times \nabla G_i(P,q) \right\} dS_q$$
$$= \begin{cases} -2\vec{E}_i(P) & \text{P inside S} \\ 0 & \text{P outside S} \end{cases} \tag{3.5}$$

The boundary conditions for the electromagnetic fields on the surface of a scatterer can be expressed in terms of the tangential field components only. Therefore, it is convenient to express equation (3.5) in terms of the tangential field components only. Applying the symmetric property of the Green's function to the term containing the normal field component in equation (3.5)

$$\hat{n} \cdot \vec{E}_i(q) \nabla G_i(P,q) = -\hat{n} \cdot \vec{E}_i(q) \nabla_P G_i(P,q) \tag{3.6}$$

The normal term can be eliminated by taking the curl of equation (3.5) at the P locations

$$\begin{aligned} -2\nabla_P \times \vec{E}_i(P) &= -2j\omega\mu_i \vec{H}_i(P) \\ &= \nabla_P \times \int_S \left[\hat{n} \times \left(\nabla \times \vec{E}_i(q) \right) \right] G_i(P,q)\, dS_q \\ &\quad -\nabla_P \times \int_S \left(\hat{n} \cdot \vec{E}_i(q) \right) \nabla_P G_i(P,q)\, dS_q \\ &\quad +\nabla_P \times \int_S \left(\hat{n} \times \vec{E}_i(q) \right) \nabla G_i(P,q)\, dS_q \end{aligned} \tag{3.7}$$

The second integral on the right hand side of equation (3.7) can be shown to be zero using the vector identity

$$\nabla \times (\nabla \varphi) = 0 \tag{3.8}$$

Therefore, equation (3.7) is simplified to

$$\begin{aligned} -2j\omega\mu_i \vec{H}_i(P) &= \nabla_P \times \int_S \left[\hat{n} \times \left(\nabla \times \vec{E}_i(q) \right) \right] G_i(P,q)\, dS_q \\ &\quad +\nabla_P \times \int_S \left(\hat{n} \times \vec{E}_i(q) \right) \nabla G_i(P,q)\, dS_q \end{aligned} \tag{3.9}$$

Using vector identity, the second integral in equation (3.9) can be shown to be equal to

$$\nabla_P \times \nabla_P \times \int_S \left(\hat{n} \times \vec{E}_i(q)\right) G_i(P,q)\, dS_q \tag{3.10}$$

Finally, equation (3.9) can be written in the form [33]

$$\nabla_P \times \int_S \left(\hat{n} \times \vec{H}_i(q)\right) G_i(P,q)\, dS_q - \nabla_P \times \nabla_P \times \frac{j}{\omega \mu_i} \int_S \left(\hat{n} \times \vec{E}_i(q)\right) G_i(P,q)\, dS_q$$
$$= \begin{cases} -2\vec{H}_i(P) & \text{P inside S} \\ 0 & \text{P outside S} \end{cases} \tag{3.11}$$

By starting out with the Helmholtz equation for the magnetic field, similar expression can be derived for the electric field $\vec{E}_i$

$$\nabla_P \times \int_S \left(\hat{n} \times \vec{E}_i(q)\right) G_i(P,q)\, dS_q + \nabla_P \times \nabla_P \times \frac{j}{\omega \varepsilon_i} \int_S \left(\hat{n} \times \vec{H}_i(q)\right) G_i(P,q)\, dS_q$$
$$= \begin{cases} -2\vec{E}_i(P) & \text{P inside S} \\ 0 & \text{P outside S} \end{cases} \tag{3.12}$$

where the subscript i denotes internal quantities. Similar steps can be taken to derive the governing integral equations for determining the fields in the exterior region. The equations are

$$\nabla_P \times \int_S \left(\hat{n} \times \vec{E}_e(q)\right) G_e(P,q)\, dS_q + \nabla_P \times \nabla_P \times \frac{j}{\omega \varepsilon_e} \int_S \left(\hat{n} \times \vec{H}_e(q)\right) G_e(P,q)\, dS_q$$
$$= \begin{cases} 2\vec{E}_e(P) & \text{P outside S} \\ 0 & \text{P inside S} \end{cases} \tag{3.13}$$

$$\nabla_P \times \int_S \left(\hat{n} \times \vec{H}_e(q)\right) G_e(P,q)\, dS_q - \nabla_P \times \nabla_P \times \frac{j}{\omega \mu_e} \int_S \left(\hat{n} \times \vec{E}_e(q)\right) G_e(P,q)\, dS_q$$
$$= \begin{cases} 2\vec{H}_e(P) & \text{P outside S} \\ 0 & \text{P inside S} \end{cases} \tag{3.14}$$

The total fields outside the scatterer are defined as

$$\vec{E} = \vec{E}_{inc} + \vec{E}_e \tag{3.15}$$

$$\vec{H} = \vec{H}_{inc} + \vec{H}_e \tag{3.16}$$

subject to the boundary conditions imposed on the scatterer surface

$$\hat{n} \times \vec{E} = \hat{n} \times \vec{E}_i \tag{3.17}$$

$$\hat{n} \times \vec{H} = \hat{n} \times \vec{H}_i \tag{3.18}$$

where $\hat{n}$ is an outward unit normal on the boundary surface S.

To obtain a set of governing integral equations for the total external fields, the incident fields are applied to the internal region characterized by the external properties

$$\nabla_P \times \int_S \left(\hat{n} \times \vec{E}_{inc}(q)\right) G_e(P,q)\, dS_q + \nabla_P \times \nabla_P \times \frac{j}{\omega \varepsilon_e} \int_S \left(\hat{n} \times \vec{H}_{inc}(q)\right) G_e(P,q)\, dS_q$$
$$= \begin{cases} -2\vec{E}_{inc}(P) & \text{P inside S} \\ 0 & \text{P outside S} \end{cases} \tag{3.19}$$

$$\nabla_P \times \int_S \left(\hat{n} \times \vec{H}_{inc}(q)\right) G_e(P,q)\, dS_q - \nabla_P \times \nabla_P \times \frac{j}{\omega \mu_e} \int_S \left(\hat{n} \times \vec{E}_{inc}(q)\right) G_e(P,q)\, dS_q$$
$$= \begin{cases} -2\vec{H}_{inc}(P) & \text{P inside S} \\ 0 & \text{P outside S} \end{cases} \tag{3.20}$$

Adding equations (3.19) and (3.20) to (3.13) and (3.14) to get

$$\nabla_P \times \int_S \left(\hat{n} \times \vec{E}(q)\right) G_e(P,q)\, dS_q + \nabla_P \times \nabla_P \times \frac{j}{\omega \varepsilon_e} \int_S \left(\hat{n} \times \vec{H}(q)\right) G_e(P,q)\, dS_q$$
$$= \begin{cases} -2\vec{E}_{inc}(P) & \text{P inside S} \\ 2\vec{E}_e(P) & \text{P outside S} \end{cases} \tag{3.21}$$

$$\nabla_P \times \int_S \left(\hat{n} \times \vec{H}(q)\right) G_e(P,q)\, dS_q - \nabla_P \times \nabla_P \times \frac{j}{\omega \mu_e} \int_S \left(\hat{n} \times \vec{E}(q)\right) G_e(P,q)\, dS_q$$

$$= \begin{cases} -2\vec{H}_{inc}(P) & \text{P inside S} \\ 2\vec{H}_e(P) & \text{P outside S} \end{cases} \tag{3.22}$$

Equations (3.11), (3.12), (3.21) and (3.22) are the governing integrals used to calculate the scattered fields located either internal or external to the scatterer body. For the sake of convenience, four integral operators are defined [33]

$$(C_\alpha \vec{a})(P) = \nabla_P \times \int_S \vec{a}(q)\, G_\alpha(P,q)\, dS_q \tag{3.23}$$

$$(M_\alpha \vec{a})(P) = \hat{n}(P) \times (C_\alpha \vec{a})(P) \tag{3.24}$$

$$(F_\alpha \vec{a})(P) = \nabla_P \times (C_\alpha \vec{a})(P) \tag{3.25}$$

$$(P_\alpha \vec{a})(P) = \hat{n}(P) \times (F_\alpha \vec{a})(P) \tag{3.26}$$

where α = e or i denotes either exterior or interior quantity, respectively. Therefore, equations (3.11), (3.12), (3.21) and (3.22) can be written as

$$C_e\{\hat{n} \times \vec{E}\} + \frac{j}{\omega\varepsilon_e} F_e\{\hat{n} \times \vec{H}\} = \begin{cases} -2\vec{E}_{inc}(P) & \text{P inside S} \\ 2\vec{E}_e(P) & \text{P outside S} \end{cases} \tag{3.27}$$

$$C_e\{\hat{n} \times \vec{H}\} - \frac{j}{\omega\mu_e} F_e\{\hat{n} \times \vec{E}\} = \begin{cases} -2\vec{H}_{inc}(P) & \text{P inside S} \\ 2\vec{H}_e(P) & \text{P outside S} \end{cases} \tag{3.28}$$

$$C_i\{\hat{n} \times \vec{E}_i\} + \frac{j}{\omega\varepsilon_i} F_i\{\hat{n} \times \vec{H}_i\} = \begin{cases} -2\vec{E}_i(P) & \text{P inside S} \\ 0 & \text{P outside S} \end{cases} \tag{3.29}$$

$$C_i\{\hat{n} \times \vec{H}_i\} - \frac{j}{\omega\mu_i} F_i\{\hat{n} \times \vec{E}_i\} = \begin{cases} -2\vec{H}_i(P) & \text{P inside S} \\ 0 & \text{P outside S} \end{cases} \tag{3.30}$$

These are commonly referred as the Stratton-Chu integral equations. Note that the unknowns in equations (3.27) through (3.30) consist of tangential components only. This is in contrast to the formulation where both the normal component as well as the tangential components are

present [18]. The major advantage of using equations (3.27) - (3.30) is that the unknowns can be solved with a significantly smaller number of equations using local coordinate systems. The resultant matrix size is 2N x 2N as opposed to 3N x 3N where N is the total number of discretization nodes in the system.

Following the field formulation approach, the unknowns to be solved are the set of tangential components of the electric and magnetic fields on the boundary surface. For continuous tangential current densities, it can be shown that as an external (internal) point P approaches a surface point p

$$\hat{n}(p)\times C_\alpha \vec{a}(p) = (\pm I + M_\alpha)\vec{a}(p) \tag{3.31}$$

where the upper (lower) sign indicates the observation point P approaches the surface point p from the external (internal) region.

Single scattering effect

As shown in Figure 3.1, there are two surfaces, namely S_R and S, that need to be considered.

As the point P approaches the surface S_R from external region e.
$P \to S_R$ from e

$$(I+M_e)|_{S_R}\{\hat{n}_{S_R}\times\vec{E}\}+\frac{j}{\omega\varepsilon_e}P_e|_{S_R}\{\hat{n}_{S_R}\times\vec{H}\}+\hat{n}_{S_R}\times\Big[C_e|_S\{\hat{n}_S\times\vec{E}\}$$
$$+\frac{j}{\omega\varepsilon_e}F_e|_S\{\hat{n}_S\times\vec{H}\}\Big]=0 \tag{3.32}$$

$$(I+M_e)|_{S_R}\{\hat{n}_{S_R}\times\vec{H}\}-\frac{j}{\omega\mu_e}P_e|_{S_R}\{\hat{n}_{S_R}\times\vec{E}\}+\hat{n}_{S_R}\times\Big[C_e|_S\{\hat{n}_S\times\vec{H}\}$$
$$-\frac{j}{\omega\mu_e}F_e|_S\{\hat{n}_S\times\vec{E}\}\Big]=0 \tag{3.33}$$

As $R \to \infty$, the Sommerfeld radiation condition requires that all integrals over the surface S_R vanish [34]. As a result, equations (3.32) and (3.33) are reduced to

$$(I+M_e)|_{S_R}\{\hat{n}_{S_R}\times\vec{E}_{inc}\}+\frac{j}{\omega\varepsilon_e}P_e|_{S_R}\{\hat{n}_{S_R}\times\vec{H}_{inc}\}+\hat{n}_{S_R}\times\Big[C_e|_S\{\hat{n}_S\times\vec{E}\}$$
$$+\frac{j}{\omega\varepsilon_e}F_e|_S\{\hat{n}_S\times\vec{H}\}\Big]=0 \tag{3.34}$$

$$(I+M_e)|_{S_R}\{\hat{n}_{S_R}\times\vec{H}_{inc}\}-\frac{j}{\omega\mu_e}P_e|_{S_R}\{\hat{n}_{S_R}\times\vec{E}_{inc}\}+\hat{n}_{S_R}\times\Big[C_e|_S\{\hat{n}_S\times\vec{H}\}$$
$$-\frac{j}{\omega\mu_e}F_e|_S\{\hat{n}_S\times\vec{E}\}\Big]=0 \tag{3.35}$$

The first two terms on the left hand side of both equations (3.34) and (3.35) can be shown to be equal to zero by taking the point P on the surface S in equations (3.19) and (3.20). The remaining two terms in equations (3.34) and (3.35) are also observed to be zero from equations (3.27) and (3.28) where

$$C_e\{\hat{n}\times\vec{E}\}+\frac{j}{\omega\varepsilon_e}F_e\{\hat{n}\times\vec{H}\}=2\vec{E}_e(P) \tag{3.36}$$

$$C_e\{\hat{n}\times\vec{H}\}-\frac{j}{\omega\varepsilon_e}F_e\{\hat{n}\times\vec{E}\}=2\vec{H}_e(P) \tag{3.37}$$

where P is on S_R. Again, the radiation condition requires that the integrals over S_R go to zero. Consequently, equations (3.32) and (3.33) equal to zero analytically.

Consider P $\to$ S from e

$$(I-M_e)|_S\{\hat{n}_S\times\vec{E}\}-\frac{j}{\omega\varepsilon_e}P_e|_S\{\hat{n}_S\times\vec{H}\}-\hat{n}_S\times\Big[C_e|_{S_R}\{\hat{n}_{S_R}\times\vec{E}\}$$
$$+\frac{j}{\omega\mu_e}F_e|_{S_R}\{\hat{n}_{S_R}\times\vec{E}\}\Big]=2\hat{n}_S\times\vec{E}_{inc} \tag{3.38}$$

$$(I-M_e)|_S\{\hat{n}_S\times\vec{H}\}+\frac{j}{\omega\mu_e}P_e|_S\{\hat{n}_S\times\vec{E}\}+\hat{n}_S\times\Big[C_e|_{S_R}\{\hat{n}_{S_R}\times\vec{H}\}$$

$$+\frac{j}{\omega\mu_e}F_e|_{S_R}\{\hat{n}_{S_R}\times\vec{E}\}\Big]=2\hat{n}_S\times\vec{H}_{inc} \tag{3.39}$$

As $R\rightarrow\infty$, the last two terms on the left hand side of equations (3.38) and (3.39) go to zero. Therefore, equations (3.38) and (3.39) reduce to

$$(I-M_e)\{\hat{n}\times\vec{E}\}-\frac{j}{\omega\varepsilon_e}P_e\{\hat{n}\times\vec{H}\}=2\hat{n}\times\vec{E}_{inc} \tag{3.40}$$

$$(I-M_e)\{\hat{n}\times\vec{H}\}+\frac{j}{\omega\mu_e}P_e\{\hat{n}\times\vec{E}\}=2\hat{n}\times\vec{H}_{inc} \tag{3.41}$$

Consider P $\rightarrow$ S from i

$$(I+M_i)\{\hat{n}\times\vec{E}_i\}+\frac{j}{\omega\varepsilon_i}P_i\{\hat{n}\times\vec{H}_i\}=0 \tag{3.42}$$

$$(I+M_i)\{\hat{n}\times\vec{H}_i\}-\frac{j}{\omega\mu_i}P_i\{\hat{n}\times\vec{E}_i\}=0 \tag{3.43}$$

Applying the boundary conditions specified in equations (3.17) and (3.18), equations (3.42) and (3.43) become

$$(I+M_i)\{\hat{n}\times\vec{E}\}+\frac{j}{\omega\varepsilon_i}P_i\{\hat{n}\times\vec{H}\}=0 \tag{3.44}$$

$$(I+M_i)\{\hat{n}\times\vec{H}\}-\frac{j}{\omega\mu_i}P_i\{\hat{n}\times\vec{E}\}=0 \tag{3.45}$$

Defining the tangential field components as equivalent surface current densities

$$\vec{M}=-\hat{n}\times\vec{E} \tag{3.46}$$

$$\vec{J} = \hat{n} \times \vec{H} \tag{3.47}$$

Equations (3.40), (3.41), (3.44) and (3.45) can be written in terms of the equivalent currents as

$$(I - M_e)\{\vec{M}\} + \frac{j}{\omega\varepsilon_e} P_e\{\vec{J}\} = 2\vec{M}_{inc} \tag{3.48}$$

$$(I - M_e)\{\vec{J}\} - \frac{j}{\omega\mu_e} P_e\{\vec{M}\} = 2\vec{J}_{inc} \tag{3.49}$$

$$(I + M_i)\{\vec{M}\} - \frac{j}{\omega\varepsilon_i} P_i\{\vec{J}\} = 0 \tag{3.50}$$

$$(I + M_i)\{\vec{J}\} + \frac{j}{\omega\mu_i} P_i\{\vec{M}\} = 0 \tag{3.51}$$

Equations (3.48) through (3.51) represent the governing BIEs for the single body scattering problem, and the solutions of these equations yield the desired equivalent surface currents. Scattered fields at any point P can subsequently be calculated using equations (3.27) through (3.30). Nevertheless, there are four BIEs and only two unknowns $\vec{J}$ and $\vec{M}$. One way to solve for this system of equations is to choose two linear combinations of equations. The two combinations considered are [33]

α_1 (3.49)+ α_2 (3.48)+ α_3 (3.51) and β_1 (3.49) + β_2 (3.48) + β_3 (3.50)

where the α's and β's are constants. A list of possible values for α_i and β_i are described by [35] and are listed in Table 3.1.

It can be shown that solutions for $(\vec{J}, \vec{M})$ *always* exist for all the combinations listed in Table 3.1[33]. However, solving scattering problems using either the electric field integral equations (EFIE) or the magnetic field integral equations (MFIE) results in a multiplicity of solutions at certain resonant frequencies as mentioned in Chapter 2. This nonuniqueness of the solution is not due to the physics of the problem but is an artifact associated with the

integral equations methods. However, the uniqueness of the solution is guaranteed if the linear combination of the integral equations are chosen [36]. For example, the combined-field formulation, the Mautz-Harrington formulation, and the Müller formulation all give unique solutions at all frequencies [37] [38]. In particular, the Mautz-Harrington formulation can be considered as the general case of the other formulations. The only condition to be met to guarantee uniqueness is that the coefficient product $\alpha\beta^*$ (where * denotes the complex conjugate) be real and positive [35] [37]. In this research, the Müller formulation is adopted to reduce the singularity of the P_α operator form a hypersingular to a weakly singular one. This point is discussed in more detail later.

The linear combination in the Müller formulation finally yields the system of equations to be solved for the surface unknowns $(\vec{J},\vec{M})$ on S

$$\left[\mu_e(I-M_e)+\mu_i(I+M_i)\right]\{\vec{J}\}-\frac{j}{\omega}[P_e-P_i]\{\vec{M}\}=2\mu_e\vec{J}_{inc} \tag{3.52}$$

$$\left[\varepsilon_e(I-M_e)+\varepsilon_i(I+M_i)\right]\{\vec{M}\}+\frac{j}{\omega}[P_e-P_i]\{\vec{J}\}=2\varepsilon_e\vec{M}_{inc} \tag{3.53}$$

Table 3.1 Choice of Possible Linear Combination Constants

Formulation	α_1	α_2	α_3	β_1	β_2	β_3
E-field	0	1	0	0	0	1
H-field	0	0	1	1	0	0
Combined field	1	0	-1	0	1	-1
Mautz-Harrington	1	0	$-\beta$	0	1	$-\alpha$
Müller	μ_e	0	$-\mu_i$	0	ε_e	$-\varepsilon_i$

For the case of electromagnetic scattering due to an electrically perfect conducting body, the problem becomes a little simpler. Since the electric field cannot exist inside and on a perfect conductor, the boundary condition in equation (3.17) becomes

$$\hat{n}\times\vec{E}=\hat{n}\times\vec{E}_i=0 \tag{3.54}$$

Consequently, the unknown surface current density $\vec{J}$ can either be solved using the magnetic field integral equation (MFIE)

$$(I-M_e)\{J\}=2\vec{J}_{inc} \tag{3.55}$$

or the electric field integral equation (EFIE)

$$\frac{j}{\omega\varepsilon_e}P_e\{\vec{J}\}=2\vec{M}_{inc} \tag{3.56}$$

There are advantages and disadvantages of using either equation (3.55) or (3.56). The major advantage of using equation (3.55) is that the kernel function is only a strongly singular one. As a result, either a Cauchy Principle Value (CPV) can be evaluated or a simple regularization procedure can be performed to reduce the singularity and evaluate the integral. However, MFIE is only applicable for closed surface scatterers that are inherently smooth. On the contrary, EFIE is well suited for both open and closed surface scatterers which may be rough. The main drawback of using the EFIE is that the kernel function associated with the EFIE is a hypersingular one, and therefore, will require more tedious regularization schemes.

Non-unique solutions at resonant frequencies

To show how the E-field formulation leads to nonunique solutions at resonant (irregular) frequencies, consider equations (2.66) and (2.67) in homogeneous form

$$\hat{n}\times\vec{E}_e^{-}(\vec{J},\vec{M})=0 \tag{3.57}$$

$$\hat{n}\times\vec{E}_i^{+}(\vec{J},\vec{M})=0 \tag{3.58}$$

where all notations are consistent with [35]. Consider the situation shown in Figure 3.2 where $\left(\vec{E}_e(\vec{J},\vec{M}),\vec{H}_e(\vec{J},\vec{M})\right)$ represent fields in the external region characterized by μ_e and ε_e, and $\left(\vec{E}_i(-\vec{J},-\vec{M}),\vec{H}_i(-\vec{J},-\vec{M})\right)$ represent fields in the internal region of S characterized by μ_i and ε_i. The fields in Figure 3.2 are supported by the equivalent current densities $(\vec{J},\vec{M})$ on the surface S given by

$$\overline{\vec{J}} = \hat{n}\times\left(\vec{H}_e^{+}(\vec{J},\vec{M}) - \vec{H}_i^{-}(-\vec{J},-\vec{M})\right) \tag{3.59}$$

$$\overline{\overline{\vec{M}}} = -\hat{n}\times\left(\vec{E}_e^{+}(\vec{J},\vec{M}) - \vec{E}_i^{-}(-\vec{J},-\vec{M})\right) \tag{3.60}$$

Also,

$$\vec{J} = \hat{n}\times\left(\vec{H}_e^{+}(\vec{J},\vec{M}) - \vec{H}_e^{-}(\vec{J},\vec{M})\right) \tag{3.61}$$

$$\vec{M} = -\hat{n}\times\left(\vec{E}_e^{+}(\vec{J},\vec{M}) - \vec{E}_e^{-}(\vec{J},\vec{M})\right) \tag{3.62}$$

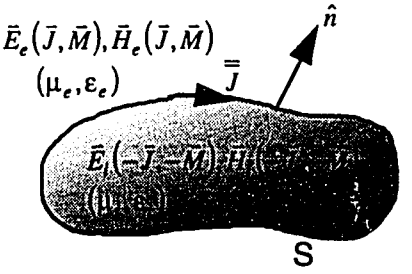

Figure 3.2 Composite equivalent system

and

$$\vec{J} = \hat{n} \times \left(\vec{H}_i^+ \left(\vec{J}, \vec{M} \right) - \vec{H}_i^- \left(\vec{J}, \vec{M} \right) \right) \tag{3.63}$$

$$\vec{M} = -\hat{n} \times \left(\vec{E}_i^+ \left(\vec{J}, \vec{M} \right) - \vec{E}_i^- \left(\vec{J}, \vec{M} \right) \right) \tag{3.64}$$

Subtracting equations (3.63) from (3.61) and (3.64) from (3.62) yield

$$\overline{\vec{J}} = \hat{n} \times \vec{H}_i^+ \left(\vec{J}, \vec{M} \right) + \hat{n} \times \vec{H}_e^- \left(\vec{J}, \vec{M} \right) \tag{3.65}$$

$$\overline{\vec{M}} = -\hat{n} \times \vec{E}_i^+ \left(\vec{J}, \vec{M} \right) - \hat{n} \times \vec{E}_e^- \left(\vec{J}, \vec{M} \right) \tag{3.66}$$

where these are identical to those given in equations (3.59) and (3.60). Since there is no resonance in the external region, equation (3.58) implies that

$$\hat{n} \times \vec{H}_i^+ \left(\vec{J}, \vec{M} \right) = 0 \tag{3.67}$$

and equations (3.57) implies that

$$\hat{n} \times \vec{H}_e^- \left(\vec{J}, \vec{M} \right) = \begin{cases} \alpha \vec{J}_R & \text{at resonant frequencies} \\ 0 & \text{at non - resonant frequencies} \end{cases} \tag{3.68}$$

where $\vec{J}_R$ is a non-zero resonant current density. Substituting equations (3.67) and (3.68) into (3.65) yields

$$\overline{\vec{J}} = \begin{cases} \alpha \vec{J}_R & \text{at resonant frequencies} \\ 0 & \text{at non - resonant frequencies} \end{cases} \tag{3.69}$$

and substituting equations (3.57) and (3.58) into (3.66) yields

$$\overline{\vec{M}} = 0 \tag{3.70}$$

To express $(\vec{J},\vec{M})$ in terms of the fields just inside S due to $(\bar{\bar{J}},0)$, substitute equations (3.67) and (3.58) into (3.63) and (3.64)

$$\vec{J}=\hat{n}\times\vec{H}_i^-(-\vec{J},-\vec{M}) \tag{3.71}$$

$$\vec{M}=-\hat{n}\times\vec{E}_i^-(-\vec{J},-\vec{M}) \tag{3.72}$$

and $(\vec{E}_i^-(-\vec{J},-\vec{M}),\vec{H}_i^-(-\vec{J},-\vec{M}))$ are the fields just inside S due to $\bar{\bar{J}}$ so equations (3.71) and (3.72) can be rewritten as

$$\vec{J}=\hat{n}\times\vec{H}_{ie}^-(\bar{\bar{J}},0) \tag{3.73}$$

$$\vec{M}=-\hat{n}\times\vec{E}_{ie}^-(\bar{\bar{J}},0) \tag{3.74}$$

where $(\vec{E}_{ie}^-(\bar{\bar{J}},0),\vec{H}_{ie}^-(\bar{\bar{J}},0))$ is the field just inside S radiated by $\bar{\bar{J}}$ given in equation (3.69) as shown in Figure 3.2. If the frequency is a resonant frequency, then the equivalent currents in equations (3.73) and (3.74) is non-trivial for $\alpha\neq 0$ because the non-trivial $\bar{\bar{J}}$ of (3.69) produces a field internal to S. However, if the frequency is not a resonant frequency, then $\bar{\bar{J}}=0$ so that the composite fields collapse to zero because of a lack of current sources. As a result, at non-resonant frequencies, the solution is unique. The proof for the existence of unique solutions at all frequencies for linear combinations of BIEs is beyond the scope of this dissertation and can be found in [39]. The numerical implementation methods and the simulation results for the single body scattering problem is presented in later chapters.

CHAPTER 4. MULTIPLE BODY SCATTERING

In electromagnetic scattering applications, a frequently encountered problem is one in which multiple scatterers are present. The multiple scattering problem, in general, is more difficult to solve than the single scattering problem. Typically, multiple scattering problems due to arbitrarily shaped objects can either be solved approximately where only a limited number of wave interactions are taken in account [40] [41], or by assuming that the scatterers are far enough apart so that the total scattered fields is approximated by the sum of the individual scattered waves [23] [24] [41] with no interaction between the individual scatterers. Rarely, if any, are there cases where the full interaction effects are accounted for in the multiple scattering problems. Alternatively, there are methods for scatterers of canonical geometry. In this case, modal expansion methods such as those described in the Mie theory can be used to take into account the full multiple scattering effects [42] [43] [44] [45] [48] [49]. This approach, once again, is only useful for scatterers of canonical shapes. In addition, an approximate method has been proposed [46] [50] where the scatterers are discretized into small spherical regions and the total scattered fields are calculated using the point dipoles approach.

Other numerical techniques such as FEM and FDM also face great difficulty when dealing with multiple scattering problems. Since FEM and FDM are both field approximation methods, the domain to be discretized includes the volumes of the scatterers *plus* the region in between the scatterers. This is a computationally expensive way for solving three dimensional scattering problems. The BIE method is a natural candidate for this type of problems for two reasons. First, since the BIE approach requires the discretization of only the bounding surface of the scatterer, a great savings is achieved with respect to the size of the problem. Second, the interactions between scatterers are exactly calculated under a steady state condition.

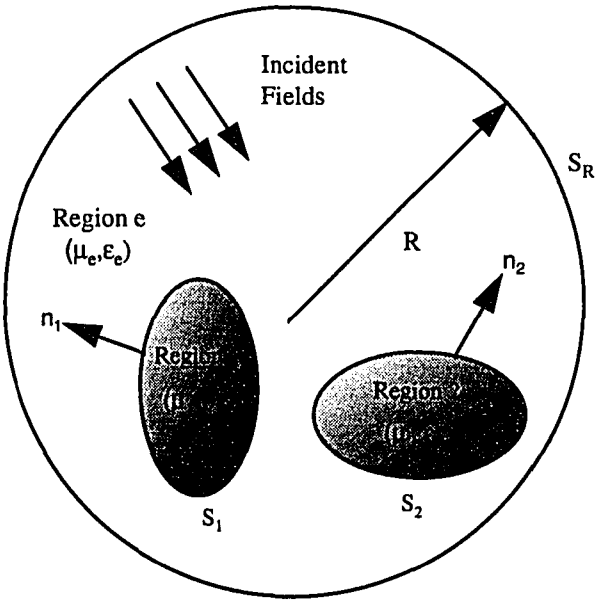

Figure 4.1 Two-scatterer problem

For the sake of simplicity, first consider a two-scatterer problem as shown in Figure 4.1. The approach described in this dissertation is general and can be extended to the case of n scatterers. Two homogeneous scatterers, 1 and 2, characterized by the constitutive parameters (μ_1,ε_1) and (μ_2,ε_2), respectively, can be of any arbitrary shape, orientation, and location. The external region e is characterized by the constitutive parameters (μ_e,ε_e). Once again, the Stratton-Chu equations given in equations (3.27) through (3.30) form the basis for deriving the governing integral equations for this problem. In order to derive the governing BIEs, the observation point P is move to each of the three surfaces, S_R, S_1, and S_2. As in the case of the single body scattering, any integration over the surface S_R goes to zero as $R \rightarrow \infty$ because of the radiation condition. Consequently, only two surfaces need to be considered, namely, S_1, and S_2. The governing BIEs are obtained by considering the following four situations.

1) Consider the observation point P $\rightarrow S_1$ from region e

$$(I-M_e)|_{S_1}\{\hat{n}_1\times\vec{E}\}-\frac{j}{\omega\varepsilon_e}P_e|_{S_1}\{\hat{n}_1\times\vec{H}\}-\hat{n}_1\times\Big[C_e|_{S_2}\{\hat{n}_2\times\vec{E}\}$$
$$+\frac{j}{\omega\varepsilon_e}F_e|_{S_2}\{\hat{n}_2\times\vec{H}\}\Big]=2\hat{n}_1\times\vec{E}_{inc} \qquad (4.1)$$

$$(I-M_e)|_{S_1}\{\hat{n}_1\times\vec{H}\}+\frac{j}{\omega\mu_e}P_e|_{S_1}\{\hat{n}_1\times\vec{E}\}-\hat{n}_1\times\Big[C_e|_{S_2}\{\hat{n}_2\times\vec{H}\}$$
$$-\frac{j}{\omega\mu_e}F_e|_{S_2}\{\hat{n}_2\times\vec{E}\}\Big]=2\hat{n}_1\times\vec{H}_{inc} \qquad (4.2)$$

2) Consider the observation P $\rightarrow S_2$ from region e

$$(I-M_e)|_{S_2}\{\hat{n}_2\times\vec{E}\}-\frac{j}{\omega\varepsilon_e}P_e|_{S_2}\{\hat{n}_2\times\vec{H}\}-\hat{n}_2\times\Big[C_e|_{S_1}\{\hat{n}_1\times\vec{E}\}$$
$$+\frac{j}{\omega\varepsilon_e}F_e|_{S_1}\{\hat{n}_1\times\vec{H}\}\Big]=2\hat{n}_2\times\vec{E}_{inc} \qquad (4.3)$$

$$(I-M_e)|_{S_2}\{\hat{n}_2\times\vec{H}\}+\frac{j}{\omega\mu_e}P_e|_{S_2}\{\hat{n}_2\times\vec{E}\}-\hat{n}_2\times\Big[C_e|_{S_1}\{\hat{n}_1\times\vec{H}\}$$
$$-\frac{j}{\omega\mu_e}F_e|_{S_1}\{\hat{n}_1\times\vec{E}\}\Big]=2\hat{n}_2\times\vec{H}_{inc} \qquad (4.4)$$

3) Consider the observation point P $\rightarrow S_1$ from region 1

$$(I+M_{i1})|_{S_1}\{\hat{n}_1\times\vec{E}_{i1}\}+\frac{j}{\omega\varepsilon_{i1}}P_{i1}|_{S_1}\{\hat{n}_1\times\vec{H}_{i1}\}=0 \qquad (4.5)$$

$$(I+M_{i1})|_{S_1}\{\hat{n}_1\times\vec{H}_{i1}\}-\frac{j}{\omega\mu_{i1}}P_{i1}|_{S_1}\{\hat{n}_1\times\vec{E}_{i1}\}=0 \qquad (4.6)$$

4) Consider the observation point P $\rightarrow S_2$ from region 2

$$(I+M_{i2})|_{S_1}\{\hat{n}_1\times\vec{E}_{i2}\}+\frac{j}{\omega\varepsilon_{i2}}P_{i2}|_{S_1}\{\hat{n}_1\times\vec{H}_{i2}\}=0 \tag{4.7}$$

$$(I+M_{i2})|_{S_1}\{\hat{n}_1\times\vec{H}_{i2}\}-\frac{j}{\omega\mu_{i2}}P_{i2}|_{S_1}\{\hat{n}_1\times\vec{E}_{i2}\}=0 \tag{4.8}$$

where the electric and magnetic fields internal to the scatterers 1 and 2 are designated $\vec{E}_{i1}$, $\vec{H}_{i1}$, $\vec{E}_{i2}$, and $\vec{H}_{i2}$, respectively. All fields are subject to the boundary conditions

$$\hat{n}_1\times\vec{E}=\hat{n}_1\times\vec{E}_{i1} \tag{4.9}$$

$$\hat{n}_1\times\vec{H}=\hat{n}_1\times\vec{H}_{i1} \tag{4.10}$$

$$\hat{n}_2\times\vec{E}=\hat{n}_2\times\vec{E}_{i2} \tag{4.11}$$

$$\hat{n}_2\times\vec{H}=\hat{n}_2\times\vec{H}_{i2} \tag{4.12}$$

where $\hat{n}_1$ and $\hat{n}_2$ represent, respectively, the outward unit normal from surfaces S_1, and S_2. Using the definition of equivalent surface current densities given in equations (3.46) and (3.47) and applying the appropriate boundary conditions, equations (4.1) through (4.8) become

$$(I-M_e)|_{S_1}\{\vec{M}_1\}+\frac{j}{\omega\varepsilon_e}P_e|_{S_1}\{\vec{J}_1\}-\hat{n}_1\times\Big[C_e|_{S_2}\{\vec{M}_2\}$$
$$-\frac{j}{\omega\varepsilon_e}F_e|_{S_2}\{\vec{J}_2\}\Big]=2\vec{M}_{inc1} \tag{4.13}$$

$$(I-M_e)|_{S_1}\{\vec{J}_1\}-\frac{j}{\omega\mu_e}P_e|_{S_1}\{\vec{M}_1\}-\hat{n}_1\times\Big[C_e|_{S_2}\{\vec{J}_2\}$$
$$+\frac{j}{\omega\mu_e}F_e|_{S_2}\{\vec{M}_2\}\Big]=2\vec{J}_{inc1} \tag{4.14}$$

$$(I-M_e)|_{S_2}\{\vec{M}_2\}+\frac{j}{\omega\varepsilon_e}P_e|_{S_2}\{\vec{J}_2\}-\hat{n}_2\times\Big[C_e|_{S_1}\{\vec{M}_1\}$$

$$-\frac{j}{\omega\varepsilon_e}F_e|_{S_1}\{\vec{J}_1\}\Big] = 2\vec{M}_{inc2} \tag{4.15}$$

$$(I-M_e)|_{S_2}\{\vec{J}_2\}-\frac{j}{\omega\mu_e}P_e|_{S_2}\{\vec{M}_2\}-\hat{n}_2\times\Big[C_e|_{S_1}\{\vec{J}_1\}$$
$$+\frac{j}{\omega\mu_e}F_e|_{S_1}\{\vec{M}_1\}\Big] = 2\vec{J}_{inc2} \tag{4.16}$$

$$(I+M_{i1})|_{S_1}\{\vec{M}_1\}-\frac{j}{\omega\varepsilon_{i1}}P_{i1}|_{S_1}\{\vec{J}_1\} = 0 \tag{4.17}$$

$$(I+M_{i1})|_{S_1}\{\vec{J}_1\}+\frac{j}{\omega\mu_{i1}}P_{i1}|_{S_1}\{\vec{M}_1\} = 0 \tag{4.18}$$

$$(I+M_{i2})|_{S_1}\{\vec{M}_2\}-\frac{j}{\omega\varepsilon_{i2}}P_{i2}|_{S_1}\{\vec{J}_2\} = 0 \tag{4.19}$$

$$(I+M_{i2})|_{S_1}\{\vec{J}_2\}+\frac{j}{\omega\mu_{i2}}P_{i2}|_{S_1}\{\vec{M}_2\} = 0 \tag{4.20}$$

where the subscript 1 and 2 denote surface values on S_1, and S_2, respectively. Again, there are more equations than there are unknowns and to avoid the problem of spurious resonance and to reduce the singularity order of the P operators from hypersingular to weakly singular, the Müller formulation is adopted. The resulting linear combinations are

$$\varepsilon_e(4.13)+\varepsilon_{i1}(4.17) \tag{4.21}$$

$$\mu_e(4.14)+\mu_{i1}(4.18) \tag{4.22}$$

$$\varepsilon_e(4.15)+\varepsilon_{i2}(4.19) \tag{4.23}$$

$$\mu_e(4.16)+\mu_{i2}(4.20) \tag{4.24}$$

These equations are the governing BIEs for a two-body scattering problem. Solving equations (4.21) through (4.24) will yield the equivalent surface current densities $\left(\bar{M}_1, \bar{J}_1, \bar{M}_2, \bar{J}_2\right)$ necessary for calculating the scattered fields.

CHAPTER 5. SCATTERER NEAR A HALF-SPACE

The problem of solving for scattered fields due to a single dielectric body situated near a surface is far more difficult to solve than both the single-body scattering and multiple-body scattering problems. To date, analytical solutions for the general case of a dielectric sphere near a dielectric half-space consisting of a different material have not been reported. Although an analytical Green's function does exist for this dielectric/half-space problem, it involves a numerical evaluation of the Sommerfeld integrals which is possible only for limited classes of problems. The exact image theory was applied for the general case of scattering of a sphere near a dielectric half-space [47]. The assumptions made, however, are that the sphere is small and far enough from the interface such that its internal fields can be treated as an uniform plane wave. In addition, the Green's function derived still requires an integration in the complex plane, a tedious task in itself. A compromising approach to modeling the sphere/surface problem is to assume that the scattered waves consist of rays which are reflected off the surface either before or after interacting with the sphere [51] [52]. This approach was further improved by explicitly including a term which accounts for the attenuation caused by the dielectric surface reflection [53]. Analytic solutions do exist, however, for the case of a dielectric sphere near a perfect conducting plane [54] where the Lorentz-Mie scattering theory has been combined with the Debye potential method. In [55], the authors derived the Müller scattering matrices for the same problem. However, the solution assumes that the scattered fields from the sphere are incident on the surface at a near-normal angle.

Conducting half-space

In this dissertation, the problem of a scatterer near a perfect conducting surface is not limited to only the case of spherical scatterers. Using the combination of BIE method and image theory, the scatterer above the conducting plane can be of arbitrary shape. The formulation for this problem is based on a simple modification of the two-scatterer problem.

Image theory

To fully appreciate the use of BIE/image theory approach for the problem of scattering due to a dielectric object near a perfect conducting half-plane, the concept of image theory must first be explained. To analyze the idea of a radiating element near an infinite plane conductor, the concept of a virtual source or an image is introduced to account for the reflections. The virtual sources, of course, are such that when combined with the real sources, form an equivalent system that replaces the original system. Consider Figure 5.1 which contains both the real source as well as the virtual source. The equivalent system, however, only gives the correct fields above the conducting plane and not below the conducting plane, where the field is zero.

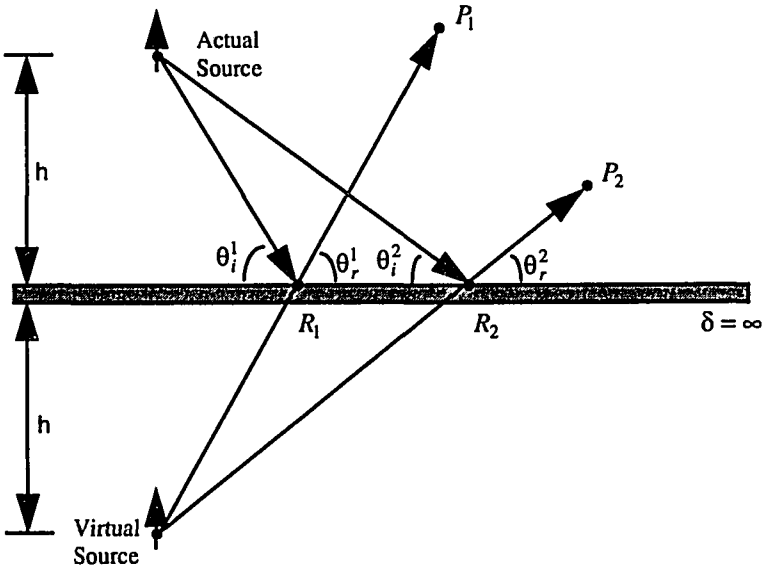

Figure 5.1 Image theory

Consider the case of a vertical electric dipole placed at a distance h above the perfect conducting plane. For an observation point P_1, there is a direct wave from the actual source to P_1. In addition, there is a reflected wave originating from the source to a point R_1 on the plane onto the point P_1. The location of R_1 is such that the Snell's law is obeyed i.e. $\theta_1^i = \theta_1^R$. For a different observation point P_2, a different reflection point R_2 can also be determined using the Snell's law. With a perfect conducting plane, the wave is totally reflected with no attenuation. Therefore, if a line along the reflected path is extended to below the conducting plane, it would appear as though that the reflected wave came from a (virtual) source situated below the plane. Consequently, the conducting plane can be removed and replaced by a vertical dipole, with the same polarization as the actual dipole, at a distance h below the interface. This is the basis for the image theory. For a horizontal dipole (parallel to the plane) above the plane, similar analysis can be used and it has been shown in [30] that the virtual source is also a horizontal dipole at a same distance below the plane but with polarization that is 180° out of phase to the actual source. Finally, the electric and magnetic source above the perfect electrically conducting half-plane will have virtual sources as shown in Figure 5.2.

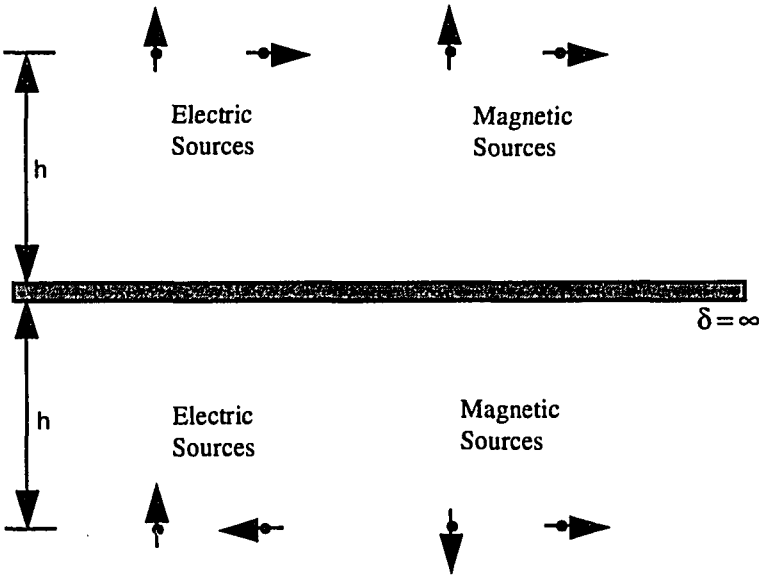

Figure 5.2 Electric and magnetic source with corresponding images

The scattering problem to be solved is shown in Figure 5.3 where a dielectric sphere is situated near a perfect electrically conducting infinite plane with an incident plane wave. Applying the image theory to this problem, the original problem can be recast into an equivalent problem as shown in Figure 5.4.

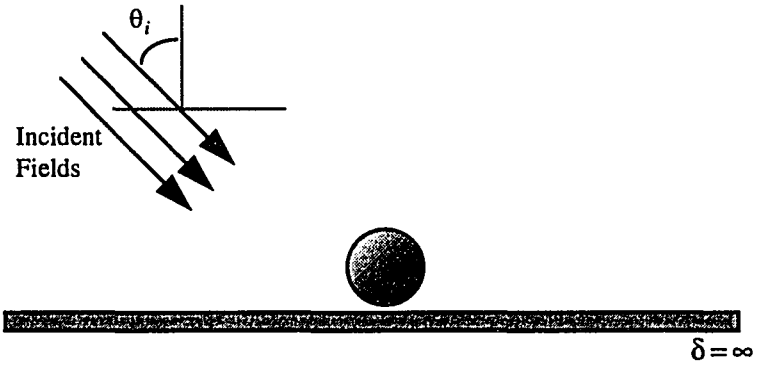

Figure 5.3 Dielectric sphere on a perfect conducting plane

The problem is now similar to the two-body scattering case as described in Chapter 4 but with two different incident fields: one representing the incident plane wave originating from the upper half-space, and the other is an equivalent reflected plane wave due to the conducting plane originating from the lower half-space. The polarization of the reflected wave is such that the electric field is zero and the magnetic field is twice the incident field at the half-space interface. The system to be solved, however, is only one half the size of the system in the two-scatterers case. This is because the magnitudes of the equivalent source on the top scatterer are the same as the magnitudes of the image equivalent sources on the bottom scatterer, with appropriate sign differences. As a result, only the unknown equivalent currents on the real scatterer need to be solved. The governing BIEs for this problem are similar to the equations for the two body scattering problem,

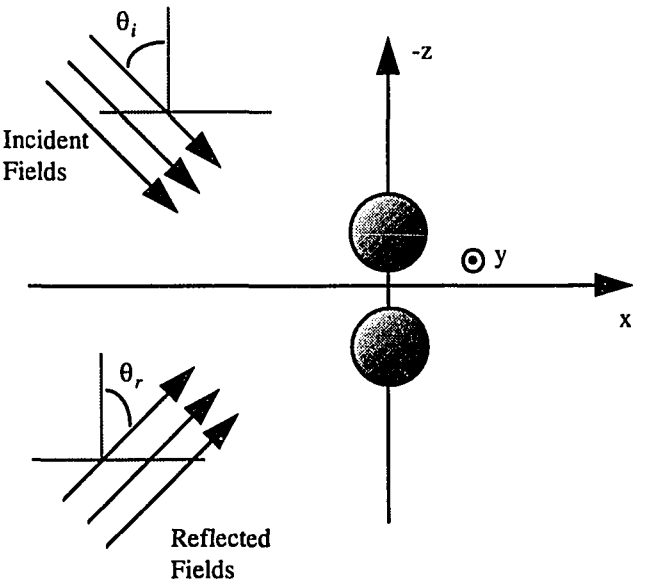

Figure 5.4 Equivalent system by application of image theory

$$(I-M_e)|_{S_1}\{\vec{M}_1\}+\frac{j}{\omega\varepsilon_e}P_e|_{S_1}\{\vec{J}_1\}-\hat{n}_1\times\left[C_e|_{S_2}\{\vec{M}_2\}\right.$$
$$\left.-\frac{j}{\omega\varepsilon_e}F_e|_{S_2}\{\vec{J}_2\}\right]=2\left[\vec{M}_{incl}+\vec{M}_{refl}\right] \tag{5.1}$$

$$(I-M_e)|_{S_1}\{\vec{J}_1\}-\frac{j}{\omega\mu_e}P_e|_{S_1}\{\vec{M}_1\}-\hat{n}_1\times\left[C_e|_{S_2}\{\vec{J}_2\}\right.$$
$$\left.+\frac{j}{\omega\mu_e}F_e|_{S_2}\{\vec{M}_2\}\right]=2\left[\vec{J}_{incl}+\vec{J}_{refl}\right] \tag{5.2}$$

$$(I-M_e)|_{S_2}\{\vec{M}_2\}+\frac{j}{\omega\varepsilon_e}P_e|_{S_2}\{\vec{J}_2\}-\hat{n}_2\times\left[C_e|_{S_1}\{\vec{M}_1\}\right.$$

$$-\frac{j}{\omega\varepsilon_e}F_e|_{S_1}\{\vec{J}_1\}\Big]=2\left[\vec{M}_{inc2}+\vec{M}_{ref2}\right] \tag{5.3}$$

$$(I-M_e)|_{S_2}\{\vec{J}_2\}-\frac{j}{\omega\mu_e}P_e|_{S_2}\{\vec{M}_2\}-\hat{n}_2\times[C_e|_{S_1}\{\vec{J}_1\}$$
$$+\frac{j}{\omega\mu_e}F_e|_{S_1}\{\vec{M}_1\}\Big]=2\left[\vec{J}_{inc2}+\vec{J}_{ref2}\right] \tag{5.4}$$

$$(I+M_{i1})|_{S_1}\{\vec{M}_1\}-\frac{j}{\omega\varepsilon_{i1}}P_{i1}|_{S_1}\{\vec{J}_1\}=0 \tag{5.5}$$

$$(I+M_{i1})|_{S_1}\{\vec{J}_1\}+\frac{j}{\omega\mu_{i1}}P_{i1}|_{S_1}\{\vec{M}_1\}=0 \tag{5.6}$$

$$(I+M_{i2})|_{S_1}\{\vec{M}_2\}-\frac{j}{\omega\varepsilon_{i2}}P_{i2}|_{S_1}\{\vec{J}_2\}=0 \tag{5.7}$$

$$(I+M_{i2})|_{S_1}\{\vec{J}_2\}+\frac{j}{\omega\mu_{i2}}P_{i2}|_{S_1}\{\vec{M}_2\}=0 \tag{5.8}$$

where S_1 and S_2 represent the bounding surfaces of the actual scatterer and the image scatterer, respectively. The variables $(\vec{M}_{ref},\vec{J}_{ref})$ represent the tangential components of the reflected wave on the surfaces of the scatterers. Additional constraints are imposed on the surface current densities on both the actual scatterer and the image scatterer. Since the BEM solves for the unknown current densities at each of the discretized nodal points, in essence, the nodal currents behave as either an equivalent electric dipole or magnetic dipole radiating the desired scattered fields. Consequently, image theory can be applied so that if a nodal current is known on the actual scatterer, the corresponding nodal current on the image scatterer can also be determined from Figure 5.2. The component relationships between the actual nodal currents and their corresponding image nodal currents are

$$J_x^a=-J_x^i \tag{5.9}$$

$$J_y^a=J_y^i \tag{5.10}$$

$$J_z^a = J_z^i \tag{5.11}$$

$$M_x^a = M_x^i \tag{5.12}$$

$$M_y^a = M_y^i \tag{5.13}$$

$$M_z^a = -M_z^i \tag{5.14}$$

By imposing these component relationships in equations (5.9) through (5.14), the size of the linear system to be solved is reduced from 4N x 4N to 2N x 2N where N is the total number of discretization nodes on both scatterers.

Dielectric half-space

The problem of solving for the scattered fields due to a dielectric particle near a dielectric half-space is more difficult than the case with a perfect conducting half-space. Numerous approximate approaches for solving this problem have been taken by researchers in the past, with the simplest being considering the total scattered fields as being made up of fields that are directly scattered from the particle plus fields reflected from the plane either before or after a number of interactions with the particle. The approach taken here, however, is an exact one where the dielectric half-space is considered to be a secondary scattering obstacle bounded by a finite flat surface S_H and the remaining surface S_R as shown in Figure 5.5.

Using this technique, the free space Green's function can be used for this problem instead of the conventional half-space Green's function where the problems of instability and integration over infinitely many wave numbers are often encountered. The problem can be considered as a two body scattering problem with the radius R, in the limit, going to infinity. The total scattered fields in the external region can be considered to be the sum of three fields.

$$\vec{E} = \vec{E}_{inc} + \vec{E}_{ref} + \vec{E}_e \tag{5.15}$$

$$\vec{H} = \vec{H}_{inc} + \vec{H}_{ref} + \vec{H}_e \tag{5.16}$$

where

$\vec{E}, \vec{H}$ are the total fields in the external region,

$\vec{E}_{inc}, \vec{H}_{inc}$ are the incident plane waves,

$\vec{E}_{ref}, \vec{H}_{ref}$ are the reflected plane waves from the half-plane in the absence of the particle, and

$\vec{E}_e, \vec{H}_e$ are the scattered waves caused by the interaction between the particle and the half-space (can be viewed as a perturbation term).

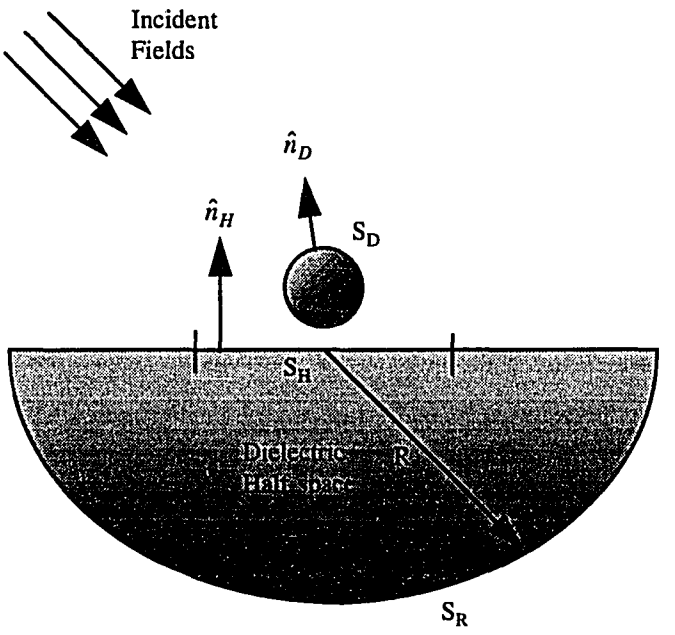

Figure 5.5 Scatterer near a dielectric half-space

Due to the attenuating nature of the scattered fields $(\vec{E}_e, \vec{H}_e)$ over distance, the problem is formulated to solve for $(\vec{E}_e, \vec{H}_e)$, instead of the total fields $(\vec{E}, \vec{H})$. This requires only a finite surface area to be discretized on the half-plane. The entire region of the bowl

plus the flat surface is considered as R goes to infinity, the integrals with $(\vec{E}_e, \vec{H}_e)$ as the surface variable can be shown to approach zero to satisfy the Sommerfeld's radiation condition. The only surface remaining that needs to be discretized is the finite surface area, S_H, on the flat plane. If the field variables were chosen to be the total fields $(\vec{E}, \vec{H})$, then the field values do not diminish as R goes to infinity since $(\vec{E}, \vec{H})$ contain plane waves. Thus, integral over the bowl cannot be discarded. Consequently, the governing BIEs for this problem are derived for $(\vec{E}_e, \vec{H}_e)$ as follows:

$$(I - M_e)|_{S_H}\{\vec{M}_{eH}\} + \frac{j}{\omega\varepsilon_e} P_e|_{S_H}\{\vec{J}_{eH}\} + \hat{n}_H \times \left[-C_e|_{S_D}\{\vec{M}_{eD}\} + \frac{j}{\omega\varepsilon_e} F_e|_{S_D}\{\vec{J}_{eD}\} \right] = 0 \quad (5.17)$$

$$(I - M_e)|_{S_H}\{\vec{J}_{eH}\} - \frac{j}{\omega\mu_e} P_e|_{S_H}\{M_{eH}\} + \hat{n}_H \times \left[-C_e|_{S_D}\{\vec{J}_{eD}\} - \frac{j}{\omega\mu_e} F_e|_{S_D}\{\vec{M}_{eD}\} \right] = 0 \quad (5.18)$$

$$\begin{aligned}&(I - M_e)|_{S_D}\{\vec{M}_{eD}\} + \frac{j}{\omega\varepsilon_e} P_e|_{S_D}\{\vec{J}_{eD}\} + \hat{n}_D \times \left[-C_e|_{S_H}\{\vec{M}_{eH}\} + \frac{j}{\omega\varepsilon_e} F_e|_{S_H}\{\vec{J}_{eH}\} \right] \\ &= -(I - M_e)|_{S_D}\{\vec{M}_{inc} + \vec{M}_{ref}\} - \frac{j}{\omega\varepsilon_e} P_e|_{S_D}\{\vec{J}_{inc} + \vec{J}_{ref}\}\end{aligned} \quad (5.19)$$

$$\begin{aligned}&(I - M_e)|_{S_D}\{\vec{J}_{eD}\} - \frac{j}{\omega\mu_e} P_e|_{S_D}\{M_{eD}\} + \hat{n}_D \times \left[-C_e|_{S_H}\{\vec{J}_{eH}\} - \frac{j}{\omega\mu_e} F_e|_{S_H}\{\vec{M}_{eH}\} \right] \\ &= -(I - M_e)|_{S_D}\{\vec{J}_{inc} + \vec{J}_{ref}\} + \frac{j}{\omega\mu_e} P_e|_{S_D}\{\vec{M}_{inc} + \vec{M}_{ref}\}\end{aligned} \quad (5.20)$$

$$\begin{aligned}&(I + M_D)|_{S_D}\{\vec{M}_{eD}\} - \frac{j}{\omega\varepsilon_D} P_D|_{S_D}\{\vec{J}_{eD}\} \\ &= -(I + M_D)|_{S_D}\{\vec{M}_{inc} + \vec{M}_{ref}\} + \frac{j}{\omega\varepsilon_D} P_D|_{S_D}\{\vec{J}_{inc} + \vec{J}_{ref}\}\end{aligned} \quad (5.21)$$

$$\begin{aligned}&(I + M_D)|_{S_D}\{\vec{J}_{eD}\} + \frac{j}{\omega\mu_D} P_D|_{S_D}\{\vec{M}_{eD}\} \\ &= -(I + M_D)|_{S_D}\{\vec{J}_{inc} + \vec{J}_{ref}\} - \frac{j}{\omega\mu_D} P_D|_{S_D}\{\vec{M}_{inc} + \vec{M}_{ref}\}\end{aligned} \quad (5.22)$$

$$(I+M_H)|_{S_H}\{\bar{M}_{eH}\}-\frac{j}{\omega\varepsilon_H}P_H|_{S_H}\{\bar{J}_{eH}\}=0 \tag{5.23}$$

$$(I+M_H)|_{S_H}\{\bar{J}_{eH}\}+\frac{j}{\omega\mu_H}P_H|_{S_H}\{\bar{M}_{eH}\}=0 \tag{5.24}$$

Numerical simulations performed thus far have demonstrated a good match for the problem where the lower half-space is characterized by the external region material properties (two material problem). This problem, in essence, is the single scatterer problem. For problems where the lower half-space is characterized by materials other than either the external region or the particle (three material problem), tests have shown that a bigger discretization surface S_H is needed to obtain a more accurate solution. However, because of memory capacity limitations of locally available computer resources, the numerical test for the three material problem is being postponed until more computing resources become available.

CHAPTER 6. NUMERICAL IMPLEMENTATION OF BOUNDARY INTEGRAL EQUATIONS

Regularization methods

Boundary integral equations (BIEs) with singular kernel functions are extensively used to solve many scattering problems with acoustic waves, elastodynamic waves, and electromagnetic waves. However, the numerical implementation often presents some serious difficulties when the integral is singular. The severity of the problem depends primarily on the order of the singularity in the kernel function. In this chapter, a procedure is developed analytically reducing the order of singularity to one that is numerically stable. This process for reducing the order of singularity is referred to as regularization [57] [59].

Until recently, most BIEs commonly used involve singular integrals that were at most strongly singular (Cauchy type singularity). These BIEs are commonly called conventional boundary integral equations (CBIEs). When solving electromagnetic scattering problems, the use of CBIEs typically results in the problem of multiplicity of solutions at certain resonant frequencies. An alternative method uses a set of integral equations which involves the gradient of the CBIEs. These integral equations, with hypersingular kernels, are commonly called the hypersingular boundary integral equations (HBIEs). The HBIE method for solving the electromagnetic scattering problems also results in nonunique solutions at certain resonant frequencies. One technique for eliminating this problem is to take the linear combination of the CBIE and the HBIE, such that the system of equations has an unique solution at all frequencies [56].

A representative singular integral in a boundary integral equation can be expressed as

$$I(p) = \int_S k(p,q)\, u(q)\, dS_q \tag{6.1}$$

where k(p,q) is the singular kernel function, u(q) is a density function, and p, q are points on the integration surface S where $R \equiv |p-q|$. The density function is usually the unknown surface variable to be solved. In the case of electromagnetic scattering, u(q) is a vector variable representing either the electric current density or the magnetic current density, For a three dimensional problem, the kernel function is hypersingular, strongly (Cauchy) singular, or weakly singular if it is of $O\left(\frac{1}{R^3}\right)$, $O\left(\frac{1}{R^2}\right)$, or $O\left(\frac{1}{R}\right)$, respectively. In order to obtain a numerically stable result, the order of the singular integrals should be reduced to a weakly singular one [60].

For integrals which are weakly singular, the singularity can be removed by transforming the coordinate system to a polar coordinate system. Gaussian quadrature is then used to compute the nonsingular integrals [57] [58] [59]. The numerical evaluation of a BIE is straightforward: The surface of integration is divided into either flat or curvilinear surface elements covering the entire surface S.

$$S = \sum_{i=1}^{m} s_i \tag{6.2}$$

where there is a total of m surface patches. The numerical integration is done by fixing the observation point p and summing the integration over each of the discretized surface patches. The variable q is typically used to represent the integration point or the source point. For cases where p and q do not fall on the same element, the integral is nonsingular (regular) and can be easily evaluated. For cases where p and q both reside on the same element, the integral becomes singular and regularization steps should be taken before evaluation. Therefore equation (6.1) can be written as

$$I(p) = \int_{S-\Delta_m} k(p,q)\,u(q)\,dS_q + \int_{\Delta_m} k(p,q)\,u(q)\,dS_q \qquad p \in \Delta_m \tag{6.3}$$

where the first integral on the right hand side is regular and can be evaluated without any difficulty. The second integral on the right hand side is, however, a singular one where both p and q fall on the element Δ_m. The second integral can be evaluated by transforming the local

coordinate system from Cartesian to a polar system. Consequently, the element Δ_m of area $d\xi$ in the local ξ space (to be described later) becomes $\rho d\rho d\phi$. The ρ in the integrand is of O(R) and for sufficiently small R allows the integral to be evaluated using the Gaussian quadrature scheme.

For strongly singular integrals, two different analytical regularization approaches can be taken to obtain weakly singular integral(s). The weakly singular integral(s) can then be evaluated using a coordinate transformation as described earlier. These ideas can be applied later to the hypersingular integrals as well. The first approach is to rewrite equation (6.1) so that the density function can be isolated from the strongly singular integral. This is done by adding and subtracting the first term of a Taylor's series expansion of the density function about the singular point p which gives

$$I(p) = \lim_{P \to p} \left\{ \int_S k(P,q)[u(q) - u(p)]\, dS_q + u(p) \int_S k(P,q)\, dS_q \right\} \tag{6.4}$$

Here, the density function, or the surface current density, is assumed to be at least Hölder one continuous [34] where the Hölder condition is stronger than continuity but weaker than differentiability. Consequently, the term $[u(q) - u(p)]$ is of at least O(R) so that the first integral is now a weakly singular integral and can be computed as before. The second strongly singular integral does not have the density function as part of the integrand and therefore, can be converted to a weakly singular or regular integral through one of two ways: Simple solutions [61] or the application of Stokes theorem [60]. The Stokes theorem approach can be used for both open and close surfaces while the simple solutions method generally requires a closed surface. The second regularization technique is to perform an integration by parts which transfers one of the gradients in the kernel function on to the density function

$$\begin{aligned} I(p) &= \lim_{P \to p} \left\{ \int_S k(P,q) u(q)\, dS_q \right\} \\ &= \lim_{P \to p} \left\{ \int_S M(P,q) \frac{\partial u(q)}{\partial S_k(q)}\, dS_q + \oint_c N(P,q) u(q)\, dl \right\} \end{aligned}$$

$$= \left\{ \int_S M(p,q) \frac{\partial u(q)}{\partial S_k(q)} dS_q + \oint_c N(p,q) u(q) dl \right\} \tag{6.5}$$

where the second integral is a closed line integral enclosing the surface S and the new kernel function M(p,q) is weakly singular, and the density function $\frac{\partial u(q)}{\partial S_k(q)}$ is the tangential gradient of u(q). The line integral is at most weakly singular for an open surface and is zero for a closed surface.

The ideas used to regularize strongly singular integrals can also be extended for regularizing hypersingular integrals. For instance, consider a three dimensional problem where u(q) satisfies the Laplace equation with an enclosed surface S and the appropriate boundary conditions, u(q) and $\frac{\partial u(q)}{\partial n(q)}$ defined on the surface S. The governing interior integral equation for this problem is

$$u(P) = \int_S \left[\overline{G}(P,q) \frac{\partial u(q)}{\partial n(q)} - \frac{\partial \overline{G}(P,q)}{\partial n(q)} u(q) \right] dS_q \tag{6.6}$$

where $\overline{G}$ is the static Greens function and n(q) is an outward directed unit normal at q and P is a point interior to S. The gradient of equation (6.6) at P is also an interior representation

$$\frac{\partial u(P)}{\partial P_r} = \int_S \left[\frac{\partial \overline{G}(P,q)}{\partial P_r} \frac{\partial u(q)}{\partial n(q)} - \frac{\partial^2 \overline{G}(P,q)}{\partial P_r \partial n(q)} u(q) \right] dS_q \tag{6.7}$$

where r represents the r^{th} component in indices notation. As the interior point P approaches the surface S, P $\rightarrow$ p, equation (6.7) becomes a hypersingular integral equation

$$\frac{\partial u(p)}{\partial P_r} = \lim_{P \rightarrow p} \left\{ \int_S \left[\frac{\partial \overline{G}(P,q)}{\partial P_r} \frac{\partial u(q)}{\partial n(q)} - \frac{\partial^2 \overline{G}(P,q)}{\partial P_r \partial n(q)} u(q) \right] dS_q \right\} \tag{6.8}$$

There are two basic approaches for regularizing a hypersingular integral into a weakly singular one. The first approach is to isolate the singularity where the first two terms of the

Taylor's expansion of the density function are subtracted and added back. This moves the density function outside the hypersingular and strongly singular integrals, and the order of these integrals is then reduced to weakly singular by employing either the simple solution method, or the Stokes theorem method. Specifically, equation (6.8) can be written using Einstein's notation as

$$\begin{aligned}\frac{\partial u(p)}{\partial P_r} = \lim_{P \to p} \Bigg\{ & \int_S \left[\frac{\partial \overline{G}(P,q)}{\partial P_r} \left[\frac{\partial u(q)}{\partial n(q)} - \frac{\partial u(p)}{\partial n(p)} \right] \right] dS_q \\ & + \frac{\partial u(p)}{\partial n(p)} \int_S \frac{\partial \overline{G}(P,q)}{\partial P_r} \, dS_q \\ & - \int_S \frac{\partial^2 \overline{G}(P,q)}{\partial P_r \, \partial n(q)} \left[u(q) - u(p) - u_{,j}(p)(q_j - p_j) \right] u(q) \, dS_q \\ & - u(p) \int_S \frac{\partial^2 \overline{G}(P,q)}{\partial P_r \, \partial n(q)} \, dS_q \\ & - u_{,j}(p) \int_S \frac{\partial^2 \overline{G}(P,q)}{\partial P_r \, \partial n(q)} (q_j - p_j) \, dS_q \Bigg\} \end{aligned} \tag{6.9}$$

Note that the first and third integral on the right hand side are weakly singular because $\left| \frac{\partial u(q)}{\partial n(q)} - \frac{\partial u(p)}{\partial n(p)} \right|$ is of O(R) and $\left| u(q) - u(p) - u_{,j}(p)(q_j - p_j) \right|$ is of $O(R^2)$. The remaining integrals are either strongly singular or hypersingular. But since the density function is isolated from the integrand, they can be regularized to weakly singular using either the Stokes theorem or a simple solution approach.

It should be emphasized that although the regularization technique stabilizes the numerical computation of singular integrals, it is not absolutely necessary for obtaining a numerical solution. In cases where the regularization procedure is difficult to perform or does not exist, singular integrals can be computed directly. This can be done by interpreting the limit of either the exterior or the interior representation as a finite part (FP) (for hypersingular integrals) or a CPV (for strongly singular integrals) [60]. Invoking the definition of the FP or the CPV and using coordinate transformation, the integral can be computed directly [62].

Regularization of single body BIEs

As mentioned in Chapter 4, the governing BIEs for the single body scattering problem contain both strongly singular as well as hypersingular kernel functions. The approach taken to regularize these integrals is the isolation technique described earlier. The regularization of the governing BIEs can be done either locally or globally. In the global regularization approach, the subtraction and addition of the expansion terms is done prior to taking the limit of the observation point approaching the surface S. The overall effect is the same as the local regularization approach where the limit is taken before the subtraction and addition of the expansion terms. It should be emphasized that in both approaches, in order to regularize the hypersingular integrals, typically two-term addition and subtraction is needed. However, in this dissertation, a special linear combination formulation is adopted, namely the Müller formulation, which analytically cancels out the high order singularity contained in the hypersingular terms. Consequently, all regularizations performed in this dissertation involve only strongly singular integrals. The global regularization is discussed first.

Global regularization approach

Prior to taking the limit P $\rightarrow$ p, the governing BIEs used are the Stratton-Chu representation of the scattered fields

$$\hat{n}(P)\times\left[C_e\left\{-\vec{M}(q)\right\}+\frac{j}{\omega\varepsilon_e}F_e\left\{\vec{J}(q)\right\}\right]=2\hat{n}(P)\times\vec{E}_e(P) \tag{6.10}$$

$$\hat{n}(P)\times\left[C_e\left\{\vec{J}(q)\right\}-\frac{j}{\omega\mu_e}F_e\left\{-\vec{M}(q)\right\}\right]=2\hat{n}(P)\times\vec{H}_e(P) \tag{6.11}$$

$$\hat{n}(P)\times\left[C_i\left\{-\vec{M}_i(q)\right\}+\frac{j}{\omega\varepsilon_i}F_i\left\{\vec{J}_i(q)\right\}\right]=-2\hat{n}(P)\times\vec{E}_i(P) \tag{6.12}$$

$$\hat{n}(P)\times\left[C_i\left\{\vec{J}_i(q)\right\}-\frac{j}{\omega\mu_i}F_i\left\{-\vec{M}_i(q)\right\}\right]=-2\hat{n}(P)\times\vec{H}_i(P) \tag{6.13}$$

where for equations (6.10) and (6.11) P is a point in the external region e and for equations (6.12) and (6.13) P is a point in the internal region i, and q is a source point on the surface S in both cases. Starting with equation (6.10) which can be written in the long form as

$$2\hat{n}(P)\times\vec{E}_e(P) = -\hat{n}(P)\times\nabla_P\times\int_S \vec{M}(q)G_e(P,q)dS_q + \frac{j}{\omega\varepsilon_e}\hat{n}(P)\times\nabla_P\times\nabla_P\times\int_S \vec{J}(q)G_e(P,q)dS_q \tag{6.14}$$

which in index notation is

$$\begin{aligned} 2\in_{ijk} n_j(P)E_{ek}(P) = &\int_S \frac{\partial G_e(P,q)}{\partial x_i(q)}\left[n_j(P)M_j(q)\right]dS_q \\ &-\int_S \frac{\partial G_e(P,q)}{\partial x_j(q)}\left[n_j(P)M_i(q)\right]dS_q \\ &+\in_{ijk}\frac{j}{\omega\varepsilon_e}n_j(P)\int_S \frac{\partial^2 G_e(P,q)}{\partial x_m(q)\partial x_k(q)}J_m(q)dS_q \\ &+\in_{ijk} j\mu_e\omega n_j(P)\int_S G_e(P,q)J_k(q)dS_q \end{aligned} \tag{6.15}$$

where $\in_{ijk}$ is the permutation constant and by using the Helmholtz's identity

$$\nabla_P\times\nabla_P\times(\vec{a}) = \nabla_P(\nabla_P\cdot\vec{a}) + k^2\vec{a} \tag{6.16}$$

where $k^2 = \omega^2\mu\varepsilon$. The first two integrals on the right hand side of equation (6.15) are strongly singular and can be regularized using the isolation technique followed by a simple application of identities from simple solutions. The last integral on the right hand side of equation (6.15) is weakly singular and therefore, can be computed directly using a local coordinate transformation. The third integral, however, is hypersingular and is more difficult to compute. But, with the use of the Müller linear combination formulation described earlier, it can be shown that the resulting integral is only weakly singular. Therefore, by subtracting and adding the first term of the Taylor series expansion of the density function and taking the limit as $P \rightarrow p$ on S and adding the incident wave in the exterior region and applying the boundary condition, equation (6.15) becomes

$$
\begin{aligned}
-2M_i(p) = {} & n_j(p)\int_S \frac{\partial G_e(p,q)}{\partial x_i(q)}\left[M_j(q)-M_j(p)\right]dS_q \\
& + n_j(p)\,M_j(p)\int_S \frac{\partial G_e(p,q)}{\partial x_i(q)}dS_q \\
& - n_j(p)\int_S \frac{\partial G_e(p,q)}{\partial x_j(q)}\left[M_i(q)-M_i(p)\right]dS_q \\
& + M_i(p)\int_S \left[\frac{\partial \overline{G}(p,q)}{\partial x_j(q)}n_j(q) - \frac{\partial G_e(p,q)}{\partial x_j(q)}n_j(p)\right]dS_q \\
& - M_i(p)\int_S \frac{\partial \overline{G}(p,q)}{\partial x_j(q)}n_j(q)\,dS_q \\
& + \in_{ijk}\frac{j}{\omega\varepsilon_e}n_j(p)\int_S \frac{\partial^2 G_e(p,q)}{\partial x_m(q)\partial x_k(q)}J_m(q)\,dS_q \\
& + \in_{ijk} j\mu_e\omega\, n_j(p)\int_S G_e(p,q)\,J_k(q)\,dS_q \\
& - 2M_i^{inc}(p)
\end{aligned}
\tag{6.17}
$$

Similarly, equations (6.11) through (6.13) can also be regularized as

$$
\begin{aligned}
2J_i(p) = {} & -n_j(p)\int_S \frac{\partial G_e(p,q)}{\partial x_i(q)}\left[J_j(q)-J_j(p)\right]dS_q \\
& - n_j(p)\,J_j(p)\int_S \frac{\partial G_e(p,q)}{\partial x_i(q)}dS_q \\
& + n_j(p)\int_S \frac{\partial G_e(p,q)}{\partial x_j(q)}\left[J_i(q)-J_i(p)\right]dS_q \\
& - J_i(p)\int_S \left[\frac{\partial \overline{G}(p,q)}{\partial x_j(q)}n_j(q) - \frac{\partial G_e(p,q)}{\partial x_j(q)}n_j(p)\right]dS_q \\
& + J_i(p)\int_S \frac{\partial \overline{G}(p,q)}{\partial x_j(q)}n_j(q)\,dS_q \\
& + \in_{ijk}\frac{j}{\omega\mu_e}n_j(p)\int_S \frac{\partial^2 G_e(p,q)}{\partial x_m(q)\partial x_k(q)}M_m(q)\,dS_q \\
& + \in_{ijk} j\varepsilon_e\omega\, n_j(p)\int_S G_e(p,q)\,M_k(q)\,dS_q \\
& + 2\mathrm{J}_{\mathrm{i}}^{\mathrm{inc}}(\mathrm{p})
\end{aligned}
\tag{6.18}
$$

$$
2M_i(p) = n_j(p)\int_S \frac{\partial G_i(p,q)}{\partial x_i(q)}\left[M_j(q)-M_j(p)\right]dS_q
$$

$$
\begin{aligned}
&+n_j(p)M_j(p)\int_S \frac{\partial G_i(p,q)}{\partial x_i(q)}dS_q \\
&-n_j(p)\int_S \frac{\partial G_i(p,q)}{\partial x_j(q)}\left[M_i(q)-M_i(p)\right]dS_q \\
&+M_i(p)\int_S \left[\frac{\partial \overline{G}(p,q)}{\partial x_j(q)}n_j(q)-\frac{\partial G_i(p,q)}{\partial x_j(q)}n_j(p)\right]dS_q \\
&-M_i(p)\int_S \frac{\partial \overline{G}(p,q)}{\partial x_j(q)}n_j(q)dS_q \\
&+\in_{ijk}\frac{j}{\omega\varepsilon_i}n_j(p)\int_S \frac{\partial^2 G_i(p,q)}{\partial x_m(q)\partial x_k(q)}J_m(q)dS_q \\
&+\in_{ijk} j\mu_i\omega n_j(p)\int_S G_i(p,q)J_k(q)dS_q
\end{aligned}
\tag{6.19}
$$

$$
\begin{aligned}
-2J_i(p) = &-n_j(p)\int_S \frac{\partial G_i(p,q)}{\partial x_i(q)}\left[J_j(q)-J_j(p)\right]dS_q \\
&-n_j(p)J_j(p)\int_S \frac{\partial G_i(p,q)}{\partial x_i(q)}dS_q \\
&+n_j(p)\int_S \frac{\partial G_i(p,q)}{\partial x_j(q)}\left[J_i(q)-J_i(p)\right]dS_q \\
&-J_i(p)\int_S \left[\frac{\partial \overline{G}(p,q)}{\partial x_j(q)}n_j(q)-\frac{\partial G_i(p,q)}{\partial x_j(q)}n_j(p)\right]dS_q \\
&+J_i(p)\int_S \frac{\partial \overline{G}(p,q)}{\partial x_j(q)}n_j(q)dS_q \\
&+\in_{ijk}\frac{j}{\omega\mu_i}n_j(p)\int_S \frac{\partial^2 G_i(p,q)}{\partial x_m(q)\partial x_k(q)}M_m(q)dS_q \\
&+\in_{ijk} j\varepsilon_i\omega n_j(p)\int_S G_i(p,q)M_k(q)dS_q
\end{aligned}
\tag{6.20}
$$

where $\overline{G}$ is the static Greens function and $\in_{ijk}$ is the permutation constant. Now, the second term on the right hand side of equations (6.17) through (6.20) are equal to zero since the surface currents have only tangential components. Therefore, taking the scalar product with the unit normal will result in zero. The fifth term of equations (6.17) through (6.20) is evaluated as

$$
\int_S \frac{\partial \overline{G}(P,q)}{\partial x_j(q)}n_j(q)\,dS_q = \int_S \frac{\partial \overline{G}(P,q)}{\partial n(q)}\,dS_q = \begin{cases} -2 & \text{P in region i} \\ 0 & \text{P in region e} \end{cases}
\tag{6.21}
$$

The final regularized form of the governing BIEs is

$$
\begin{aligned}
-2M_i(p) = {} & n_j(p)\int_S \frac{\partial G_e(p,q)}{\partial x_i(q)}\left[M_j(q)-M_j(p)\right]dS_q \\
& -n_j(p)\int_S \frac{\partial G_e(p,q)}{\partial x_j(q)}\left[M_i(q)-M_i(p)\right]dS_q \\
& +M_i(p)\int_S \left[\frac{\partial \overline{G}(p,q)}{\partial x_j(q)}n_j(q)-\frac{\partial G_e(p,q)}{\partial x_j(q)}n_j(p)\right]dS_q \\
& +\in_{ijk}\frac{j}{\omega\varepsilon_e}n_j(p)\int_S \frac{\partial^2 G_e(p,q)}{\partial x_m(q)\partial x_k(q)}J_m(q)\,dS_q \\
& +\in_{ijk} j\mu_e\omega\, n_j(p)\int_S G_e(p,q)\,J_k(q)\,dS_q \\
& -2\mathrm{M}_\mathrm{i}^{\mathrm{inc}}(\mathrm{p})
\end{aligned}
\tag{6.22}
$$

Similarly, equations (6.11) through (6.13) can also be regularized as

$$
\begin{aligned}
2J_i(p) = {} & -n_j(p)\int_S \frac{\partial G_i(p,q)}{\partial x_i(q)}\left[J_j(q)-J_j(p)\right]dS_q \\
& +n_j(p)\int_S \frac{\partial G_e(p,q)}{\partial x_j(q)}\left[J_i(q)-J_i(p)\right]dS_q \\
& -J_i(p)\int_S \left[\frac{\partial \overline{G}(p,q)}{\partial x_j(q)}n_j(q)-\frac{\partial G_e(p,q)}{\partial x_j(q)}n_j(p)\right]dS_q \\
& +\in_{ijk}\frac{j}{\omega\mu_e}n_j(p)\int_S \frac{\partial^2 G_e(p,q)}{\partial x_m(q)\partial x_k(q)}M_m(q)\,dS_q \\
& +\in_{ijk} j\varepsilon_e\omega\, n_j(p)\int_S G_e(p,q)\,M_k(q)\,dS_q \\
& +2\mathrm{J}_\mathrm{i}^{\mathrm{inc}}(\mathrm{p})
\end{aligned}
\tag{6.23}
$$

$$
\begin{aligned}
0 = {} & n_j(p)\int_S \frac{\partial G_i(p,q)}{\partial x_i(q)}\left[M_j(q)-M_j(p)\right]dS_q \\
& -n_j(p)\int_S \frac{\partial G_i(p,q)}{\partial x_j(q)}\left[M_i(q)-M_i(p)\right]dS_q \\
& +M_i(p)\int_S \left[\frac{\partial \overline{G}(p,q)}{\partial x_j(q)}n_j(q)-\frac{\partial G_i(p,q)}{\partial x_j(q)}n_j(p)\right]dS_q
\end{aligned}
$$

$$+\in_{ijk}\frac{j}{\omega\varepsilon_i}n_j(p)\int_S\frac{\partial^2 G_i(p,q)}{\partial x_m(q)\partial x_k(q)}J_m(q)\,dS_q$$
$$+\in_{ijk} j\mu_i\omega\, n_j(P)\int_S G_i(P,q)J_k(q)\,dS_q \qquad (6.24)$$

$$0=-n_j(p)\int_S\frac{\partial G_i(p,q)}{\partial x_i(q)}\left[J_j(q)-J_j(p)\right]dS_q$$
$$+n_j(p)\int_S\frac{\partial G_i(p,q)}{\partial x_j(q)}\left[J_i(q)-J_i(p)\right]dS_q$$
$$-J_i(p)\int_S\left[\frac{\partial\overline{G}(p,q)}{\partial x_j(q)}n_j(q)-\frac{\partial G_i(p,q)}{\partial x_j(q)}n_j(p)\right]dS_q$$
$$+\in_{ijk}\frac{j}{\omega\mu_i}n_j(p)\int_S\frac{\partial^2 G_i(p,q)}{\partial x_m(q)\partial x_k(q)}M_m(q)\,dS_q$$
$$+\in_{ijk} j\varepsilon_i\omega\, n_j(p)\int_S G_i(p,q)M_k(q)\,dS_q \qquad (6.25)$$

The fourth term in equations (6.22) through (6.25) contains a hypersingular kernel function which can be reduced to a weakly singular one by using the Müller combined field formulation. This can be seen by expanding the Green's function using Taylor's series and taking the second derivative of the series. After taking the linear combination and canceling terms, it can be shown that the highest order of singularity remaining is a weak one. Consequently, the resulting governing BIEs can be computed numerically through the use of a coordinate transformation.

Local regularization approach

In the local regularization approach, the limit of $P\rightarrow p$ is taken prior to the addition and subtraction of Taylor series expansion terms. Consequently, equations (3.48) through (3.51) constitute the starting point for regularization. Writing equation (3.48) in index form

$$-M_i(P)=\int_S\frac{\partial G_e(P,q)}{\partial x_i(q)}\left[n_j(P)M_j(q)\right]dS_q$$
$$-\int_S\frac{\partial G_e(P,q)}{\partial x_j(q)}\left[n_j(P)M_i(q)\right]dS_q$$
$$+\in_{ijk}\frac{j}{\omega\varepsilon_e}n_j(P)\int_S\frac{\partial^2 G_e(P,q)}{\partial x_m(q)\partial x_k(q)}J_m(q)\,dS_q$$

$$+\in_{ijk} j\mu_e \omega n_j(P)\int_S G_e(P,q)J_k(q)dS_q$$
$$-2M_i^{inc}(P) \qquad (6.26)$$

Since the singularity problem only occurs in the case where p and q fall on the same element, the addition and subtraction of expansion terms only need to take place on an element by element basis. Therefore, if ΔS is the element for which both p and q reside, equation (6.26) can be regularized to be

$$\begin{aligned}
-M_i(p) = &\int_{S-\Delta S} \frac{\partial G_e(p,q)}{\partial x_i(q)}\left[n_j(p)M_j(q)\right]dS_q \\
&-\int_{S-\Delta S} \frac{\partial G_e(p,q)}{\partial x_j(q)}\left[n_j(p)M_i(q)\right]dS_q \\
&+\in_{ijk} \frac{j}{\omega\varepsilon_e} n_j(p)\int_S \frac{\partial^2 G_e(p,q)}{\partial x_m(q)\partial x_k(q)} J_m(q)dS_q \\
&+\in_{ijk} j\mu_e\omega n_j(p)\int_S G_e(p,q)J_k(q)dS_q \\
&-2M_i^{inc}(p) \\
&+\int_{\Delta S} \frac{\partial G_e(p,q)}{\partial x_i(q)} n_j(p)\left[M_j(q)-M_j(p)\right]dS_q \\
&+\int_{\Delta S}\left[\frac{\partial \overline{G}(p,q)}{\partial n(q)}M_i(p)-\frac{\partial G_e(p,q)}{\partial x_j(q)}n_j(p)M_i(q)\right]dS_q \\
&-M_i(p)\int_{\Delta S}\frac{\partial \overline{G}(p,q)}{\partial n(q)}dS_q
\end{aligned} \qquad (6.27)$$

Similarly, the remaining three equations can be regularized in a same fashion

$$\begin{aligned}
-J_i(p) = &\int_{S-\Delta S} \frac{\partial G_e(p,q)}{\partial x_i(q)}\left[n_j(p)J_j(q)\right]dS_q \\
&-\int_{S-\Delta S} \frac{\partial G_e(p,q)}{\partial x_j(q)}\left[n_j(p)J_i(q)\right]dS_q \\
&-\in_{ijk} \frac{j}{\omega\mu_e} n_j(p)\int_S \frac{\partial^2 G_e(p,q)}{\partial x_m(q)\partial x_k(q)} M_m(q)dS_q \\
&-\in_{ijk} j\varepsilon_e\omega n_j(p)\int_S G_e(p,q)M_k(q)dS_q \\
&-2J_i^{inc}(p)
\end{aligned}$$

$$+\int_{\Delta S}\frac{\partial G_e(p,q)}{\partial x_i(q)}n_j(p)\left[J_j(q)-J_j(p)\right]dS_q$$
$$+\int_{\Delta S}\left[\frac{\partial \overline{G}(p,q)}{\partial n(q)}J_i(p)-\frac{\partial G_e(p,q)}{\partial x_j(q)}n_j(p)J_i(q)\right]dS_q$$
$$-J_i(p)\int_{\Delta S}\frac{\partial \overline{G}(p,q)}{\partial n(q)}dS_q \qquad (6.28)$$

$$-M_i(p)=\int_{S-\Delta S}\frac{\partial G_i(p,q)}{\partial x_i(q)}\left[n_j(p)M_j(q)\right]dS_q$$
$$-\int_{S-\Delta S}\frac{\partial G_i(p,q)}{\partial x_j(q)}\left[n_j(p)M_i(q)\right]dS_q$$
$$+\in_{ijk}\frac{j}{\omega\varepsilon_i}n_j(p)\int_S\frac{\partial^2 G_i(p,q)}{\partial x_m(q)\partial x_k(q)}J_m(q)dS_q$$
$$+\in_{ijk} j\mu_i\omega n_j(p)\int_S G_i(p,q)J_k(q)dS_q$$
$$+\int_{\Delta S}\frac{\partial G_i(p,q)}{\partial x_i(q)}n_j(p)\left[M_j(q)-M_j(p)\right]dS_q$$
$$+\int_{\Delta S}\left[\frac{\partial \overline{G}(p,q)}{\partial n(q)}M_i(p)-\frac{\partial G_i(p,q)}{\partial x_j(q)}n_j(p)M_i(q)\right]dS_q$$
$$-M_i(p)\int_{\Delta S}\frac{\partial \overline{G}(p,q)}{\partial n(q)}dS_q \qquad (6.29)$$

$$-J_i(p)=\int_{S-\Delta S}\frac{\partial G_i(p,q)}{\partial x_i(q)}\left[n_j(p)J_j(q)\right]dS_q$$
$$-\int_{S-\Delta S}\frac{\partial G_i(p,q)}{\partial x_j(q)}\left[n_j(p)J_i(q)\right]dS_q$$
$$-\in_{ijk}\frac{j}{\omega\mu_i}n_j(p)\int_S\frac{\partial^2 G_i(p,q)}{\partial x_m(q)\partial x_k(q)}M_m(q)dS_q$$
$$-\in_{ijk} j\varepsilon_i\omega n_j(p)\int_S G_i(p,q)M_k(q)dS_q$$
$$+\int_{\Delta S}\frac{\partial G_i(p,q)}{\partial x_i(q)}n_j(p)\left[J_j(q)-J_j(p)\right]dS_q$$
$$+\int_{\Delta S}\left[\frac{\partial \overline{G}(p,q)}{\partial n(q)}J_i(p)-\frac{\partial G_i(p,q)}{\partial x_j(q)}n_j(p)J_i(q)\right]dS_q$$
$$-J_i(p)\int_{\Delta S}\frac{\partial \overline{G}(p,q)}{\partial n(q)}dS_q \qquad (6.30)$$

where the last term on the right hand side of equations (6.27) through (6.28) can be evaluated by converting it into a line integral and numerically calculating the line integral. The local regularization approach is generally preferred since it is easy to implement and it imposes no restrictions on the problem to consist of only closed surface boundaries, as it does with the global regularization technique.

Regularization of multiple body BIEs

The process of regularizing the governing BIEs for the multiple scattering problem is very similar to that of a single-body scattering problem. The regularized form obtained in equations (6.22) through (6.25) can be used for the multiple scattering problem. Note that the first two terms on the left hand side of equations (4.13) through (4.20) all take on the same form as BIEs for the single scattering problem shown in equations (3.48) through (3.51). As a result, the regularization steps are the same for the first two terms in equations (4.13) through (4.20). The remaining two terms in equations (4.13) through (4.16) do not need any regularization since the collocation point and the source point never reside on the same element surface. Consequently, the kernel functions in these integrals are always regular.

Regularization of scatterer near a half-space

The regularized form of the governing BIEs for the problem of a dielectric scatterer situated near the perfect conducting half-space and near the dielectric half-space is identical to that of the multiple scattering problem. This is because both problem are similar to the two-scatterer problem.

Boundary element method

The boundary element method {BEM} is a numerical method used to obtain solutions to BIEs. This method was first applied to the problem of evaluating the electrical capacitance of a cube in 1951 [63] and later popularized to the structural mechanics community in the 1960's and 1970's [64] [65]. At around the same time, a numerical method called the method of moments (MOM) was developed by Harrington which is closely linked to the BEM [66].

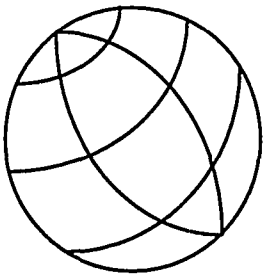

Figure 6.1 A typical discretized three dimensional surface

The concept of solving BIEs is not a difficult one. In the three dimensional BEM approach, the surface domain is discretized into patches of surface elements covering the entire boundary surface. The shapes of the elements are usually either quadrilateral or triangular mainly for the purpose of directly using the Gaussian quadrature integration method. A typical discretized surface is shown in Figure 6.1. Within each element, there are a fixed number of nodes residing at various locations. Two types of elements are defined depending on the location of the nodes. Nonconforming elements have their nodes located just inside the element edges so that adjacent elements do not share nodes. On the other hand, conforming elements have their nodes located right on the element edges and are shared by the adjacent elements. Each type of element has its own advantages and disadvantages and these will be described later. The elements can be further divided into either planar elements or curvilinear elements. Typically, for a complex shaped object, it requires more planar elements than curvilinear elements to cover the entire surface. However, for curvilinear elements the shape functions used for interpolating the unknowns are higher order polynomials, thus, more expensive to compute. Some typical conforming planar and curvilinear quadrilateral elements are shown in Figure 6.2 and nonconforming planar and curvilinear triangular elements are shown in Figure 6.3.

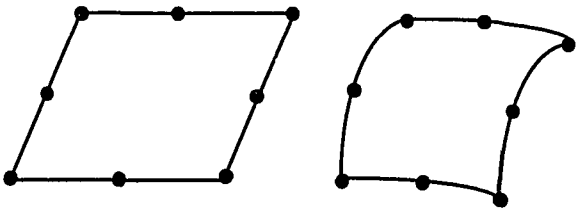

Figure 6.2 Different types of comforming quadrilateral elements

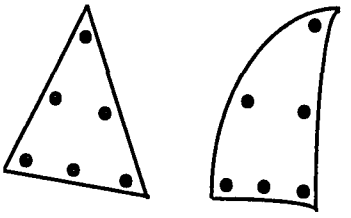

Figure 6.3 Different types of nonconforming triangular elements

The governing BIEs used for the electromagnetic scattering problem contain both strongly singular and hypersingular kernel functions. Theory imposes a C^1 smoothness requirement on the density function of the HBIEs. The conforming elements, however, only establish C^0 continuity at the nodes, and therefore, are not suitable for HBIEs. On the other hand, because adjacent elements do not share nodes, the gradients of the density functions on the nonconforming elements are always unique, and therefore, enforce the C^1 continuity requirements of the HBIEs [67]. In the special case of Müller field formulation where the hypersingular kernel function is reduced to a weakly singular one, conforming elements can also be used. Nevertheless, in order to keep the computer program developed for this research general enough so that all formulations can be used, the nonconforming elements are adopted for discretization. The tradeoff is that the use of nonconforming elements typically increases the size of the system to be solved. In general, for an m element system, there are

approximately 7m nodes for the nonconforming elements and in contrast to 3m nodes for the conforming elements. However, it should be noted that for a given problem, in order to achieve a comparable level of accuracy, it usually requires about 1.5 - 2 times more conforming elements than nonconforming elements to cover the same surface. This results in an increase of the size of the system for conforming elements to 4.5m - 6m nodes in contrast to 7m nodes for nonconforming elements.

With the BEM, the unknown surface density function on an element is approximated by expanding (or interpolating) a set of basis functions defined on each of the nodes on that element. Specifically,

$$J_m(\xi) = \sum_{\alpha} N_\alpha(\xi) J_{m\alpha} \tag{6.31}$$

where m denotes the m^{th} component of the vector density function, α is the index of the nodes on an element (8 for quadrilaterals and 6 for triangulars), ξ is a local coordinate system defined on each element, N is the appropriate basis function or shape function, and $J_{m\alpha}$ is the current density function defined at each node. The geometrical location of any point on the element is approximated in the same manner

$$x_m(\xi) = \sum_{\alpha} N_\alpha(\xi) x_{m\alpha} \tag{6.32}$$

where N is a set of shape functions and $x_{m\alpha}$ is the m^{th} component of the node location in reference to the global coordinate system. If the same set of shape functions (M=N) is used for both the density function expansion and the geometrical expansion, then it is called an isoparametric formulation. For curvilinear elements, the typical set of shape functions used are

i) For quadrilateral elements

$$N_1(\xi) = \frac{1}{4}(\xi_1 + 1)(\xi_2 + 1)(\xi_1 + \xi_2 - 1)$$
$$N_2(\xi) = \frac{1}{4}(\xi_1 - 1)(\xi_2 + 1)(\xi_1 - \xi_2 + 1)$$

$$
\begin{aligned}
N_3(\xi) &= \frac{1}{4}(1-\xi_1)(\xi_2-1)(\xi_1+\xi_2+1) \\
N_4(\xi) &= \frac{1}{4}(\xi_1+1)(\xi_2-1)(\xi_1-\xi_2+1) \\
N_5(\xi) &= \frac{1}{2}(\xi_1+1)(1-\xi_2^2) \\
N_6(\xi) &= \frac{1}{2}(\xi_2+1)(1-\xi_1^2) \\
N_7(\xi) &= \frac{1}{2}(\xi_1-1)(\xi_2^2-1) \\
N_8(\xi) &= \frac{1}{2}(1-\xi_2)(1-\xi_1^2)
\end{aligned}
\tag{6.33}
$$

ii) For triangular elements

$$
\begin{aligned}
N_1(\xi) &= \xi_1(2\xi_1-1) \\
N_2(\xi) &= \xi_2(2\xi_2-1) \\
N_3(\xi) &= \xi_3(2\xi_3-1) \\
N_4(\xi) &= 4\xi_1\xi_3 \\
N_5(\xi) &= 4\xi_1\xi_2 \\
N_6(\xi) &= 4\xi_2\xi_3
\end{aligned}
\tag{6.34}
$$

where ξ_1, ξ_2, ξ_3 is a local coordinate system on each element which will be defined later, and equation (6.32) is an implicit transformation in which a surface curvilinear element is mapped onto a parent plane square or plane equilateral triangle as shown in Figure 6.4. This mapping process is necessary when performing the numerical integration using the Gaussian quadrature method. ξ_3 for the triangular elements is not an independent component and can be derived from ξ_1 and ξ_2. After the transformation to the standard parent element, an established Gaussian quadrature method can be applied to integrate over the surface by specifying a fixed number of Gaussian points on the surface element. An empirical formula proposed by [58] is used to determine the number of Gaussian points needed on an element. The method uses a measure called the severity number to account for factors such as the distance between the collocating point and the integration element, the number of oscillations of the kernel functions over an element, and so forth.

Let $O(\xi_1\xi_2 n)$ be a local (curvilinear) coordinate system on a boundary element where ξ_1 and ξ_2 are along the two tangential directions and n is along the normal direction as shown in Figure 6.5. The transformation from the global Cartesian coordinate system to the local coordinate system is through the Jacobian matrix [68]

$$|JAC(\xi)| = \det \begin{bmatrix} \frac{\partial x_1}{\partial n} & \frac{\partial x_2}{\partial n} & \frac{\partial x_3}{\partial n} \\ \frac{\partial x_1}{\partial \xi_1} & \frac{\partial x_2}{\partial \xi_1} & \frac{\partial x_3}{\partial \xi_1} \\ \frac{\partial x_1}{\partial \xi_2} & \frac{\partial x_2}{\partial \xi_2} & \frac{\partial x_3}{\partial \xi_2} \end{bmatrix} \tag{6.35}$$

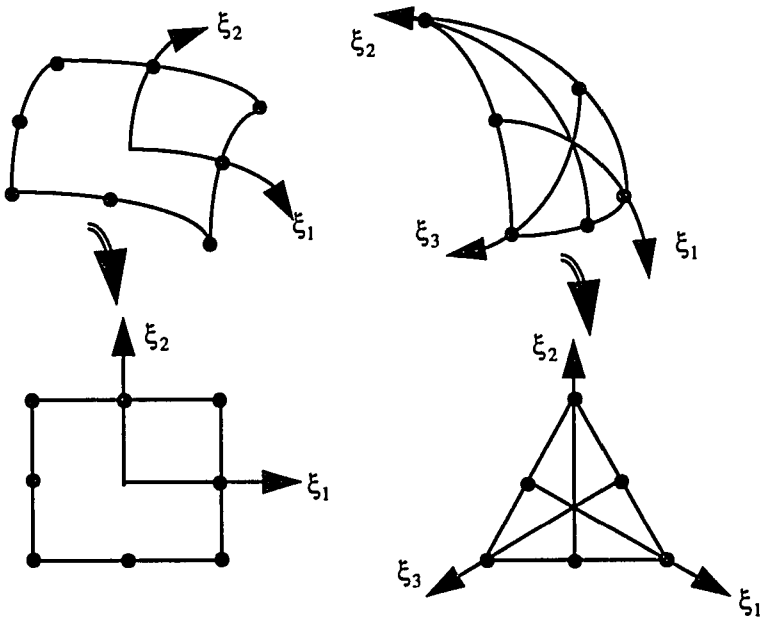

Figure 6.4 Curvilinear elements and their parent elements

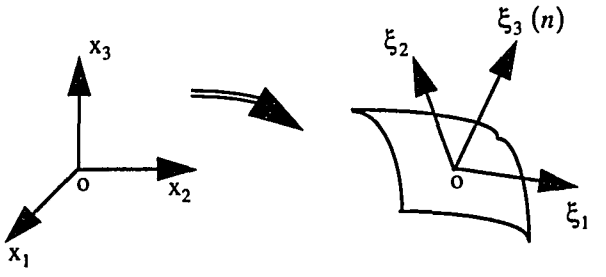

Figure 6.5 Coordinate transformation

and

$$\left|JAC(\xi)\right| = \frac{dS_q}{d\xi} \tag{6.36}$$

$$dS_q = \left|JAC(\xi)\right| d\xi \tag{6.37}$$

$$dS_q = \left|JAC(\xi)\right| d\xi_1\, d\xi_2 \tag{6.38}$$

Substituting equations (6.31), (6.32) and (6.38) into the Müller combination of equations (6.22) through (6.25) yields a set of algebraic equations with the unknowns being the surface current densities $(\vec{J}, \vec{M})$ defined at each of the discretization nodes

$$\begin{bmatrix} A_{11} & A_{12} \\ A_{21} & A_{22} \end{bmatrix} \begin{bmatrix} \vec{M} \\ \vec{J} \end{bmatrix} = \begin{bmatrix} 2\vec{M}_{inc} \\ 2\vec{J}_{inc} \end{bmatrix} \tag{6.39}$$

Solving this system of equations in the local coordinate system instead of the global coordinate system implies that the size of the matrix is 4N x 4N instead of 6N x 6N, where N is the total number of discretized nodes in the system. The reason why the local system is smaller than the global system is because the unknown density functions do not have any normal components in the local coordinate systems. For a realistic electromagnetic scattering

problem, considerable savings in matrix formation and solution time is achieved. Equation (6.39) can be solved using any standard linear solver routine. The solution obtained is the equivalent current densities on the surface of the scatterer. The scattered fields anywhere in space are calculated by substituting these current densities into equations (3.32) through (3.35). For this calculation, the kernel functions are no longer singular since the observation point P does not reside on the surface of integration.

CHAPTER 7. NUMERICAL SIMULATION RESULTS

The validity of the BEM program developed for this research is confirmed by comparing the BEM numerical results with those obtained using either analytical methods or other numerical methods. In all cases, the external region of the problems is assumed to be air. For the single-body scattering problem, The BEM solution is compared with the Mie theory with varying parameters such as the radius of the spherical scatterer and the refractive index of the scatterer to test the robustness of the BEM program. For the two-body scattering problem, the numerical BEM results are compared with those calculated in [42]. Once again, spheres with different sizes and different separation are compared. For the problem of a single scatterer near a perfect conducting half-plane, the solutions obtained using the BEM are compared with those presented in [69]. For the scattering problem of dielectric sphere near a dielectric half-space, the memory requirement needed to solve for the actual three material problem is beyond the capability of locally available computing resources. Therefore, this test is postponed until more computing resources become available. Instead, as a preliminary check, results from the special case of modeling the half-space as air are compared with the results obtained from Mie theory.

Single scatterer problem

The test configuration for the single scatterer problem is shown in Figure 7.1. The incident fields are unit-amplitude plane waves polarized in the y-direction. The scattered waves are calculated in the far-field region along the y-z plane as a function of the scattering angle θ, where $\theta = 0^o$ is in the forward scattering direction and $\theta = 180^o$ is in the backward scattering direction. The scattering cross sections are obtained from the calculated scattered fields. In figures 7.2 through 7.14, the y-axis represents the scattering cross section and the x-axis represents the scattering angle. Also, M denotes the number of elements used to discretize a particular problem, N represents the refractive index of the sphere which can be either a real (dielectric material) or a complex (lossy material) quantity, and ka represents a dimensionless quantity for the radius of the sphere.

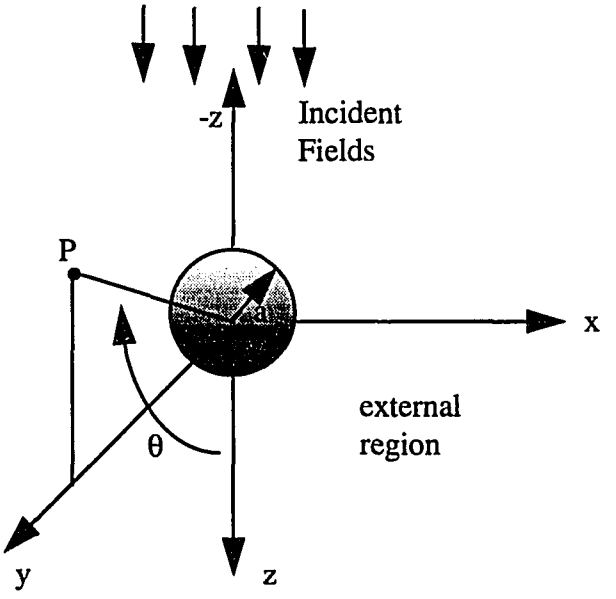

Figure 7.1 Single scatterer test configuration

Conforming elements

As explained in Chapter 6, in BEM, conforming elements can be used in problems which involve only strongly or weakly singular integrals. In this dissertation, although hypersingular integrals are present in the BIEs, but through the use of Müller formulation, these hypersingular integrals can be shown to be analytically reduced to weakly singular integrals. Consequently, conforming elements can be employed. Figures 7.2 through 7.5 illustrate some simulation results with varying refractive indices and the number of discretizing elements. The analytical results are obtained by using the Mie solution program found in [23]. As can be seen in the next section, in order to achieve a similar accuracy for a problem, it typically requires more conforming elements than nonconforming elements to cover the surface.

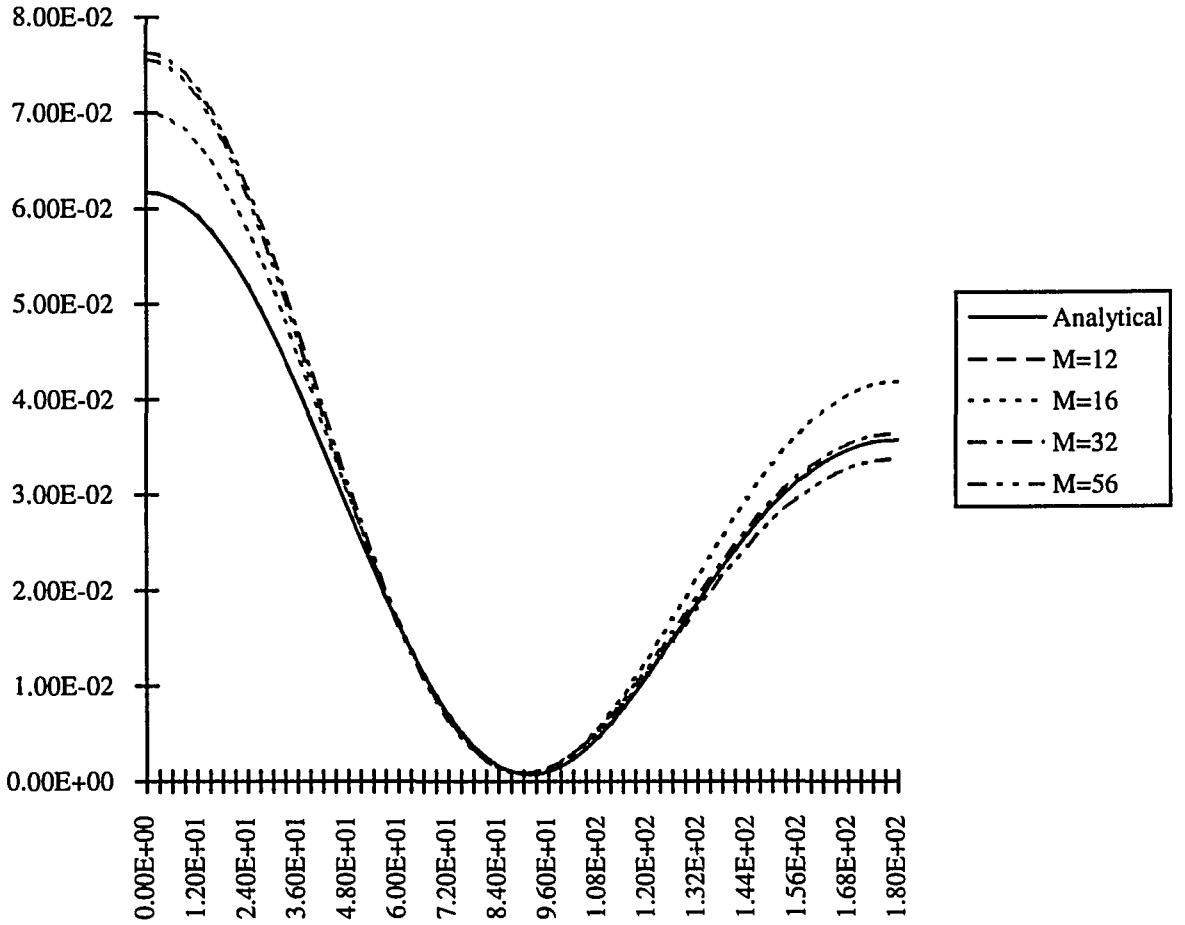

Figure 7.2 Conforming elements N = 1.2 ka = 1.0

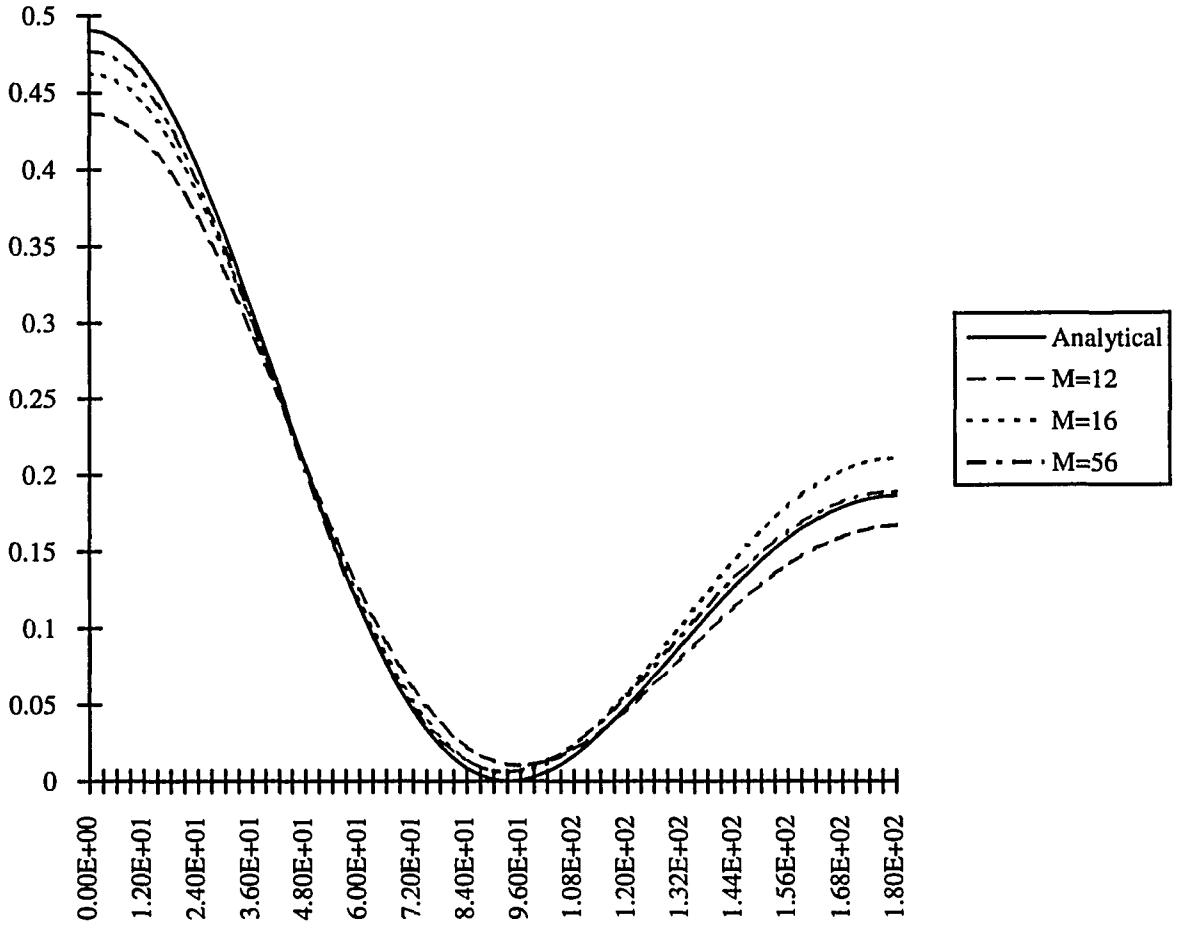

Figure 7.3 Conforming elements N = 1.5 ka = 1.0

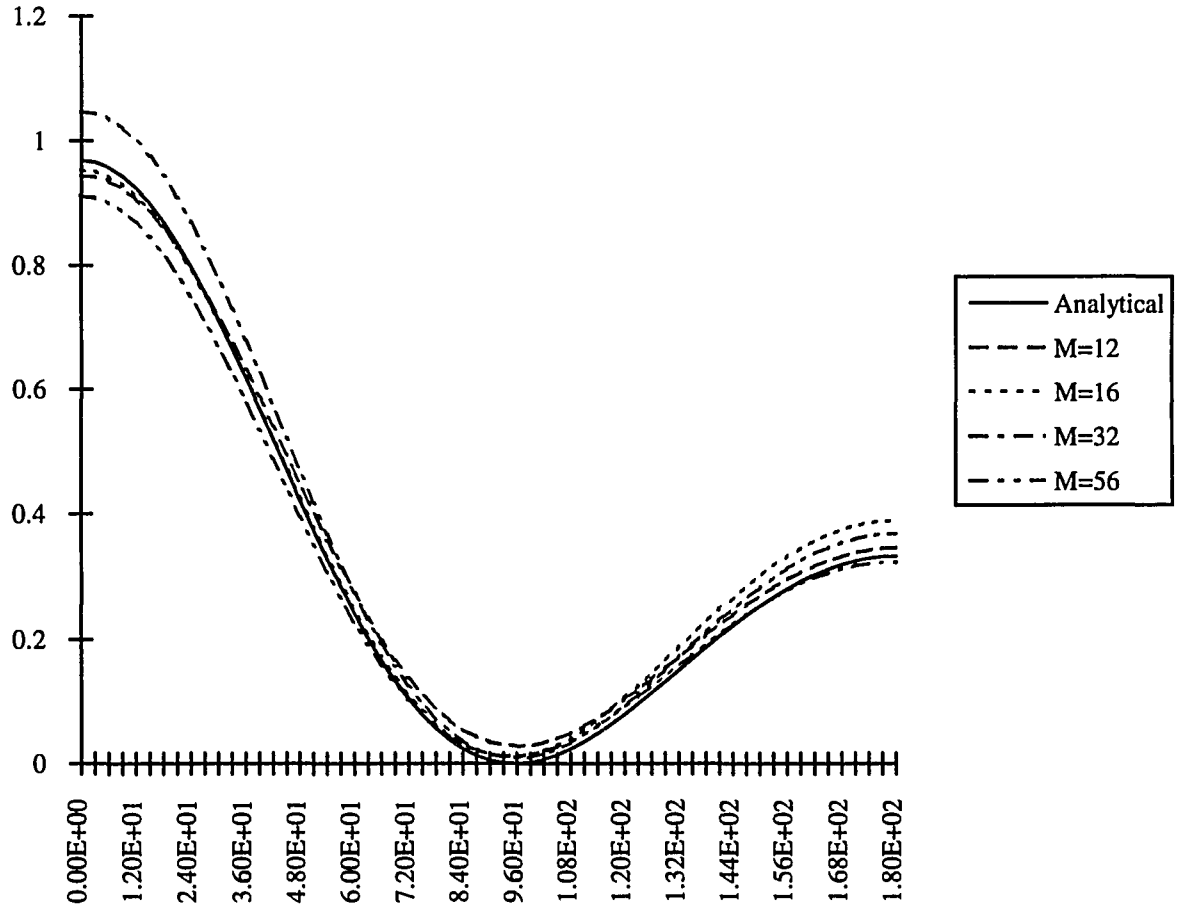

Figure 7.4 Conforming elements N = 1.7 ka = 1.0

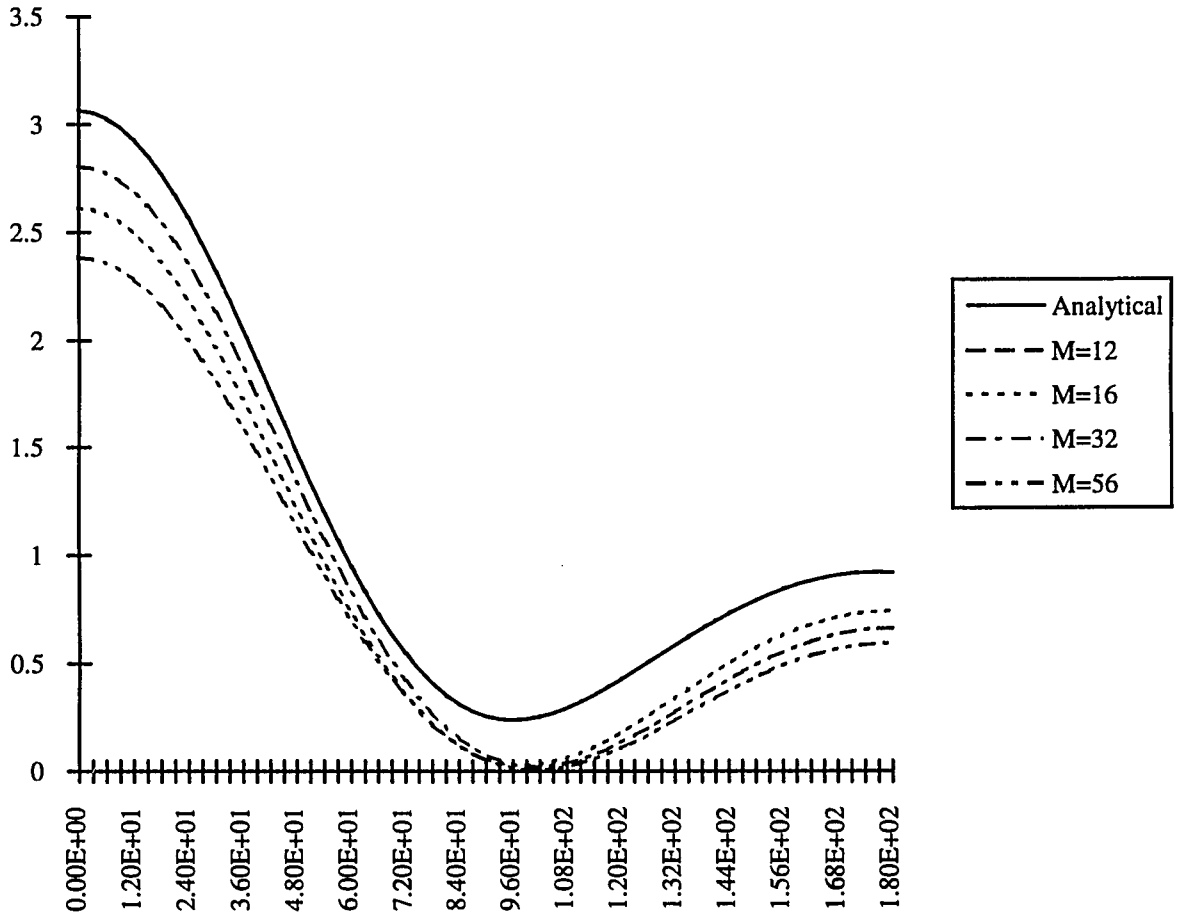

Figure 7.5 Conforming elements N = 2.1 ka = 1

Nonconforming elements

Dielectric scatterers To test for the robustness of the program, the relative radius of the sphere is also varied in addition to varying the M and N parameters. The simulation results are shown in Figures 7.6 through 7.10. As can be seen in figures, as the radius increases, it requires more discretizing elements to cover the surface in order to obtain an accurate solution.

Lossy scatterers The program is tested for lossy scatterers by making the refractive index of the scatterer a complex number. The simulation results are shown in Figures 7.11 through 7.12. Once again, there is a good agreement between the analytical solution and the BEM solutions.

Perfect conducting scatterer As mentioned in Chapter 3, the scattering problem of a single perfect conducting scatterer can be solved using either the EFIE or the MFIE. In this case, the MFIE is employed to avoid the evaluation of hypersingular integrals. The result is shown in Figure 7.13 and is in good agreement with the result found in [70].

Multiple scatterer problem

The test configuration for the multiple scatterer problem is shown in Figure 7.14. The incident fields are unit-amplitude plane waves polarized in the y-direction. The scattered waves are calculated in the far-field region along the x-z plane as a function of θ. The vertical intensity is calculated by dividing the scattered fields obtained from the two scatterer problem by the scattered fields obtained from the single scatterer problem. In Figure 7.15, the y-axis represents the vertical intensity and the x-axis represents the scattering angle. The index of refraction for this problem is 1.2 for both spheres and the dimensionless quantity ka represents the radius of the spheres. The results are in excellent agreement with those found in [42].

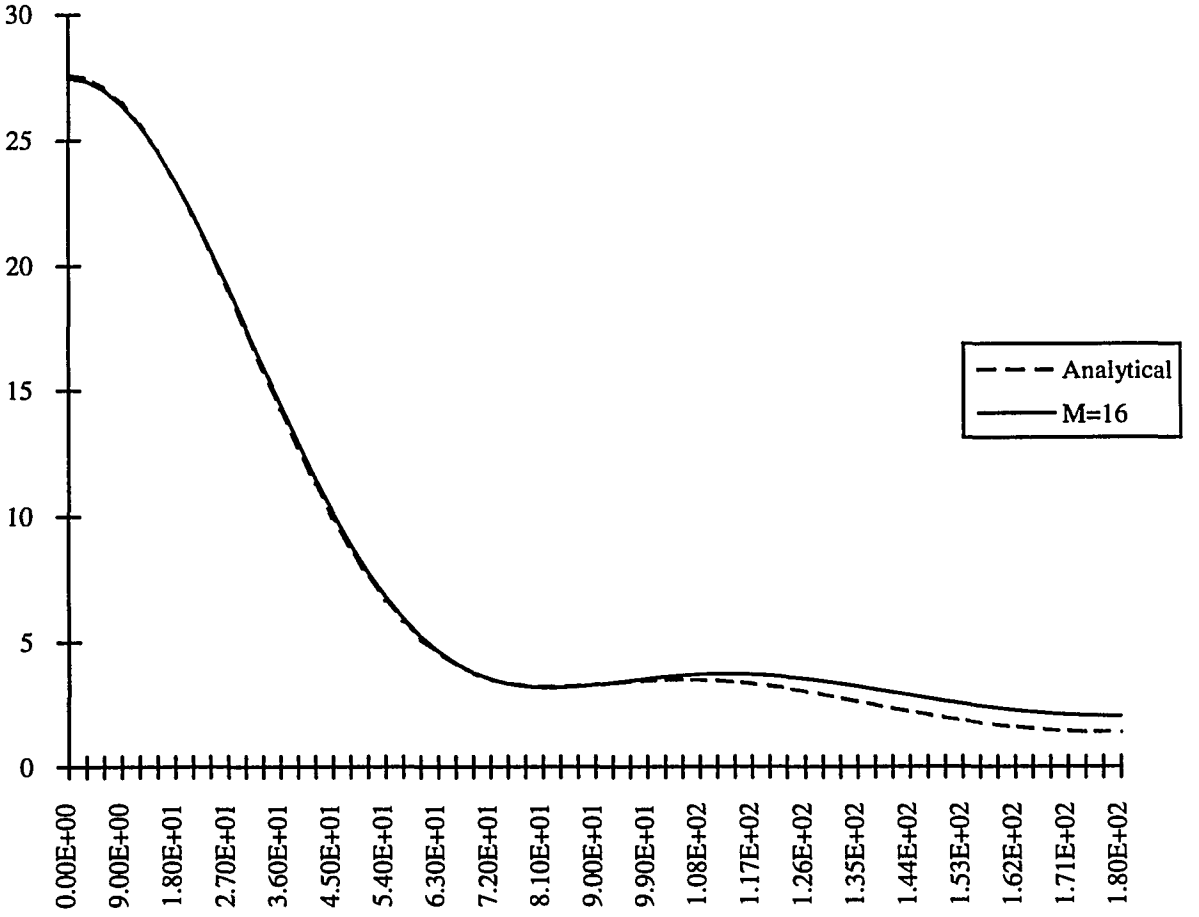

Figure 7.6 Nonconforming elements ka = 2 N = 2

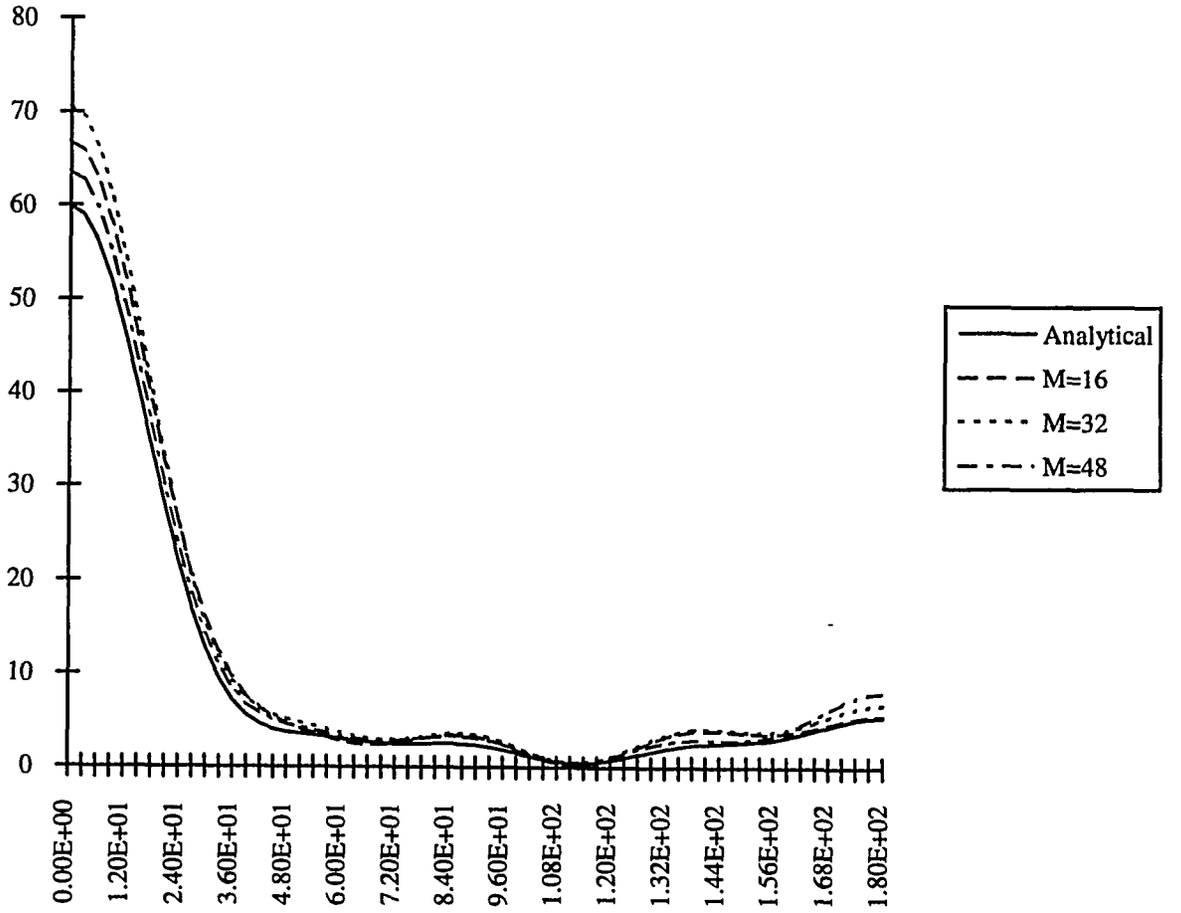

Figure 7.7 Nonconforming elements ka = 4 N = 1.7

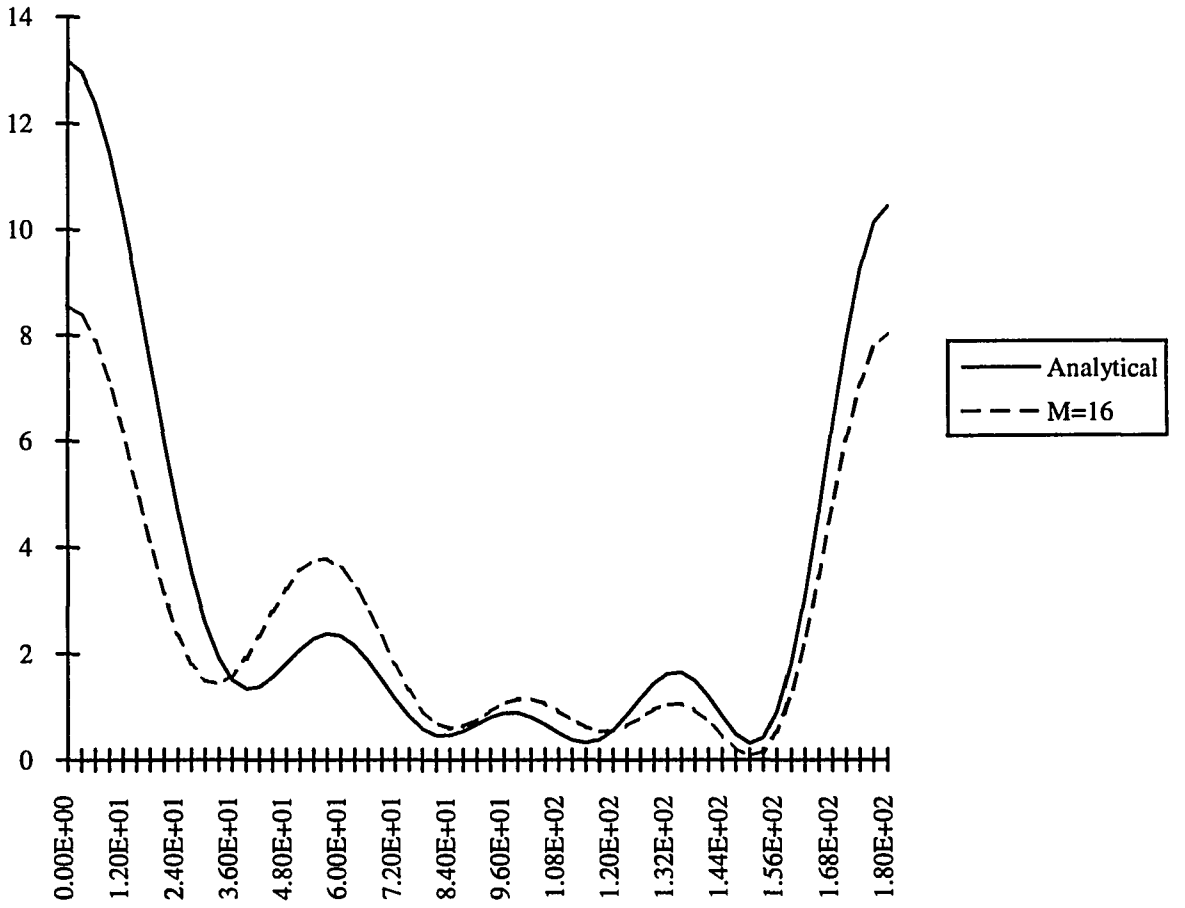

Figure 7.8 Nonconforming elements ka = 4 N = 2.0

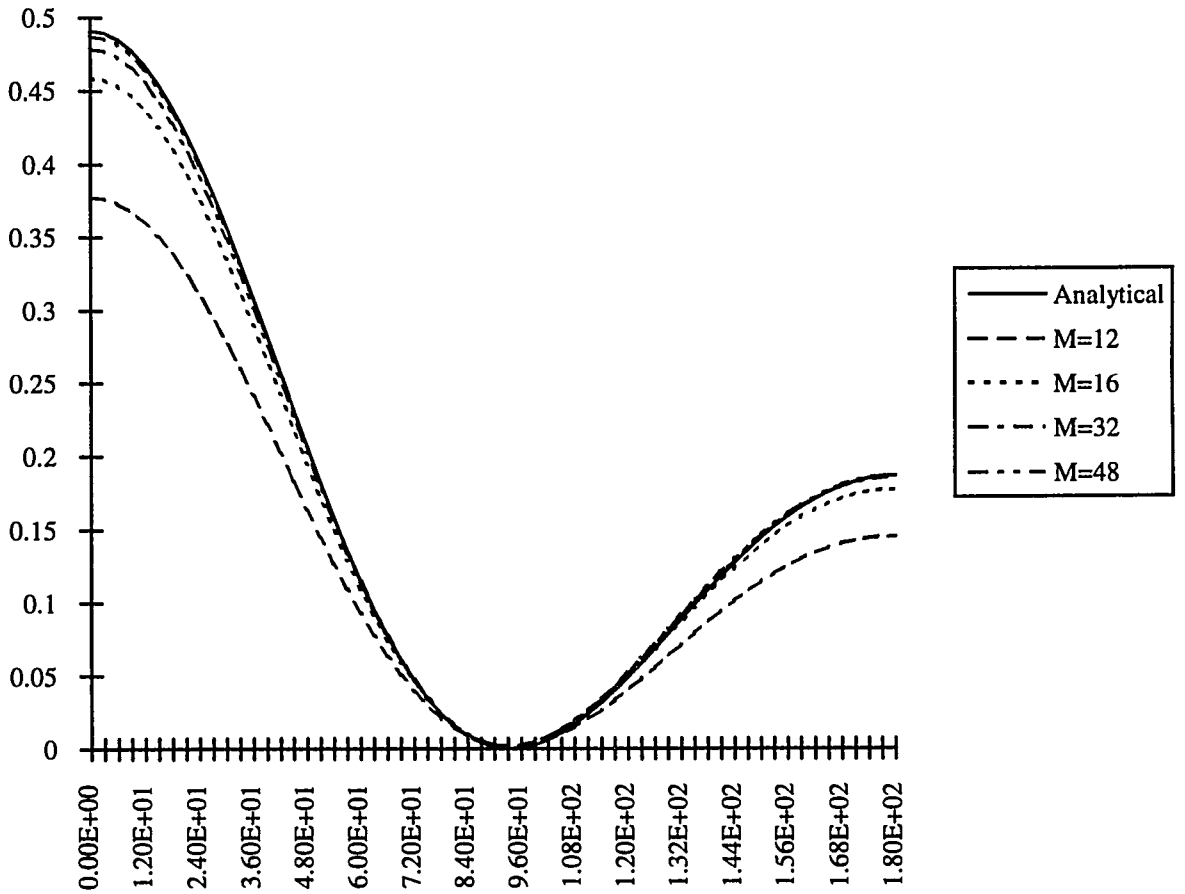

Figure 7.9 Nonconforming elements ka = 1.0 N = 1.5

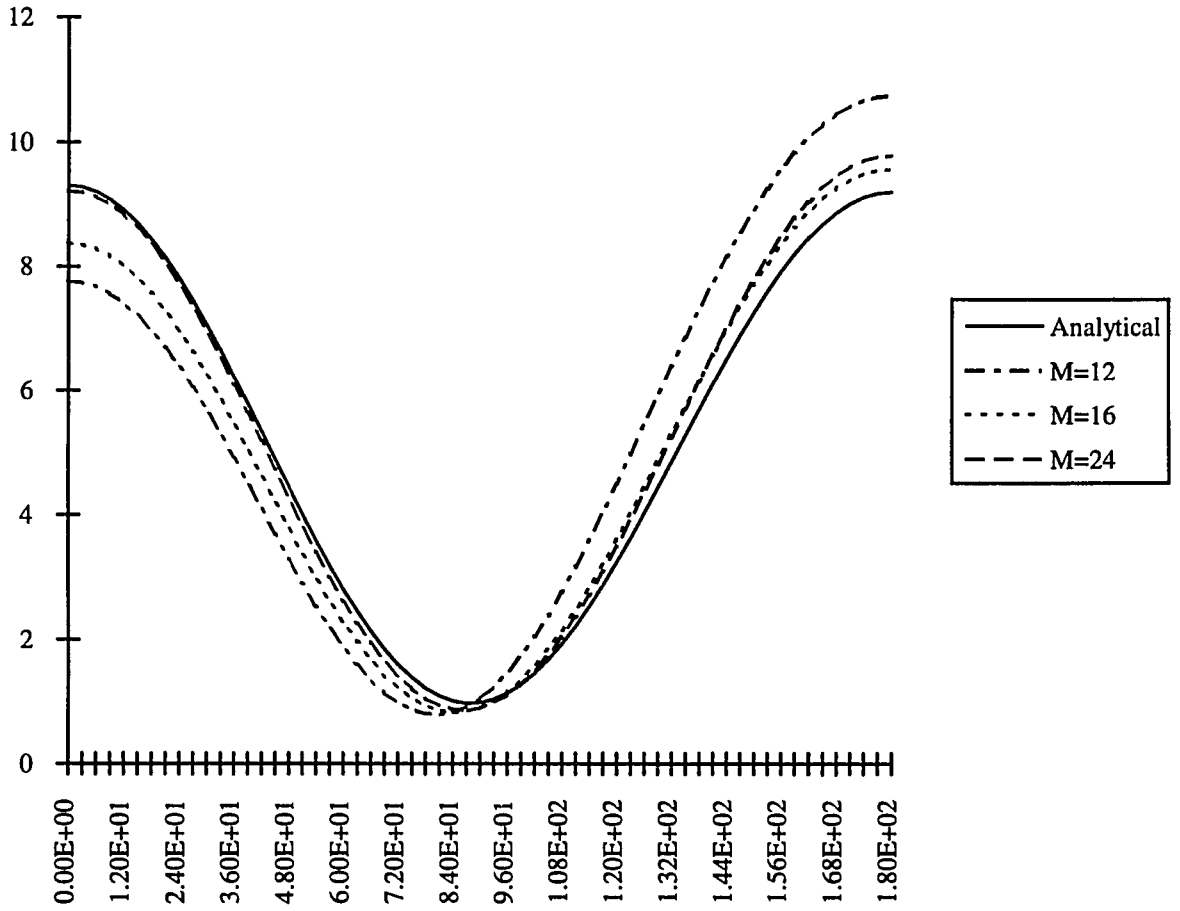

Figure 7.10 Nonconforming elements ka = 1 N = 4

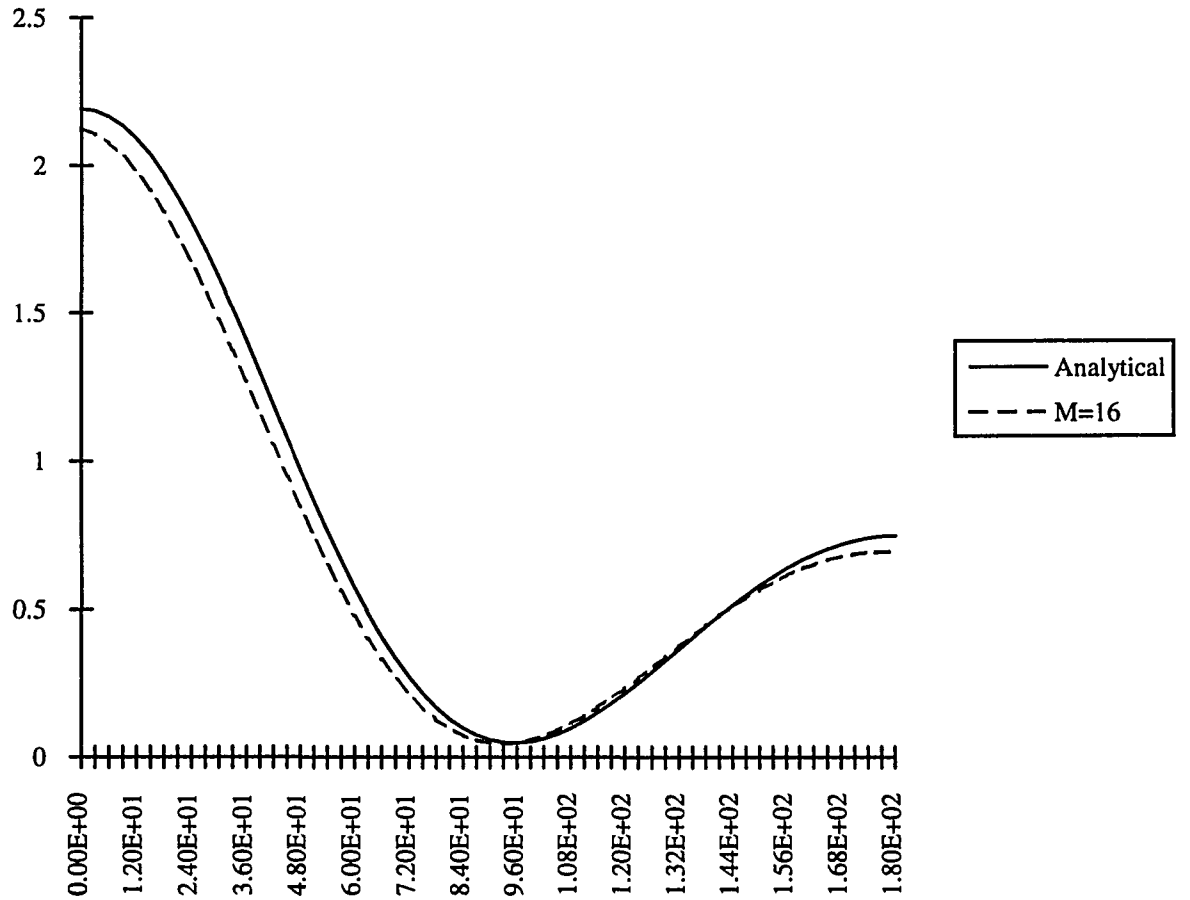

Figure 7.11 Nonconforming elements ka = 1 N = 2.0 + j 1

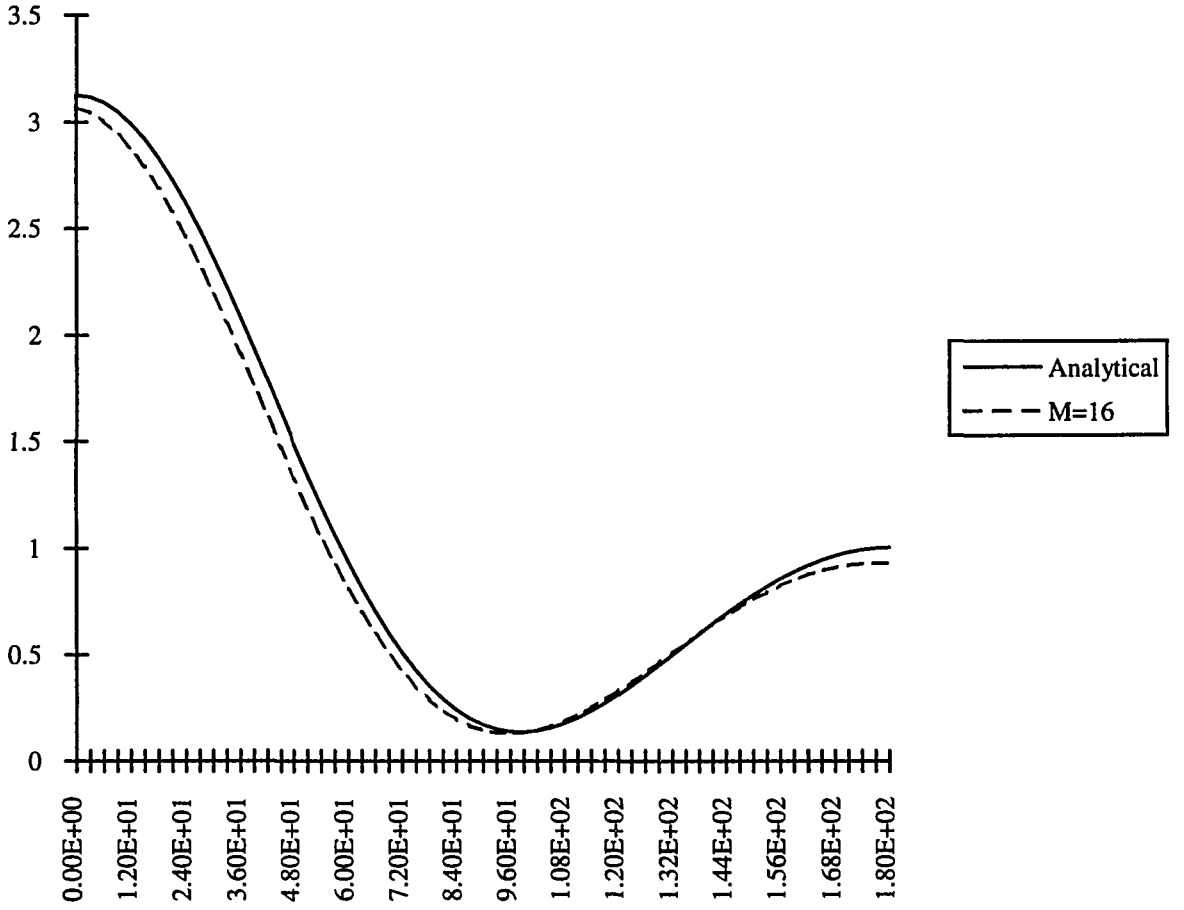

Figure 7.12 Nonconforming elements ka = 1 N = 2.5 + j 1

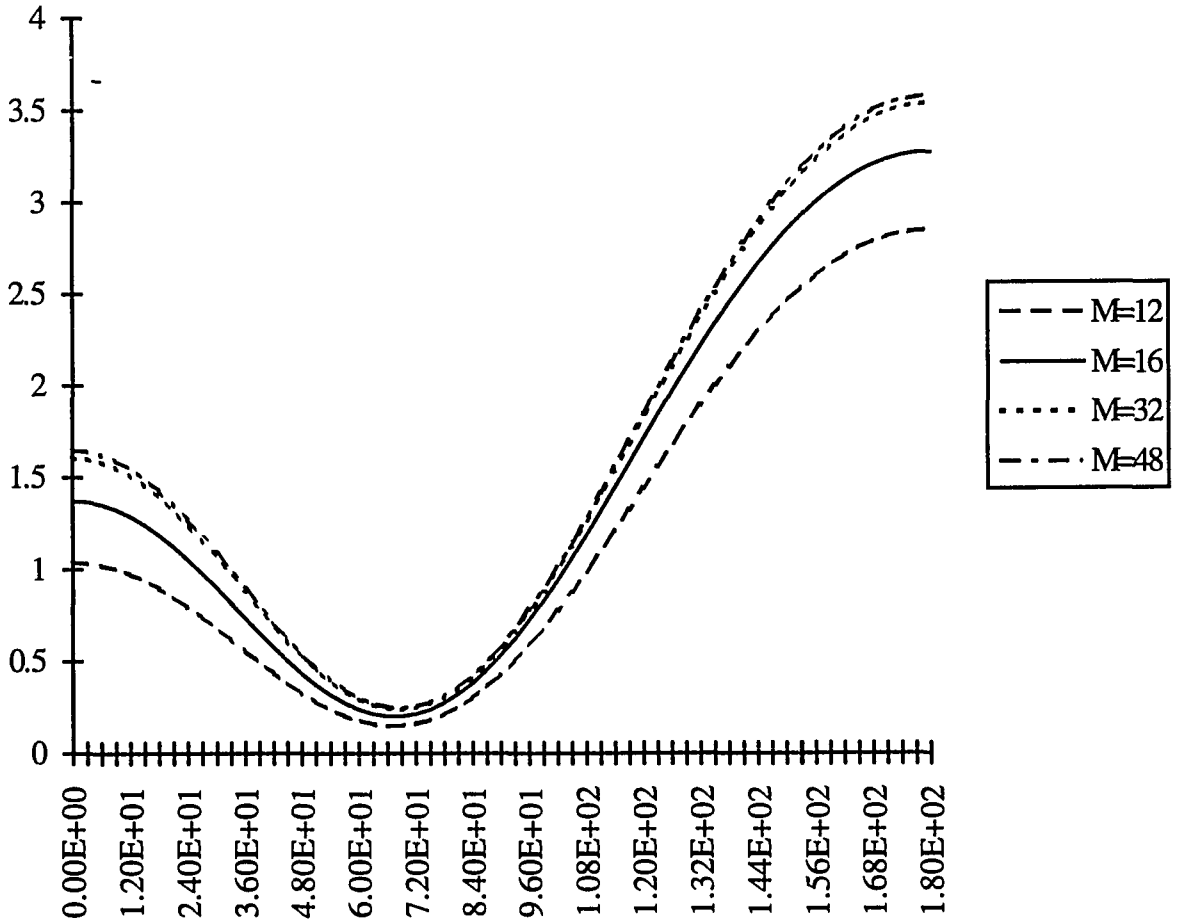

Figure 7.13 Perfect conducting sphere ka = 1

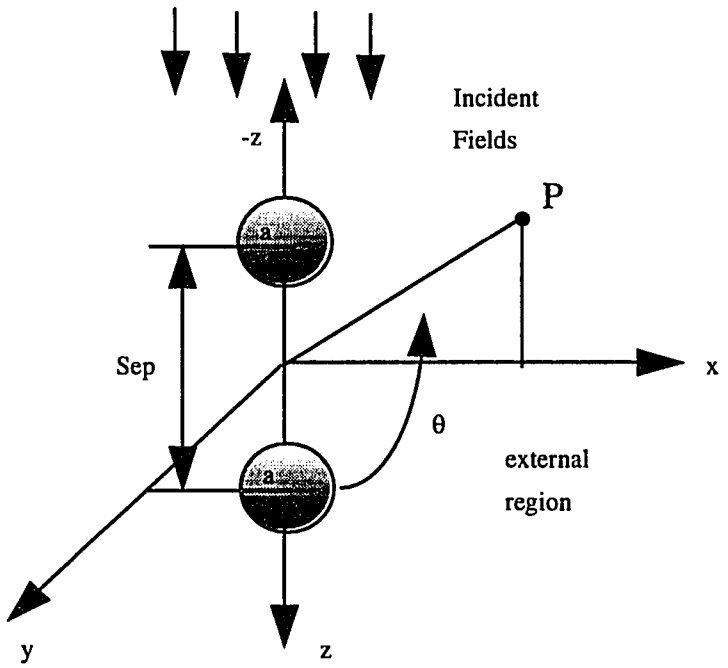

Figure 7.14 Two scatterer test configuration

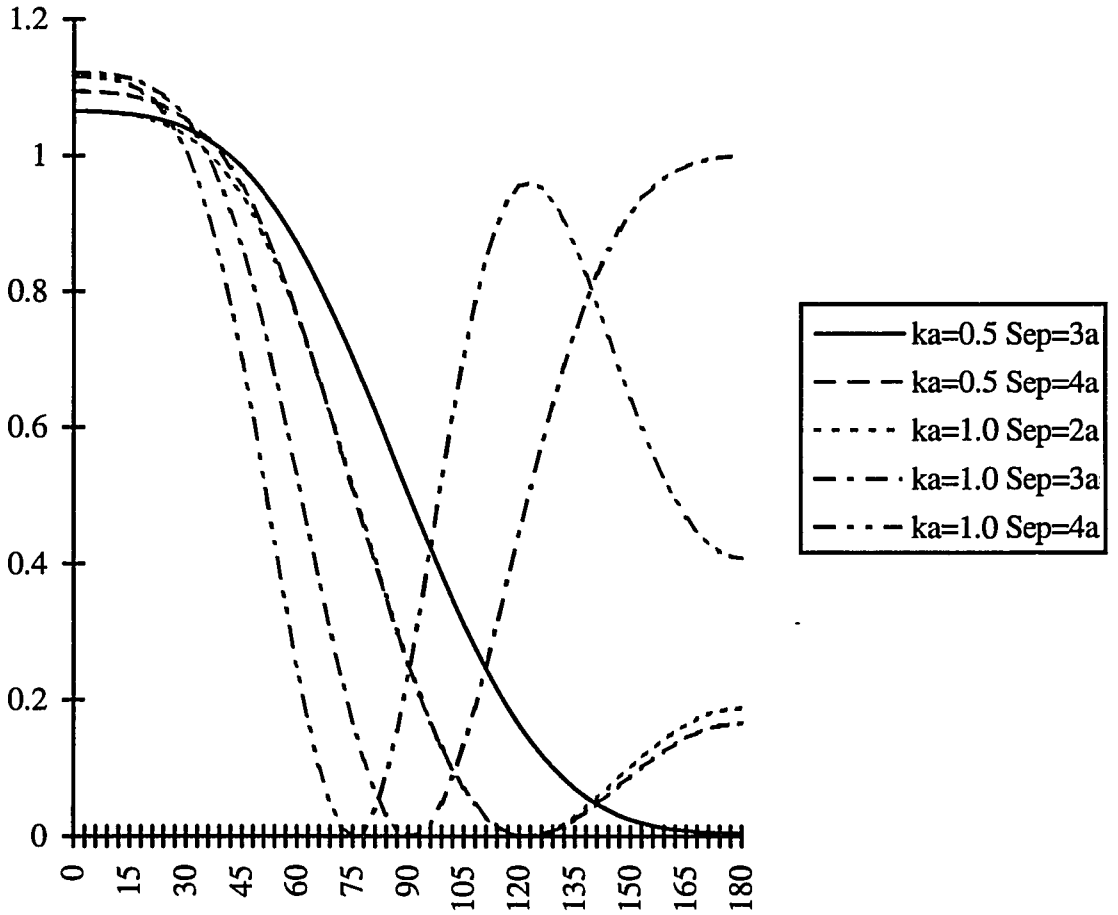

Figure 7.15 Two sphere nonconforming elements scattering problem N = 1.2

Scatterer on a perfect conducting half-space

The test configuration for the problem of single dielectric scatterer situated above a perfect conducting half-space is shown in Figure 7.16. The incident wave is an unit-amplitude plane polarized in the y-direction and differential scattering cross section is calculated from the scattered fields obtained in the far-field region. For this problem, the refractive index of the scatterer is 1.46 and the radius of the sphere is $ka = 0.4\pi$. The simulated result is shown in Figure 7.17 where the y-axis represents the differential scattering cross section in logarithmic scale and the x-axis represents the scattering angle, θ. The result is in good agreement with the result obtained using the multipole expansion method [69].

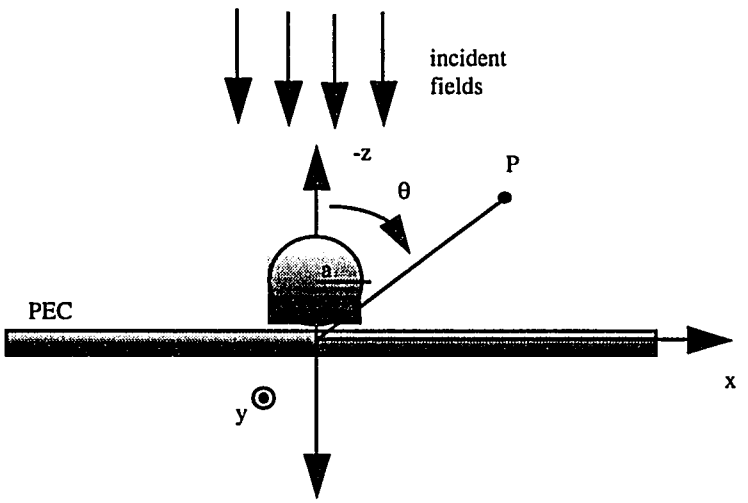

Figure 7.16 Dielectric scatterer on perfect conducting half-space

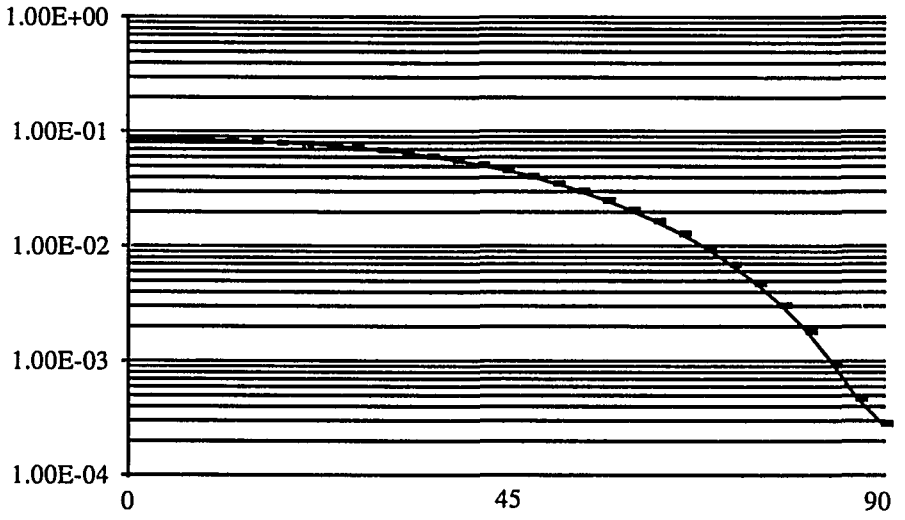

Figure 7.17 Dielectric sphere on perfect conducting half-space ka = 1

Dielectric scatterer on dielectric half-space

The problem of dielectric scatterer situated above a dielectric half-space is shown in Figure 7.18. Similar as before, the incident field is an unit-amplitude plane wave polarized in the y-direction. However, since no analytical results have been reported for this problem yet, the program is tested with the special case of modeling the half-space as air and results are compared with the analytical Mie solution. The scattering cross section is plotted as a function of the scattering angle. The half-space surface is truncated at 5 times the radius of the scatterer. The simulation result is shown in Figure 7.19. As can be seen from the Figure 7.19, there is a good match between the analytical solution and the BEM solution. This gives an optimistic indication that the program is working for the three-material problem as well.

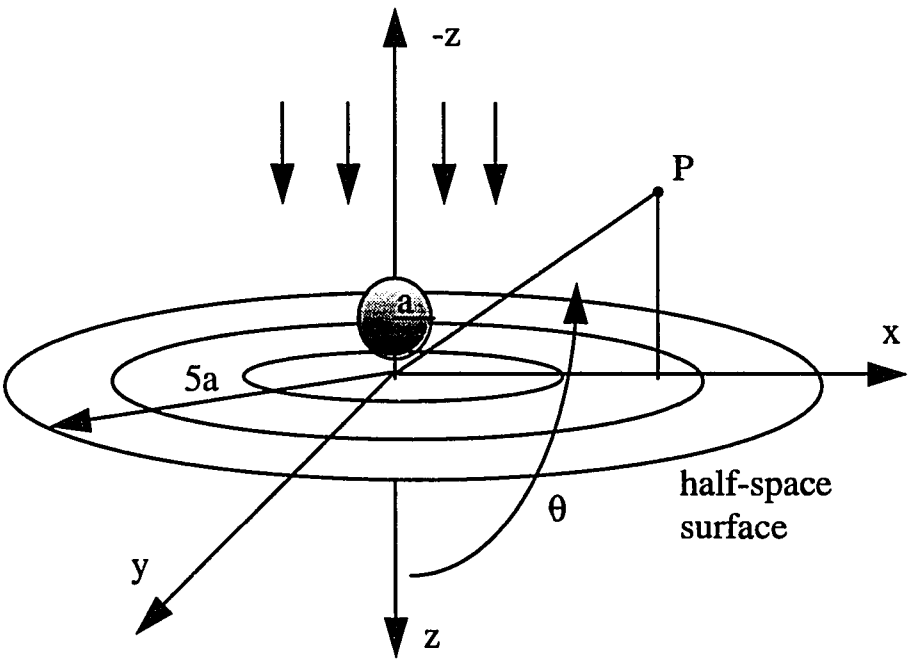

Figure 7.18 Test configuration of dielectric scatterer on dielectric half-space

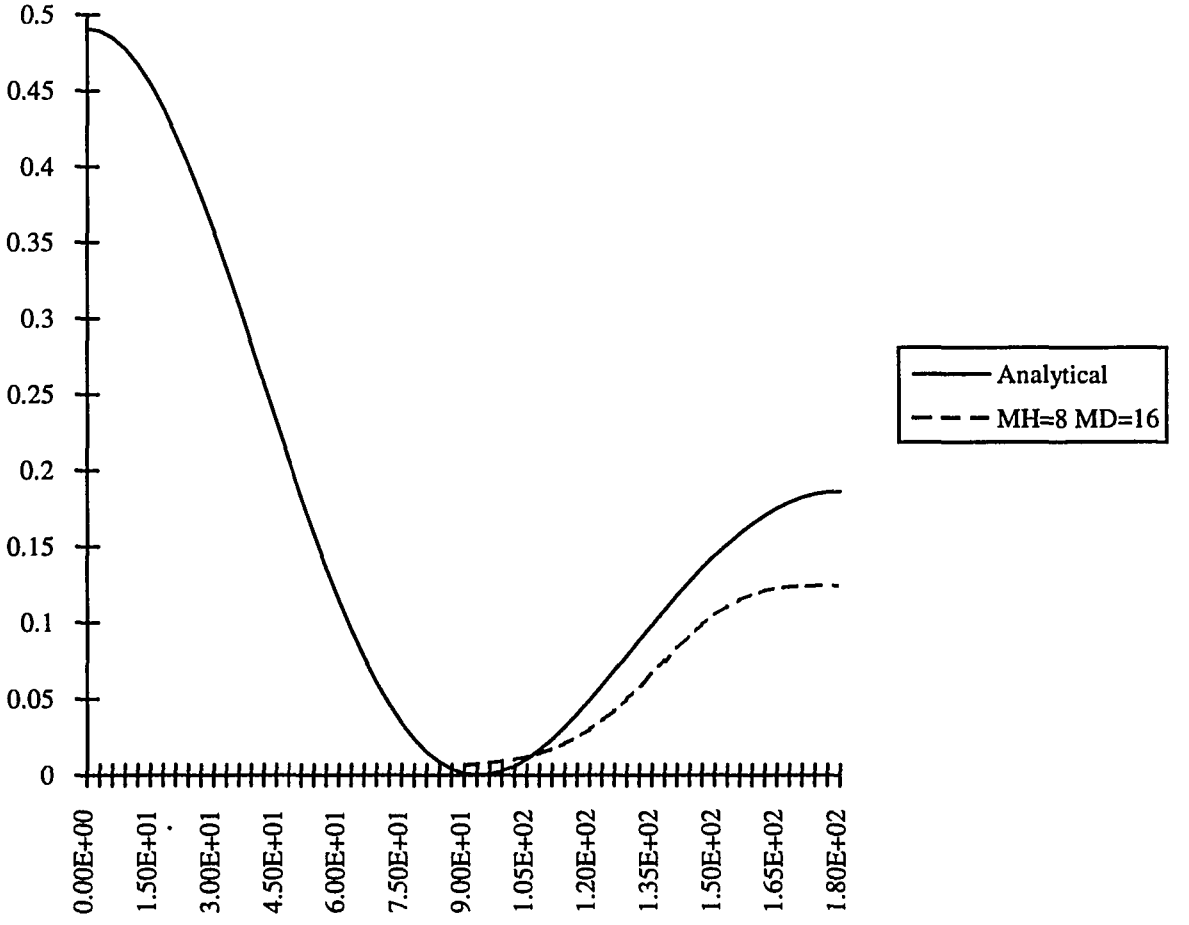

Figure 7.19 Dielectric scatterer on a dielectric half-space ka = 1 N = 1.5

CHAPTER 8. CONCLUSIONS AND FUTURE WORK

The main objective of this dissertation is the development of a BIE model for solving electromagnetic scattering problems. This chapter summarizes the major contributions and suggests areas of future research.

Summary of major contributions

The development of an accurate forward model for scattering problems is essential in many applications ranging from nondestructive evaluation to atmospheric studies. By using the forward model, spatial distribution of the scattered fields can be accurately predicted prior to the experiment implementation. This is advantageous in providing valuable information for optimizing experimental parameters and operator training. This dissertation has illustrated that the BIE method is a powerful tool for solving electromagnetic scattering problems. The primary advantage of this method, as opposed to methods governed by differential equations, is that the problem domain consists of a surface rather than a volume for three dimensional problems. This, in turn, presents a significant saving in computation time and memory storage requirement. The disadvantage of the BIE method, however, is that it is difficult to solve for problems involving nonlinear media.

The BIE formulation developed was then validated by application to some fundamental problem geometries for which analytical solutions are available. To do this, four general scattering configurations were considered:

1) Single scatterer suspended in an infinite medium.
2) Multiple scatterers suspended in an infinite medium.
3) Scatterer(s) situated near a perfect conducting half-space.
4) Scatterer(s) situated near a dielectric half-space.

The solutions to the four configurations include the special case where the scatterer(s) is made of perfect conducting material. In most applications, the scattering problem of interest typically falls under one of the four configuration models listed above. Presently, the first three configurations have been thoroughly tested for a variety of material parameters and the simulation results obtained are in good agreement with either analytical solutions or other published results. The fourth configuration has been tested for the special case where the dielectric half-space is assigned the same properties as the external region. This reduces the problem to the configuration in case 1 which allows the comparison with the Mie solution. Further testing needs to be done for the more general case of a problem consisting of three distinct materials. In all cases, validation work was done using only spherical scatterers. This was necessary for comparison with analytical results that are readily available for spherical scatterers. However, the model is not limited to spherical scatterers and consequently, further testing needs to be done for cases where scatterers are of arbitrary shapes.

As was seen from the numerical results in Chapter 7, in most cases, a discretization density of 16 elements per scatterer was sufficient to achieve an accurate solution. This translates to about 80 nodes per scatterer, a number which is significantly lower than the number of nodes required if the problem were solved using the FEM or the FDM. To further reduce the computational effort needed to solve the matrix equation, all calculations are done in the local coordinate system, rather than the global coordinate system. This is to take advantage of the fact that the vector current densities have two tangential components in the local coordinate system but have three components in the global coordinate system. This results in a reduction of the matrix by one-third of the original matrix size. All numerical simulations have been done on the DEC 5000/240 work stations. The computer run time is typically 20 - 30 minutes per run.

In order to calculate the scattered fields in a much shorter time for practical purposes, developments are underway to take advantage of the readily available large storage media, such as CD ROM's, and create a library of scattering coefficient matrices stored for various scatterer size, shape and other properties. This library will allow the scattered fields to be calculated almost instantaneously as the orientation and the type of the incident fields are varied. The calculation procedure would then simply involve a multiplication step between

the inverse of the coefficient matrix and the user-supplied incident field vector. This procedure is both cost-effective and user-friendly, and could potentially be the direction in which most numerical models are headed. Users of this new capability need not have the expertise or any of the usual skills required to set up and execute a computer solution to electromagnetic scattering problems.

Finally, it should be emphasized that the BIE method is by no means the best technique for solving *ALL* scattering problems. Instead, the BIE method simply serves as an alternative way to complement other numerical methods such as FEM and FDM. Depending on the nature of the problem, FEM and FDM may happen to be a more well-suited candidate than the BIE method. Yet, there may be situations where both the BIE method and the FEM can be used in conjunction with each other to achieve the best result. But in general, the BIE method is a more efficient method for problems involving infinite boundaries and linear, homogeneous media.

Future work

The work reported in this dissertation clearly demonstrates the versatility of the BIE method for solving electromagnetic scattering problems. Further developments and studies are still necessary. Some additional areas of study include

1) The test on the problem of a dielectric scatterer situated near a dielectric half-space should be completed. This test, however, requires more computation resources than what is locally available.

2) The computer program developed should be parallelized to achieve lower computation time. This task is currently being implemented.

BIBLIOGRAPHY

[1] R. Mittra, O. Ramahi, A. Khebir, R. Gordon and A. Kouki, "A Review of Absorbing Boundary Conditions for Two- and Three- Dimensional Electromagnetic Scattering Problems," *IEEE Trans. on Mag.*, vol. 25, pp 3034-3040, July 1989.

[2] J. D'Angelo and I. Mayergoyz, "On the Use of Local Absorbing Boundary Conditions for RF Scattering Problems," *IEEE Trans. on Mag.*, vol. 25, pp 3040-3043, July 1989.

[3] K. K. Mei, "Unimoment Method for Solving Antenna and Scattering Problems," *IEEE Trans. on Ant. and Prop.*, vol. AP-22, pp 760-766, Nov. 1974.

[4] A. Cangellaris and R. Lee, "The Bymoment Method for Two-Dimensional Electromagnetic Scattering," *IEEE Trans. on Ant. and Prop.*, vol. 38, pp 1429-1438, Sept. 1990.

[5] T. Cwik, "Coupling Finite Element and Integral Equation Solutions Using Decoupled Boundary Meshes," *IEEE Trans. on Ant. and Prop.*, vol. 40, pp 1496-1504, Dec. 1992.

[6] Z. Gong and A. Glisson, "A Hybrid Equation Approach for the Solution of Electromagnetic Scattering Problem Involving Two-Dimensional Inhomogeneous Dielectric Cylinders," *IEEE Trans. on Ant. and Prop.*, vol. 38, pp 60-68, Jan. 1990.

[7] J. M. Jin and V. Liepa, "Application of Hybrid Finite Element Method to Electromagnetic Scattering From Coated Cylinders," *IEEE Trans. on Ant. and Prop.*, vol. 36, pp 50-54, Jan. 1988.

[8] O. C. Zienkiewicz, D. Kelly and P. Bettess, "The Coupling of the Finite Element Method and Boundary Solution Procedures," *Intern. Journal Numerical Methods Eng.*, vol. 11, pp 355-375, Nov. 1977.

[9] X. Yuan, D. Lynch and J. Strohbehn, "Coupling of Finite Element and Moment Methods for Electromagnetic Scattering from Inhomogeneous Objects," *IEEE Trans. on Ant. and Prop.*, vol. 38, pp 386-394, Mar. 1990.

[10] M. Morgan and K. K. Mei, "Finite Element Computation of Scattering by Inhomogeneous Penetrable Bodies of Revolution," *IEEE Trans. on Ant. and Prop.*, vol. AP-27, pp 202-214, Mar. 1979.

[11] B. McDonald and A. Wexler, "Finite Element Solution of Unbounded Field Problems," *IEEE Trans. on Microwave Theory Techn.*, vol. MTT-20, pp 841-847, Dec. 1972.

[12] B. Beker, K. R. Umashankar and A. Taflove, "Numerical Analysis and Validation of the Combined Field Surface Integral Equations for Electromagnetic Scattering by Arbitrarily Shaped Two-Dimensional Anisotropic Objects," *IEEE Trans. on Ant. and Prop.*, vol. 37, pp 1573-1581, Dec. 1989.

[13] K. Yashiro and S. Ohkawa, "Boundary Element Method for Electromagnetic Scattering from Cylinders," *IEEE Trans. on Ant. and Prop.*, vol. AP-33, pp 383-389, April 1985.

[14] H. A. El-Mikati and B. Davies, "Improved Boundary Element Techniques for Two-Dimensional Scattering Problems with Circular boundaries," *IEEE Trans. on Ant. and Prop.*, vol. AP-35, pp 539-544, May 1987.

[15] S. M. Rao, D. Wilton and A. Glisson, "Electromagnetic Scattering by Surfaces of Arbitrary Shape," *IEEE Trans. on Ant. and Prop.*, vol. AP-30, pp 409-418, May 1982.

[16] K. Umashankar, A. Taflove and S. Rao, "Electromagnetic Scattering by Arbitrarily Shaped Three-Dimensional Homogeneous Lossy Dielectric Objects," *IEEE Trans. on Ant. and Prop.*, vol. AP-34, pp 758-766, June 1986.

[17] M. G. Andreason, "Scattering from Bodies of Revolution," *IEEE Trans. on Ant. and Prop.*, vol. AP-13, pp 303-310, Mar. 1985.

[18] W. S. Hall, X. Mao and W. Robertson, "Quadratic, Isoparametric BEM Formulation for Electromagnetic Scattering from Arbitrarily Shaped Three-Dimensional Homogeneous Dielectric Objects," in *Boundary Elements XIV*, ed. C. A. Brebbia, J. Dominguez, and F. Parvis, Computational Mechanics Publications, Southampton, 1992.

[19] M. S. Ingbar and R. H. Ott, "An Application of the Boundary Element Method to the Magnetic Field Integral Equation," *IEEE Trans. on Ant. and Prop.*, vol. 39, pp 606-611, May 1991.

[20] J. R. Mautz, " A Stable Integral Equation for Electromagnetic Scattering from Homogeneous Dielectric Bodies," *IEEE Trans. on Ant. and Prop.*, vol. 37, pp 1070-1071, Aug. 1987.

[21] E. Marx, "Integral Equation for Scattering by a Dielectric," *IEEE Trans. on Ant. and Prop.*, vol. AP-32, pp 166-172, Feb. 1984.

[22] A. Glisson, " An Integral Equation for Electromagnetic Scattering from Homogenous Dielectric Bodies," *IEEE Trans. on Ant. and Prop.*, vol. AP-32, pp 173-175, Feb. 1984.

[23] C. F. Bohren and D. R. Huffman, *Absorption and Scattering of Light by Small Particles*, John Wiley and Sons, New York, 1983.

[24] H. C. van de Hulst, *Light Scattering by Small Particles*, Dover Publications, Inc., New York, 1957.

[25] E. Yamashita, *Analysis Methods for Electromagnetic Wave Problems*, Artech House, Inc., Norwood, 1990.

[26] A. Ishimaru, *Wave Propagation and Scattering in Random Media, Vol I, Single Scattering and Transport Theory*, Academic Press, New York, 1978.

[27] J. A. Stratton, *Electromagnetic Theory*, McGraw-Hill, New York, 1941.

[28] J. B. Keller, "Geometrical Theory of Diffraction," *Journal Opt. Soc. Amer.*, vol. 52, pp 116-130, 1962.

[29] G. L. Games, *Geometrical Theory of Diffraction*, Peter Peregrinus, Stevenage, 1976.

[30] C. A. Balanis, *Advanced Engineering Electromagnetics*, John Wiley and Sons, New York, 1989.

[31] O. C. Zienkiewicz, *Finite Element Method*, 3rd edition, McGraw-Hill, London, 1977.

[32] V. V. Varadan, A. Lakhtakia and V. K. Varadan, *Field Representations and Introduction to Scattering, Vol. I*, North-Holland, Elsevier Science Publishers, New York, 1991.

[33] P. A. Martin and P. Ola, "Boundary Integral Equations for the Scattering of Electromagnetic Waves by Homogeneous Dielectric Obstacle," *Proceedings of the Royal Society of Edinburgh*, vol. 123A, pp 185-208, 1993.

[34] J. J. H. Wang, *Generalize Moment Methods in Electromagnetics*, Wiley and Sons, New York, 1991.

[35] R. F. Harrington, "Boundary Integral Formulations for Homogeneous Material Bodies," *Journal of Electromagnetic Waves and Applications*, vol. 3, pp 1-15, 1989.

[36] D. S. Jones, *Methods in Electromagnetic Wave Propagation*, Clarendon Press, Oxford, 1979.

[37] J. R. Mautz and R. F. Harrington, "Electromagnetic Scattering from a Homogenous Body of Revolution," *Achiv Für Elektronik und Übertagungstechnik,* vol. 33, pp 71-80, 1979.

[38] C. Müller, *Foundations of the Mathematical Theory of Electromagnetic Waves*, Springer, Berlin, 1969.

[39] D. Colton and R. Kress, *Integral Equation Methods in Scattering Theory*, Wiley and Sons, New York, 1983.

[40] E. J. Bawolek and E. D. Hirleman, "Light Scattering by Submicron Spherical Particles on Semiconductor Surfaces," in *Particle on Surfaces,* ed. K. Mittal, Plenum Publishing Co., New York, 1991.

[41] P. Spyak and W. L. Wolfe, "Scatter from Particulate Contaminated Mirrors," *Optical Engineering*, vol. 31, pp 1746-1763, Aug. 1992.

[42] S. Levine and G. O. Olaofe, "Scattering of Electromagnetic Waves by Two Equal Spherical Particles," *Journal of Colloid and Interface Science*, vol. 27, pp 442-457, July 1968.

[43] M. F. R. Cooray and I. R. Ciric, "Scattering of Electromagnetic Waves by a System of Two Dielectric Spheroids of Arbitrary Orientation," *IEEE Trans. on Ant. and Prop.*, vol. 39, pp 680-684, May 1991.

[44] A. C. Ludwig, "Scattering by Two and Three Spheres Computed by the Generalized Multipole Technique," *IEEE Trans. on Ant. and Prop.*, vol. 39, pp 703-705, May 1991.

[45] J. H. Bruning and Y. T. Lo, "Multiple Scattering of Waves by Spheres," *IEEE Trans. on Ant. and Prop.*, vol. AP-19, pp 378-390, May 1971.

[46] G. W. Kattawar and C. E. Dean, "Electromagnetic Scattering from Two Dielectric Spheres: Comparison Between Theory and Experiment," *Optics Letters*, vol. 8, pp 48-50, Jan. 1983.

[47] I. V. Lindell, A. Sihvola, K. Muinonen and P. Barber, "Scattering by a Small Object Close to an Interface. I. Exact Image Theory Formulation," *Journal Opt. Soc. Am. A.*, vol. 8, pp 472-476, 1991.

[48] C. Liang and Y. T. Lo, "Scattering by Two Spheres," *Radio Science*, vol. 2, pp 1481-1495, 1967.

[49] A. L. Aden and M. Kerker, "Scattering of Electromagnetic Waves from Two Concentric Spheres," *Journal Appl. Phys.*, vol. 22, pp 1242-1246, 1951.

[50] G. W. Kattawar and T. J. Humphreys, "Electromagnetic Scattering from Two Identical Pseudo Spheres," in *Light Scattering by Irregularly Shaped Particles*, ed. D. W. Schuernam, pp 177-190, Plenum Press, New York, 1980.

[51] K. B. Nahm and W. L Wolfe, "Light Scattering Models for Sphere on a Conducting Plane: Comparison with Experiments," *Appl. Optics*, vol. 26, pp 2995-2999, 1987.

[52] R. P. Young, "Low Scatter Mirror Degradation by Particle Contamination," *Optical Engineering*, vol. 15, pp 516-520, 1976.

[53] D. C. Weber and E. D. Hirleman, "Light Scattering Signatures of Individual Spheres on Optically Smooth Conducting Surfaces," *Appl. Optics*, vol. 19, pp 4019-4026, 1988.

[54] P. A. Bobbert and J. Vlieger, "Light Scattering by a Sphere on a Substrate," *Physica.*, vol. 137A, pp 209-242, 1986.

[55] G. Videen, "Light Scattering From a Sphere on or Near a Surface," *Journal Opt. Soc. Am. A.*, vol. 8, pp 483-489, 1991.

[56] A. J. Burton and G. F. Miller, "The Application of the Integral Equation Methods to the Numerical Solution of Some Exterior Boundary-Value Problems," *Proc. Roy. Soc. London*, vol. A323, pp 201-210, 1971.

[57] M. Rezayat, D. j. Shippy and F. J. Rizzo, "On Time-Harmonic Elastic-Wave Analysis by the Boundary Element Method For Moderate to High Frequencies," *Computer Methods in Applied Mechanics and Engineering*, vol. 55, pp 349-367, 1986.

[58] F. J. Rizzo and D. J. Shippy, "An Advanced Boundary Integral Equation Method for Three-Dimensional Thermoelasticity," *Internal. Journ. Numer. Methods Eng.*, vol. 11, pp 1753-1768, 1977.

[59] F. J. Rizzo, D. J. Shippy and M. Rezayat, "A Boundary Integral Equation Method for Radiation and Scattering of Elastic Waves in Three Dimensions," *Internal. Journ. Numer. Methods Eng.*, vol. 21, pp 115-129, 1985.

[60] G. Krishnasamy, F. J. Rizzo and T. J. Rudolphi, "Hypersingular Integral Equations: Their Occurrence, Interpretation, Regularization and Computation," *Developments in BEM*, vol. 7, Chap. 7, Elsevier Applied Science Publisher, Feb. 1991.

[61] P. K. Banerjee and P. K. Butterfield, *Boundary Element Method in Engineering*, McGraw-Hill, London, 1981.

[62] M. Guiggiani, G. Krishnasamy, T. J. Rudolphi and F. J. Rizzo, "A General Algorithm for the Numerical Solution of Hypersingular BIEs," *Journal of Apply Mech.*, to appear.

[63] D. K. Reitan and T. J. Higgins, "Calculations of Electrical Capacitance of a Cube," *Journal of Appl. Phys.*, vol. 22, pp 223-226, 1951.

[64] T. A. Cruse and F. J. Rizzo, "Boundary Integral Equation Method: Computational Application in Applied Mechanics," *ASME Proc.* AMD - vol. 1, 1975.

[65] T. A. Cruse, "Application of the Boundary Element Method to Three Dimensional Stress Analysis," *Computers and Structures*, vol. 3, pp 509-527, 1973.

[66] R. Harrington, *Field Computation by Moment Methods*, Macmillan, New York, 1968.

[67] Y. Liu and F. J. Rizzo, "A Weakly Singular Form of the Hypersingular Boundary Integral Equation Applied to 3-D Acoustic Wave Problems," *Computer Methods in Applied Mechanics and Engineering*, vol. 96, pp 271-287, 1992.

[68] A. F. Seybert, B. Soenarko, F. J. Rizzo and D. J. Shippy, "An Advanced Computational Methods for Radiation and Scattering of Acoustic Waves in Three Dimensions," *Journal Acoustic Soc. Am.*, vol. 77, pp 362-368, Feb. 1985.

[69] B. R. Johnson, "Light Scattering from a Spherical Particle on a Conducting Plane: I. Normal Incidence," *Journal Opt. Soc. Am. A.*, vol. 9, pp 1341-1351, Aug. 1992.

[70] G. Ruck, D. Barrick, W. Stuart and C. Krichbaum, *Radar Cross Section Handbook, Volume I*, Plenum Press, New York, 1970.

APPENDIX. EQUIVALENCE CONCEPT

The concept of equivalence plays a vital role in solving problems using the boundary integral equation approach. This section describes some fundamental concepts of the equivalence principle. In electromagnetic theory, a BIE is one which deals with an integral of an unknown source multiplied by a Green's functions and integrated over the bounding surface of an object in interest. In the BIE method, the electromagnetic fields both internal and external to the homogeneous body can be calculated using a set of equivalent currents on the surface of the scatterer. These equivalent currents act as sources to produce the desired scattered fields in both regions of interest. There are two general classes of formulation of the BIE for the electromagnetic scattering problems, specifically, the source formulation (indirect BIE method) and the field formulation (direct BIE method). Although both formulations are described in this section, the one adopted in this research is the field formulation.

A typical scattering problem to be solved is sketched in Figure A.1 where the homogeneous scatterer, with a bounding surface S, can be of any arbitrary shape. S^- represents the surface just inside of S and S^+ represents the surface just outside of S. Following the notation of [35], $\vec{J}_e$, $\vec{M}_e$ denote the equivalent currents on S radiating into the medium characterized by the external constitutive parameters μ_e and ε_e and $\vec{J}_i$, $\vec{M}_i$ denote the equivalent currents on S radiating into the medium characterized by the internal constitutive parameters μ_i and ε_i. $\vec{E}_e(\vec{J}_e,\vec{M}_e)$, $\vec{H}_e(\vec{J}_e,\vec{M}_e)$ represent the fields produced by $\vec{J}_e$, $\vec{M}_e$ and $\vec{E}_i(\vec{J}_i,\vec{M}_i)$, $\vec{H}_i(\vec{J}_i,\vec{M}_i)$ represent the fields produced by $\vec{J}_i$, $\vec{M}_i$. The Greens function used in both formulations is the free space Greens function

$$G_\alpha(p,q)=\frac{e^{-jk_\alpha|p-q|}}{2\pi|p-q|} \qquad \text{(A.1)}$$

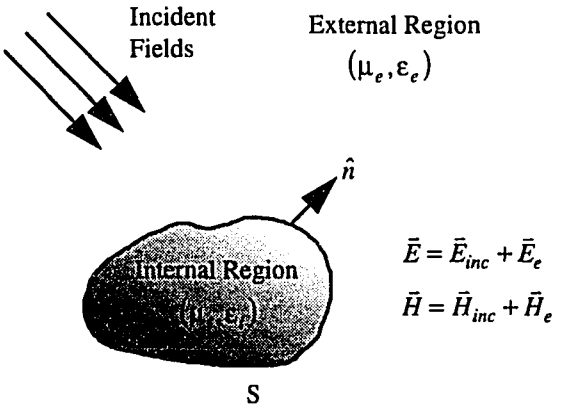

Figure A.1 A general scattering problem

where the subscript α = e or i is to denote either the exterior or the interior material, respectively. The spatial point p is an observation point and q is a source point located on S. The notation

$$\hat{n} \times \vec{E}^{+}(\vec{J}_e, \vec{M}_e) \tag{A.2}$$

$$\hat{n} \times \vec{H}^{+}(\vec{J}_e, \vec{M}_e) \tag{A.3}$$

represents the tangential components of the fields produced by $\vec{J}_e$, $\vec{M}_e$ evaluated on S^+ while the notation

$$\hat{n} \times \vec{E}^{-}(\vec{J}_i, \vec{M}_i) \tag{A.4}$$

$$\hat{n} \times \vec{H}^{-}(\vec{J}_i, \vec{M}_i) \tag{A.5}$$

represents the tangential components of the fields produced by $\vec{J}_i$, $\vec{M}_i$ evaluated on S^-. The two definitions are depicted graphically in Figures A.2 and A.3.

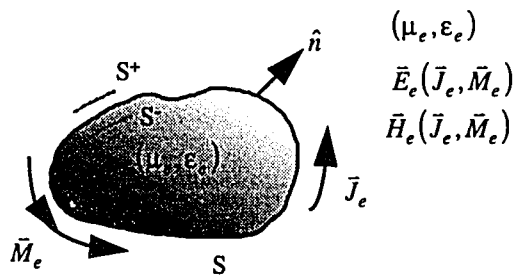

Figure A.2 Equivalent external currents

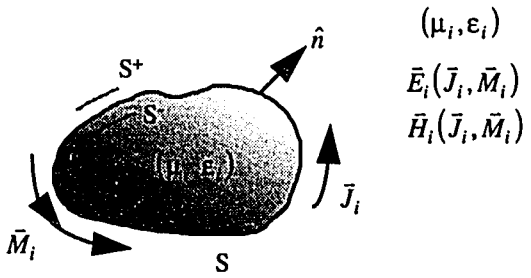

Figure A.3 Equivalent internal currents

Source formulation

In the source formulation, the problem is formulated in terms of unknown electric and magnetic current densities acting as sources on the surface of the scatterer. The equivalent current densities are defined separately for the internal region as well as the external region. The boundary conditions are then applied to the tangential electric field and the tangential magnetic field on the scatterer surface.

Using equivalent currents $\bar{J}_e$, $\bar{M}_e$ over S radiating into media e everywhere, as shown in Figure A.2, the fields in region e can be expressed as

$$\bar{E}_e = \bar{E}_{inc} + \bar{E}_e(\bar{J}_e, \bar{M}_e) \tag{A.6}$$

$$\bar{H}_e = \bar{H}_{inc} + \bar{H}_e(\bar{J}_e, \bar{M}_e) \tag{A.7}$$

Similarly, equivalent currents $\bar{J}_i$, $\bar{M}_i$ over S radiating into media i everywhere, as shown in Figure A.3 , give the fields in region i and can be expressed as

$$\bar{E}_i = \bar{E}_i(\bar{J}_i, \bar{M}_i) \tag{A.8}$$

$$\bar{H}_i = \bar{H}_i(\bar{J}_i, \bar{M}_i) \tag{A.9}$$

Equations (A.6) and (A.7) give the total fields in the external region while equations (A.8) and (A.9) give the fields in the internal region. Applying the boundary conditions (2.11) and (2.12) which require that the tangential components of $\bar{E}$ and $\bar{H}$ be continuous across the surface S yield

$$\hat{n} \times \left[\bar{E}_{inc} + \bar{E}_e^+(\bar{J}_e, \bar{M}_e)\right] = \hat{n} \times \bar{E}_i^-(\bar{J}_i, \bar{M}_i) \tag{A.10}$$

$$\hat{n} \times \left[\bar{H}_{inc} + \bar{H}_e^+(\bar{J}_e, \bar{M}_e)\right] = \hat{n} \times \bar{H}_i^-(\bar{J}_i, \bar{M}_i) \tag{A.11}$$

Equations (A.10) and (A.11) represent two equations in four unknowns $(\vec{J}_e, \vec{M}_e, \vec{J}_i, \vec{M}_i)$. In order to obtain an unique solution, two more relationships must be established.

Electric current formulation

A simple way to uniquely determine the solutions is to force the magnetic current densities to be zero.

$$\vec{M}_e = \vec{M}_i = 0 \tag{A.12}$$

As a result, equations (A.10) and (A.11) reduce to

$$\hat{n} \times \left[\vec{E}_{inc} + \vec{E}_e^{+}(\vec{J}_e, 0) \right] = \hat{n} \times \vec{E}_i^{-}(\vec{J}_i, 0) \tag{A.13}$$

$$\hat{n} \times \left[\vec{H}_{inc} + \vec{H}_e^{+}(\vec{J}_e, 0) \right] = \hat{n} \times \vec{H}_i^{-}(\vec{J}_i, 0) \tag{A.14}$$

One drawback as shown in [35] is that the operators in equations (A.13) and (A.14) become singular at frequencies for which S, when covered by a perfect electric conductor and filled with the external dielectric medium, forms a resonator. Thus, numerical results of (A.13) and (A.14) will fail in the proximity of these frequency values.

Magnetic current formulation

Similarly, a unique solution can be obtained by setting the electric current densities to zero

$$\vec{J}_e = \vec{J}_i = 0 \tag{A.15}$$

and equations (A.10) and (A.11) reduce to

$$\hat{n} \times \left[\vec{E}_{inc} + \vec{E}_e^{+}(0, \vec{M}_e) \right] = \hat{n} \times \vec{E}_i^{-}(0, \vec{M}_i) \tag{A.16}$$

$$\hat{n} \times \left[\vec{H}_{inc} + \vec{H}_e^{+}(0, \vec{M}_e) \right] = \hat{n} \times \vec{H}_i^{-}(0, \vec{M}_i) \tag{A.17}$$

Once again, the operators in equations (A.16) and (A.17) become singular at frequencies for which S, when covered by a perfect magnetic conductor and filled with the external dielectric medium, forms a resonator. These frequencies are precisely the same as in the case of the electric current formulation.

Combined source formulation

An alternative to the two previous formulations is to set

$$\vec{J}_e = -\vec{J}_i = \vec{J} \tag{A.18}$$

$$\vec{M}_e = -\vec{M}_i = \vec{M} \tag{A.19}$$

and equations (A.10) and (A.11) become

$$\hat{n}\times\left[\vec{E}_{inc} + \vec{E}_e^{+}\left(\vec{J},\vec{M}\right)\right] = \hat{n}\times\vec{E}_i^{-}\left(-\vec{J},-\vec{M}\right) \tag{A.20}$$

$$\hat{n}\times\left[\vec{H}_{inc} + \vec{H}_e^{+}\left(\vec{J},\vec{M}\right)\right] = \hat{n}\times\vec{H}_i^{-}\left(\vec{J},\vec{M}\right) \tag{A.21}$$

As shown in [35], the combined source formulation is equivalent to the combined field formulation in which the singularity problem at the eigenfrequencies is eliminated.

Field formulation

In the field formulation, a single set of equivalent current densities $\vec{J}$, $\vec{M}$ is used to produce the fields in both the internal and external regions, and the boundary conditions are applied to the tangential fields on S. According to the equivalence principle, an electromagnetic field can be terminated by placing the appropriate electric and magnetic current densities on S. Using the convention specified in Figure A.1, the current densities

$$\vec{J} = \hat{n}\times\vec{H} = \hat{n}\times\left(\vec{H}_{inc} + \vec{H}_s\right) \tag{A.22}$$

$$\bar{M} = -\hat{n} \times \bar{E} = -\hat{n} \times \left(\bar{E}_{inc} + \bar{E}_s \right) \tag{A.23}$$

do not change the fields external to S but produce zero field inside of S. Since the field is zero in the interior, the internal medium properties can be arbitrarily changed to any value. For instance, the internal medium can be assumed to be characterized by (μ_e, ε_e) of the external medium. This external equivalence is shown in Figure A.4.

The equivalence principle can also be applied to the internal region where the fields internal to S remain the same and the fields external to S become zero. Similarly, the external medium can now be arbitrarily changed to that of the internal material. This requires the termination currents $-\hat{n} \times \bar{H}$ and $-\hat{n} \times \left(-\bar{E} \right)$ where the minus sign comes from the fact that the surface normal now points inward into the internal region of S. Hence, the currents are simply the negatives of those in equations (A.22) and (A.23). The internal equivalence is shown in Figure A.5. Applying the boundary conditions, just inside of S in Figure A.4, the fields are

$$\hat{n} \times \left[\bar{E}_e^- \left(\bar{J}, \bar{M} \right) + \bar{E}_{inc} \right] = 0 \tag{A.24}$$

$$\hat{n} \times \left[\bar{H}_e^- \left(\bar{J}, \bar{M} \right) + \bar{H}_{inc} \right] = 0 \tag{A.25}$$

Just inside of S in Figure A.5, the fields are

$$-\hat{n} \times \bar{E}_i^+ \left(\bar{J}, \bar{M} \right) = 0 \tag{A.26}$$

$$-\hat{n} \times \bar{H}_i^+ \left(\bar{J}, \bar{M} \right) = 0 \tag{A.27}$$

Now, these are four equation with two unknowns, and hence, additional constraints must be imposed to yield an unique solution.

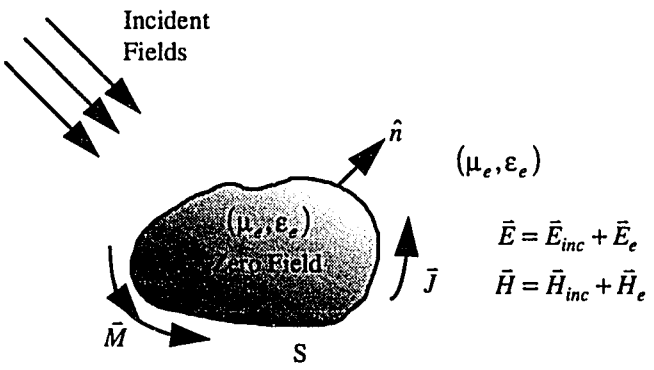

Figure A.4 External equivalence representation

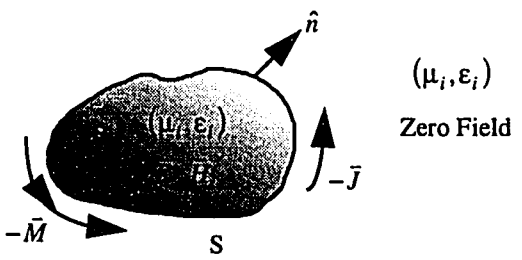

Figure A.5 Internal equivalence representation

Electric field formulation

In this approach, only two equations involving the electric field are considered

$$\hat{n}\times\left[\vec{E}_e^-\left(\vec{J},\vec{M}\right)+\vec{E}_{inc}\right]=0 \tag{A.28}$$

$$\hat{n}\times\vec{E}_i^+\left(\vec{J},\vec{M}\right)=0 \tag{A.29}$$

This yields in two equations and two unknowns. However, it can be shown that the electric field formulation will fail at precisely the same frequencies as the electric current formulation.

Magnetic field formulation

Similar to the previous formulation, in this case, only the two equations involving the magnetic field are considered

$$\hat{n}\times\left[\vec{H}_e^-\left(\vec{J},\vec{M}\right)+\vec{H}_{inc}\right]=0 \tag{A.30}$$

$$\hat{n}\times\vec{H}_i^+\left(\vec{J},\vec{M}\right)=0 \tag{A.31}$$

Once again, this formulation will fail at the same frequencies as the magnetic current formulation.

Combined field formulation

In this approach, linear combinations of equations (A.24) through (A.27) are taken to reduce the number of equations from four to two.

$$\alpha_1\left[\hat{n}\times\left[\vec{E}_e^-\left(\vec{J},\vec{M}\right)+\vec{E}_{inc}\right]\right]+\beta_1\left[\hat{n}\times\vec{E}_i^+\left(\vec{J},\vec{M}\right)\right]=0 \tag{A.32}$$

$$\alpha_2\left[\hat{n}\times\left[\vec{H}_e^-\left(\vec{J},\vec{M}\right)+\vec{H}_{inc}\right]\right]+\beta_2\left[\hat{n}\times\vec{H}_i^+\left(\vec{J},\vec{M}\right)\right]=0 \tag{A.33}$$

various choices of α_1, β_1, α_2, and β_2 exist with some being preferred over others. The formulation used in this research is the Müller formulation. Specific advantages of using this formulation are described in Chapter 6.